FATIGUE OF TWO-PHASE IRON POLYCRYSTALS

FATIGUE OF TWO-PHASE IRON POLYCRYSTALS

By

MALCOLM J. BROWN, B.Sc.

A Thesis
Submitted to the School of Graduate Studies
in Partial Fulfilment of the Requirements
for the Degree
Master of Science

McMaster University
April 1971

MASTER OF SCIENCE (1971
(Metallurgy and Materials Science)

McMASTER UNIVERSITY
Hamilton, Ontario

TITLE: Fatigue of Two-Phase Iron Polycrystals

AUTHOR: Malcolm J. Brown, B.Sc. (University College, Swansea)

SUPERVISOR: Professor J. D. Embury

NUMBER OF PAGES: (v); 131

SCOPE AND CONTENTS:

Quench-aged low carbon iron specimens, containing various distributions of carbide particles were fatigued in tension-compression under low amplitude strain control.

Observations of the influence of second phase particles upon the development of dislocation substructures were made using transmission electron microscopy of thin foils. These observations were correlated with the cyclic mechanical response of the material, and with the response of material containing a fatigue saturation substructure to subsequent tensile overstrain.

A rationale for the development of cyclic softening in the material is proposed, based on the requirements of continuity in plastically inhomogeneous materials. A source model for the observed instability of the cyclic substructure in tensile overstrain is described.

ACKNOWLEDGEMENTS

The author gratefully acknowledges the continued interest, guidance and stimulation of his supervisor, Dr. J. D. Embury throughout the course of the present work.

To Dr. D. J. Lloyd and to other members of the research group, the author would like to offer his thanks for much useful discussion and advice.

The author would further wish to acknowledge the assistance of Mr. R. Jarochowicz with the electron optical facilities, and to thank Mr. M. van Oosten for draughting the diagrams in this thesis, and Mrs. A. Miltimore, for rapidly and accurately typing the manuscript.

Financial support from the National Research Council of Canada is gratefully acknowledged.

TABLE OF CONTENTS

CHAPTER 1

INTRODUCTION

The phenomenon of fatigue of metals exerts costly effects throughout technology. While recent investigations of the detailed development of dislocation substructures during cyclic deformation of single phase materials have established many of the fundamental characteristics of the fatigued state, the investigation of structural materials, which are largely multi-phase alloys, is still heavily weighted towards the acquisition of fatigue failure data, with little attention being paid to the sub-structural changes.

There exists a need, therefore, for experimental observations in systems representative of useful materials. In particular, information about two-phase, precipitation-hardened systems is highly desirable, for many steels and commercial alloys are used in this form.

A substantial number of experiments with simple systems, usually single crystals of pure metals, have determined the dislocation sub-structures associated with the well-recognised phenomena of cyclic hardening, cyclic softening and saturation, observed when one of the testing variables is held constant. A similar depth of understanding of the substructural development in two-phase materials has not been achieved.

The present investigation therefore attempts to analyse the cyclic stress response of polycrystalline low-carbon iron, quenched and aged to give various carbide precipitate particle sizes and spacings, during controlled low strain amplitude fatigue, in tension-compression. Substructural changes were monitored by transmission electron microscopy and ancilliary techniques. The experiments were designed to examine the influence of the second phase particle on the dislocation accumulation, and to delineate the stability of both

the particle distribution and the dislocation substructure, during cyclic deformation and subsequent tensile strain. The stability of structures produced by low-temperature, thermal-mechanical treatments was also examined.

The results will be interpreted in terms of some of the current rationales for deformation in plastically inhomogeneous materials. It is of particular importance to understand in such materials how microscopic inhomogenieties may influence the nucleation and propagation of macroscopic instability, for this understanding is essential to the ultimate relation of macroscopic data for crack propagation to the observed structure and mechanical properties of the material, in a predictive and useful manner.

CHAPTER 2

REVIEW OF THE LITERATURE

2.1 Introduction

Metallic materials in engineering applications subject to fatigue deformation are usually selected on the basis of the S-N diagram. The fatigue limit: Ultimate tensile strength ratio is consequently the most widely used criterion in assessing the fatigue resistance of a material in a generalized design context. Neither of the quantities in this criterion has a viable theoretical basis; this is particularly apparent in modern engineering materials, the development of which has been based on two strengthening mechanisms, the first by dislocation substructure, the second from precipitation hardening. It is clearly very important, therefore, to understand not only how such materials are strong in unidirectional deformation, but also how they perform under reversed stresses.

Two phase materials may be broadly categorized, according to Kelly and Nicholson (1963) into those containing rigid non-deformable particles that contribute to the work-hardening capacity of the material by the generation of dislocations to satisfy continuity requirements as described by Ashby (1970) and those possessing obstacles which are sheared by glide deformation, absorbing energy of deformation in the process. The first property of a two-phase material to be considered in fatigue, therefore, is the stability of the second phase, under cyclic strain.

The second property of interest is the stability of the dislocation substructure developed under cyclic strain, or modified by cyclic strain, in the case of cold-worked materials, or materials with a pre-existing substructure from a phase transformation. In a tensile test the Considere

construction (which defines the plastic strain beyond which the residual work-hardening capacity of the solid is unable to restrict the development of plastic deformation caused by the increasing stress acting as the load-bearing area decreases i. e. as the material necks down) gives us the onset of plastic instability. In cyclic deformation, we observe the phenomena of cyclic hardening, cyclic softening and saturation. At saturation, the material is subject to continued plastic strain, at the same stress level; in softening, the deformation is absorbed at decreasing applied stress levels; this is substructural instability as defined by Forsyth and Stubbington (1960).

The purpose of this literature review will thus be to determine what information is available about substructural stability in fatigue, with emphasis on the cyclic response of b. c. c. materials, in particular iron -iron carbide alloys which are representative of the commercially significant iron-base materials, and constitute the simplest system capable of yielding fundamental information.

The most detailed substructural information describing the spread of plasticity during fatigue comes from numerous investigations of the response of f. c. c. rather than b. c. c. materials, simply because in an f. c. c. material it is possible to predict the type of slip system which will exhibit reversed flow, whereas a b. c. c. material offers a multiple choice. Furthermore, f. c. c. materials are available in higher purities than b. c. c. materials, and the two solute effect complications observable in b. c. c., strain ageing, and the precipitation of both metastable and stable carbides can be avoided by using pure f. c. c. metals. In the next section we shall examine detailed f. c. c. observations, and show their relevance to the b. c. c. case. We shall then evaluate such data as is available in the iron-carbon system, particularly for quench-aged materials, and in other b. c. c. materials.

An experimental programme of investigation into the problems

of stability in two-phase iron-carbon alloys may then be constructed.

2.2 Investigations in f.c.c. Materials

2.2.1 Definition of slip behaviour

That general similarities exist between the fatigue response of the pure b.c.c. and f.c.c. metals has been demonstrated by the investigations of Feltner and Laird (1967a, 1967b, 1968). They define the response in terms of the cyclic stress-strain curve, derived from hysteresis loop data either by incremental stress increases performed on one specimen, or by the use of a series of specimens. It is found that materials exhibiting wavy slip, a definition based loosely on the ease of cross-slip, and hence applicable to materials of high stacking-fault energy, have unique cyclic stress-strain curves, which are independent of the prior history of the material. This is a useful engineering definition, enabling us to differentiate between copper or iron and lowered stacking fault alloys such as Cu-7.5% Al which slips on planar systems without cross-slipping, and does not respond uniquely to cyclic stresses.

The general characteristics of the fatigue process depend strongly on the amplitude of cyclic deformation per cycle, and whether the stress or strain is applied as the controlled parameter. In order to follow in detail the substructural development in a system it is essential to control the deformation put into the specimen per cycle by controlling the plastic strain amplitude rather than allow the specimen to respond in an uncontrolled manner to an imposed stress amplitude. Further, fairly low plastic strain amplitudes must be employed to slow the process sufficiently for its development to be monitored; in this review basically only low or low to medium amplitude investigations (giving lives $> 10^4$ cycles) will be considered.

Controlled stress amplitude investigations are examined where appropriate.

2.2.2 General characteristics

Feltner and Laird (1967 a, b) tested copper and Cu-7.5% Al specimens in tension-compression at different temperatures and after different annealing and cold-working pre-treatments. The transient deformation behaviour produces symmetrical hysteresis rapidly with wavy slip, but for a planar mode, especially at low temperatures, this behaviour is retarded. In general deformed samples softened, whilst annealed samples hardened to a saturation stress uniquely defined for a given applied strain amplitude, but only for wavy slip. The mode of slip did not appear to influence the rate of hardening in polycrystals of comparable grain size. The comparisons of rates of softening mode were suspect in that such comparisons must be made for comparable changes in the flow stress i.e. the initial structures should be similar, and the structures at the point of measurement should be similar. Apart from the irreproducibility of polycrystalline data, the measurement of softening rates at similar cumulative plastic strains is not meaningful in terms of substructural modification. The history dependence of fatigue may extend therefore only to the saturation state produced in planar slip materials.

Reinforcing evidence for this view is that in copper, the temperature dependence of the cyclic flow stress: monotonic flow stress ratio is greater than in Cu-7.5% Al, as expected if cross-slip is the important process, but the saturation stress in copper can be characterized by a cyclic mechanical equation of state. A similar conclusion can be drawn for iron. From this evidence, by considering the change in the elastic modulus with temperature, the same saturation flow stress - cell size relationship can be established as 295^{o}K as at 78^{o}K in polycrystalline copper, according to Pratt (1967). The dislocation cell structure which was observed by transmission electron microscopy (TEM) at saturation was of a scale determined only by the applied strain amplitude, according to both Feltner and Laird, and Pratt.

The former authors further found that some cell walls at saturation consisted of three sets of parallel screw dislocations, composing a twist wall, similar to single crystal observations after low temperature annealing of fatigued copper, made by Laufer and Roberts (1966). In addition more complex dislocation boundaries, plus very simple tilt boundaries, which could consist of edge dipoles or multipoles, were found.

Clearly it is very difficult to determine whether the cell wall structure after hardening or softening is similar and unique. The similarity in strain rate sensitivity at saturation of both annealed and cold-worked specimens, and the similarity of the flow stress-temperature sensitivity after fatigue of specimens with different histories recorded in copper by Kemsley (1958) do reinforce the idea that the wavy slip structure is truly unique.

The influence of history on the hardening or softening process is not clear, however. This is a detailed problem to be examined in the next section.

2.2.3 Details of the cyclic structure

Most observations have been made in single crystals of copper, cycled under controlled low amplitude strain. Behaviour is most conveniently categorized into that of hardening, softening and saturation.

2.2.3.1 Hardening

The process of cyclic hardening has been more thoroughly examined than the corresponding mechanism of softening. The observations of Shinozaki and Embury (1969) on crystals of an orientation such that the primary and coplanar systems were almost equally stressed, were that slip on each system operated rapidly to form long dipoles, and then localised dipole

tangles associated with forest dislocations. Lomer-Cottrell locks are observed to form, and eventually secondary systems are activated according to the stress-relief theory of Hirsch and Mitchell (1967). At the low strain amplitude employed a cell structure per se was not completed. Analogous observations have been made by Hancock and Grosskreutz (1967); they determined that at higher amplitudes the density of braids of dipoles increased, along with the dipole density, whilst the length of the constituent dipoles increased and the Frank (faulted) dipole density decreased (due to their sessile nature, which results firstly in hardening, but ultimately in shearing by secondary dislocations) as the fatigue process continued.

The early stages of fatigue, prior to the full localization of strain, have been investigated by Basinski, Basinski and Howie (1969), who did not observe intense surface slip lines unless the specimen was overstrained beyond the cyclic limits imposed, even when using high resolution Nomarski interference contrast. Their thesis that strain is not localized as described by Watt, Embury and Ham (1968) but rather forms a three-dimensional array, the dipole mats breaking up on the slip plane, was illustrated by etch-pitting the primary and cross-slip planes and by TEM during hardening at $\Delta\epsilon_p = 0.01$. A cell structure did not result, however. Slip line studies showed that surface slip lines became very short as the structure localized and became more complex, the aspect of surface slip correlating well with the scale of the substructure. Most important to the present investigation, the instability to subsequent deformation was shown dramatically by the sudden formation of long, intense reversible slip-lines analogous to the persistent slip bands of Watt et al. (loc. cit.), during overstrain. Furthermore the authors record that the initial rate of work-hardening in overstrain was very low. Indeed Watt (1971) records that the rate of work-hardening of crystals overstrained at saturation was virtually zero so that the substructure was completely unstable.

Arguments have been made that the formation of persistent slip

bands (which return after electropolishing and recycling) is associated with unique surface structures, for example those of Laufer (1969) and Lukas, Klesnil, Krejci and Rys (1966). Such differences are not significant to the growth of instabilities in the bulk of the material, but could possibly affect crack nucleation.

Otherwise, several theories of fatigue hardening utilise the observed high density of dislocation loops and defect contrast observed in TEM as a basis for obstacle hardening. While loops may be pinched off from dipoles, evidence for defects aggregating from vacancy concentrations enhanced during fatigue is indirect (Broom and Ham (1957)). In fact the experiments of Adamson (1968) on neutron-irradiated copper single crystals indicated that radiation induced defects were removed by interaction with slip dislocations in fatigue, producing fatigue softening. The microstructure exhibited defect-free channels on primary planes, the width of which increased as fatigue continued. Channels on cross-slip planes, of virtually constant width, also form. The important result was that surface slip, accurately monitored by an electron shadowgraph technique, ceased early in life, even though much of the crystal was unslipped. Subsequent cyclic stress is borne predominantly by the soft unstable defect-free channels created in the matrix. Adamson suggested that this was possibly due to the internal stress distribution of the dipole clusters which eventually are observed to build up, as in pure copper, but here principally in the channels.

The consensus would appear to be that dipole formation and interaction contributes significantly to the hardening process.

2.2.3.2 Softening

Wood (1962-63), in an early investigation of fatigue softening, observed the effect of subsequent low amplitude fatigue upon torsed pre-strained aluminium cylinders. He recorded that an asymmetry of the

flow stresses induced by the imposed pre-strain was relieved rapidly in a few hundred cycles. Similarly, large cyclic prestrains could be relieved. Since the Bauschinger effect was initially large, the compressive semi-amplitude of the flow-stress exhibited hardening, whilst the tensile semi-amplitude softened. Wood indicated that such behaviour must reflect a fundamental cyclic rearrangement; he also produced stress-strain curves after softening to saturation. Such curves exhibited lower rates of work-hardening than during pre-strain of the virgin material; this indicates that the cyclic structures are also unstable.

Clarebrough, Hargreaves, West and Head (1957) made one of the original observations of softening by stored energy comparisons in deformed, and deformed and fatigued copper, as a function of temperature. The cold-work recrystallisation peak is replaced by a smaller recrystallization peak and a large recovery peak after fatigue. This correlates well with modern TEM observations of softening as a dipole based tidying process analogous to recovery.

A detailed investigation of softening of pre-strained copper single crystals by Huggard (1970) showed that the Bauschinger effect induced by prestrain could be reduced by cyclic softening. The resulting structure at saturation may still have a back stress, however, as shown by the very accurate measurements of Wadsworth and Hutchings (1964) in cyclic hardening, albeit. Huggard observed the production of dipoles and conversion of primary dislocations into dipoles during softening. The temperature dependence of the degree of softening was similar to that of τ_{III} in unidirectional deformation, usually associated with the onset of cross-slip controlled processes. The general reduction of misorientation across cell walls and tidying of the structure resulted in a unique saturation stress. Slip line studies showed that persistent slip lines formed suggesting the resultant

structure was probably unstable with respect to overstrain. An interesting corroberative result from the careful investigation of Steeds (1966) is that at the end of stage two unidirectional hardening the secondary dislocation density greatly exceeds the primary density, presumably of edge dipoles. Since the formation of saturation structures such as cell walls would require the interaction of primary glide loops with secondary loops, either in inclined planes, to form a tilt wall, or in parallel planes to form a twist wall, the τ_{III} analogy is to be expected.

2.2.3.4 Saturation

Observations are probably most frequently made of the saturated state, for example at fracture. Similarly the stability criteria are most easily established for well-defined structures such as simple cell walls. One method of assessing stability is the examination of reversibility of slip monitored by surface observations. In this manner, Watt, Embury and Ham, loc. cit. have examined the properties of dipole mats formed in very low amplitude fatigue hardening of copper single crystals. These structures, which extend into the bulk of the material at saturation, and exhibit plastic strain bearing capacity partly by mechanical reversibility are thus persistent slip bands that slip and unslip, as revealed by electropolishing gradually down into the bulk. On the basis that such structures must be embryo saturation stress-producing structures, their strain bearing capacity was calculated. It was found that motion of dislocations between mats was required, and the dipole-flip model of Feltner (1965) for example, is inadequate. The general applicability of the experimental observations upon which a theory is based similarly restricts the validity of the simple theory of Kuhlmann-Wilsdorf and Nine (1967) who postulated that the growth of an instability relative to the strain-free matrix, such as a persistent slip band, could bear the strain. This concentration of slip, according to the model, has to occur on primary planes to produce extensive twist boundaries with

self-cancelling misorientations about axes perpendicular to the primary planes, before persistent slip bands are observed. Later, tilt boundaries perpendicular to the primary planes can form if slip occurs mainly on two co-planar systems.

Avery and Backofen (1963) have analysed the accommodation of strain by emission of segments of dislocation from suitable sources, and concluded that strain could be borne at saturation for the hardening case, provided that the source density was a function of the square of the applied stress; then the reversible plastic strain was also parabolic with stress and the irreversible component tended to zero at saturation. They observed that instability is not a unique property of the hardened state however. Intermittent overstrain resulted in subsequent softening to a unique saturation stress in copper, but not in Cu-6% Al. Further, the saturation state is shown to be prerequisite to the onset of cracking, regardless of stacking-fault energy; propagation decreases as the stacking-fault energy decreases, demonstrating that the factors controlling initiation and true growth differ. This point will be examined in the discussion.

It is instructive finally to consider the results of the strain-burst experiments of Neumann (1969). Single crystals of copper were subjected to linear increases of applied stress during fatigue, which caused strong maxima in the strain response, increasing as the structure developed, rather than monotonic increases. Interrupting the test and overstraining the crystal produced strong, wide long slip lines, which had large offsets and obviously propagated along paths of instability.

2.2.4 Investigations in other f.c.c. systems

Aluminium and silver respond similarly to copper under cyclic stress, being both wavy slip mode metals according to Feltner's definition. Weissman, Shrier and Greenhut (1966), working with single and bicrystals under reversed bending, followed the build-up of cell structures with regular twist

walls by TEM and X-ray diffractometry for rocking-curve half-width determination. The effect of a boundary was found to reduce the failure life by a factor of five. The observed structures correlated well with those in copper, showing elongated loop tangles in low-strain regions. The stability of the saturated structure was examined by careful recording of the structure at various amplitudes of strain, then changing the strain amplitude. By TEM it was observed that complex interactions, nucleated at cell walls, produce new cell sizes by a process analogous to recovery. The new developing cells decorated the structure delineating nucleation sites. Crack propagation could be retarded, by reducing the strain amplitude at a transverse strain boundary so that "cyclic stress-induced ductility is hence a vital property of plasticity ahead of a crack tip."

Grosskreutz and Waldon (1963) using X-ray microbeam analysis of the plastic zone ahead of a crack tip concluded that subgrain formation is a necessary requirement for crack propagation in aluminium. Sweeping up mechanisms for loop debris and defect production during hardening contribute little to the instability of the plastic zone as the strain is raised, until such a structure is developed, in these authors' opinion. McEvily and Boettner (1963) found that crack initiation /stage I propagation by persistent slip is followed by a stage II process strongly dependent on the nominal stresses at the crack tip. None of the simple exponential growth rate relations are applicable over the entire process and in single crystals, orientations with high work hardening rates in fact show high propagation rates in aluminium. An understanding of instability would be exceedingly valuable as an adjunct to understanding these stages of crack propagation. A complete analysis of this problem cannot be approached in this thesis.

2.3 Investigations in Iron-Carbon Alloys

The literature of detailed TEM observations in iron reflects the

difficulties of making any reliable, unambiguous crystallographic observations. Unfortunately, the experimental techniques used to acquire the data, particularly the mechanical property measurements (or absence thereof) are rarely reported in sufficient detail for useful comparisons to be made. In particular, many investigations have been carried out in reversed bending, without any reference to specimen geometry; further, electron micrographs are seldom related to their location in the specimen, so that under the variable strain amplitude applied it is impossible to determine the state of strain at the region of substructure described. In addition, many investigations are carried out under stress amplitude control; adding the further complication that many oscillatory or reciprocating constant load high-frequency testing machines apply initial loading in a progressive manner, we have a considerable interpretative problem.

An exception is some of the first controlled low strain amplitude, tension-compression fatigue tests on iron by Wei and Baker (1965a). TEM gave observations of bulk substructures consisting of dislocation loops and dipoles, similar to those observed by Keh and Weissman (1963) in unidirectional deformation at small strains. Surface layer structures of linear arrays of loops increasing in density as fatigue progressed were also seen. In a subsequent paper, Wei and Baker (1965b) showed that at larger fractions of the life slip processes concentrated into localized regions. At the very low strain amplitude used a wall structure built up adjacent to grain boundaries, but a regular cell structure was not seen amongst the structures retained in the foils. Surface slip lines were roughly correlated with the partition of strain, and jogged screw type mechanisms rather than double cross slip considered for the formation of the preponderant loop density.

Under cyclic reversed bending, annealed polycrystalline ferrovac E also exhibited a high density of fine dislocation loops, according to McGrath and Bratina (1965a). These loops concentrated around heavily jogged

dislocations, but above certain values of the controlled stress amplitude used, well-defined subgrain boundaries developed in addition. Parallel studies in tension-compression, under a controlled strain amplitude $\Delta\epsilon_p = 0.012$ by Lukas, Klesnil and Rys (1965) traced the development of the fatigued structure at a slightly higher imposed amplitude. In polycrystals, they observed that substantial dislocation tangling occurred during the first half-cycle, producing loops and dipoles, leading to well-defined embryo sub-boundaries being observed by cycle 100. A regular, localised slip cell structure then developed. The life was $> 4.7 \times 10^4$ cycles. In stress amplitude control tests the dislocation density increased an order of magnitude in the first half cycle, but thereafter changed little. Interestingly, the Bauschinger effect was virtually eliminated by cycle 10.

The interpretive problems posed by stress-amplitude controlled testing is illustrated by the interesting investigations of Lukas, Klesnil, Kreju and Rys (1966) to verify the grain-size dependence of the fatigue limit, using stress amplitudes below the macroscopic yield point. The resulting development of strain amplitude by a process analogous to Luders instability gives macroscopic softening followed by dominant microscopic hardening. The slow growth of the plastic regions masks the hardening process, however, and the important overstrain experiments made at various early stages of the life, which suggest that a tangled dipole structure can generate further mobile segments to accommodate strain yet still harden adequately by interaction with debris such as loops, vacancies and their aggregates, cannot be simply interpreted. The effects of grain size were restricted to the control of the expansion of plastic micro-volume in initial softening, which was greatest at fine grain sizes, as was Lüders extension. The saturation strain reached after cyclic hardening was found to be a unique function of the imposed stress amplitude only, obeying the wavy-slip definition.

Klesnil and Lukas (1967) further examined surface foils by TEM

from low and high-amplitude fatigued specimens. They showed that slip bands, bounded by loops or dislocation tangles, 2-12 μm below the surface correlated well with surface slip-line spacing; this constitutes important evidence for the localisation of slip at free surfaces, a key factor in the life of cyclically loaded engineering structures.

McGrath and Bratina (1965b) fatigued furnace cooled Ferrovac E in bending at low stress amplitudes, and found simple jogged dislocations and loop structures. No Burgers vectors were determined but the dislocations appeared to be predominantly screws rather than extended dipoles. Similar structures were found after reasonable fractions of the life in a low carbon Swedish iron and an iron-0.08%C alloy with low dissolved carbon contents. Normalized 0.28%C steel with a transformation induced substructure in the ferrite resisted fatigue better than the other alloys at low stress amplitudes, but the best performance was obtained by spheroidization; it was suggested that carbon atmospheres around the cementite interfaces exerted a drag on slip dislocations.

The paper reported briefly observations of the response of quench-aged iron containing a fine metastable precipitate and an associated substructure. It was observed that fatigue appeared to change the precipitate morphology in regions of localised slip; however the original distribution of carbide was inhomogeneous and the suggestion that shearing of precipitates in such local regions reduced the precipitate size to the extent that reversion might occur or at least TEM image contrast be lost required further evidence. McGrath and Bratina (1967) therefore extended the study in quench-aged 0.08%C iron to both stable and metastable dispersions of carbide of differing size and spacing, cycled in fully reversed bending. In the fine dispersions, which frequently showed no detectable slip activity by TEM, occasionally regions adjacent to grain boundaries displayed different electron image contrast, suggestive of denuding as in precipitate or loop-free zones. Such regions were suggested to be precipitate

free due to extensive slip activity. For dispersions with spacings $\sim 1000\text{Å}$ dislocation-particle interaction was more clearly seen; whether the process constituted nucleation of a tangle of dislocations, an active source, or a shearing event, could not be resolved. Coarser dispersions were connected by a fairly uniform network of dislocations at a correspondingly early stage of the life. Unfortunately, none of the observations are related to their location in the specimen; nor is its geometry described. Hence the magnitude of the stress acting on the foil area described is unknown; it is not even possible to assess if the situations described were even fully plastic in bending. The fractions of the life undergone were small, but again unsepecified. Surface observations showed that slip was restricted by fine dispersions relative to coarser dispersion behaviour at the same amplitude and fraction of the life. Microcracks eventually open up at 45° to the specimen axis at the end of the life, associated only with active slip bands. They are best observed in the fine dispersions, as the gross slip at the end of the life in coarse dispersions masks such observations.

Cyclic hardening and softening data supplementary to the above investigation was produced by McGrath and Bratina (1969) in an attempt to correlate the behaviour of specimens cycled in tension-compression with the observed substructure. It was determined that while quenched and furnace cooled iron both hardened, after the Luders instability had propagated, fine metastable carbide distributions hardened initially, but subsequently softened. The softening behaviour was attributed to the establishment of persistent slip channels which denuded the matrix of hard particles. Coarse dispersions hardened continuously; hardening was not attributed to strain-ageing however, on the basis that iron with an interstitial-getter, such as Fe-0.25% Zr shows rather similar behaviour; modification of the substructure alone must produce the hardening. The authors also pointed out that yielding after strain ageing results in a higher initial density of dislocations, generated from many pinning points, than non strain-aged

material, and such an enhanced density does not appear to be available in fatigue. There appears to be considerable scope for an investigation in more detail to examine particle stability and the ultimate development of substructure not examined in the above work; such an extension of the investigation is presented in this thesis.

In addition to the basic problem of the distribution of plastic instability, the stability of coherent and noncoherent carbides poses an extensive problem, that of the affect of reversed strain on the solid solubility of carbon in ferrite after quenching. Ferro and Montalenti (1962) prepared quenched, annealed, and quench-aged specimens and endeavoured to test the hypothesis that the sharp knee frequently exhibited by the S-N curve was associated with the occurrence of a sharp yield-point in the material. Since fatigue endurance is such a variable quantity it is difficult to correlate such data with explanations based either on accelerated fatigue ageing, or the simple plastic stability of the deformed matrix. No correlation between sharp yielding and a sharp endurance limit was found however; one would not expect initial Snoek or Cottrell type locking to influence eventual endurance unless the specimen was rested in any case.

Mintz and Wilson (1965) attempted to investigate the kinetics of strain-ageing during continuous cycling at room temperature. Any accelerated process of strengthening will of course be masked by changes of plasticity during fatigue, especially during cyclic hardening of the substructure. In an effort to overcome these difficulties, coarse grained steels of varying carbon contents were cycled under incrementally increasing stresses, and the temperature rises, attributed partly to a damping decrement which varies with solute concentration, and hence varies through an ageing reaction, were monitored with differential thermocouples. The results in quenched 0.7%C steel showed that as the stress increased to failure the decrement increased; however the cyclically deformed material was unable to repeat this behaviour after resting until restrained through yield, suggesting that

a strain-ageing reaction was facilitated, for stressing cycles began in the elastic range. On unlocking the structure the damping decreased rapidly, suggestive of a Lüders type of instability. By assuming an ageing reaction rate function , similar to the static description, a temperature dependence significant even at -40°C was determined. In a bainitic quenched and tempered steel of similar composition, with a very fine carbide precipitate, a different dependence, still operative at -40°C, was observed; in these tests the structure did not become strongly locked after fatiguing and testing. Annealed samples behaved similarly. By comparing static and cyclic ageing rates, it was determined that quenched specimens showing the locking-type of ageing, aged up to six times faster at the testing frequency than statically. No frequency dependence in the range 80-200 cps. was detected. The other type of reaction, however, was up to fifty times faster at a particular stage of fatigue (the rate of reaction is a function of the degree of completion). This observation was explained in terms of shearing and reversion of fine carbides producing increased supplies of carbon in solution. The observed activation energies (0.5eV) differed markedly from the activation energy of carbon diffusion in iron (0.86eV) so that purely thermal activation provided by the temperature rise could not account for the rate changes. In the absence of a knowledge of the variation in Koster damping it is possible only to say that the solid solution behaviour is based more on the dragging, interaction and formation of Cottrell atmospheres, whereas fine precipitate particles may be subject to reversion and subsequent overageing during fatigue. In order to analyse resting data or the temperature dependence of the fatigue life in annealed steels of widely differing grain sizes, and hence yielding behaviour, such as that of Oates and Wilson (1964), we need far more detailed frequency-dependence and damping data than is available at the present time. It is constructive however to observe from the unidirectional strain-ageing data of Wilson and Russell (1960), that segregation of solute to dislocations does not stop

when atmosphere formation is complete, but that subsequent segregation has little effect on the unpinning stress. Neither is the Luders instability further affected. In order to alter the flow stress, solute clustering or actual precipitation is required, and these processes alone alter the work-hardening capacity of the material.

More direct observations of ageing behaviour during fatigue of low carbon steels were made by Wilson and Tromans (1970). Portions of the rim of a 0.03%C steel were cycled in reversed bending at temperatures between 20°C and 130°C, after quenching. Surface slip was retarded as the test temperature increased so that ageing was facilitated. The electron metallography, supplemented by optical metallography on polished and etched sections, showed the usual dislocation tangles characteristic of low-amplitude fatigue. The dislocation-free matrix developed a fine carbide precipitate but increasingly as the temperature was raised undecorated narrow bands free of extensive electron image contrast in the reflections used in TEM, were observed. Optical micrographs at high magnification showed analogous etching effects. A requirement for this 'channelling' of slip would appear to be freedom from intersection with other structural features; the problem may well be formulated for single slip in a favourable stress system, where local work-hardening is not permitted, reflecting an instability propagating under a local strain concentration in an unstable two-phase system. For in detail, the situation may be more complex; the structures observed close to the neutral axis of the bend specimen did not show channels, (Wilson (1970)). Furthermore, envelope contrast around the channels was not well resolved, though it could have been reprecipitated carbide, possibly supplied by carbon from sheared, reverted metastable carbides. We might thus deduce that a gradient of strain is required to produce this type of instability, and that the details of the localisation of strain are not simple. Experimental evidence will be presented in this thesis to support those deductions. In addition, it becomes obvious that

such instabilities must be particularly important at the tip of a propagating fatigue crack; although high amplitude cell structures generally build up, intense fatigue ageing apparently limits the slip propagation paths to channels, whilst lower ageing temperatures permit paths subject only to the original constraints in the material. Again further information about the stability of distributions of fine metastable carbide is required. Some detailed observations of cell structure build-up by etch-pitting $\{100\}$ planes of a single crystal of iron with a propagating fatigue crack have been made by Lawrence and Jones (1970), but their observation of the lack of orientation dependence of the S-N curve, previously investigated by Hempel (1959) confirms the complexity of the process of plastic strain development in single phase iron, without the added complications of solute redistribution as a further restriction on slip processes.

2.4 Investigations in Other Iron Base Alloys and b.c.c. Materials

Although carried out under low-cycle, high stress-amplitude controlled conditions, the work of Morrow (1965) on quenched and tempered 1045 steel is of direct interest to the problems of stability in fatigue. On tempering such a material, the strain hardening exponent decreases to a minimum and then increases as the tempering temperature is raised to fully soften the steel. Measurements on hysteresis loops showed that cyclic softening of up to two orders of magnitude of cyclic strain occurs on cycling, being greater, the higher the amplitude. The best resistance to softening is obtained from optimum tempering for monotonic deformation. This result negates previous observations that slightly softer (and therefore more coarsely dispersed carbide aggregates) materials perform best. This may be due to the effects of detrimental metallurgical constituents and defects used in other investigations, but probably most important of all, to the imposed state of stress, particularly in surface layers or at internal surfaces where cracks nucleate.

Such an influence may be deduced from the results of Eckert (1958) for the torsion of axle shafts.

On this rationale, Morrow, Halford and Millan (1966), employing the fracture mechanics concept of engineering brittle failure, suggested that a transition from shear to tensile failure occurs on increasing the hardness of a tempered steel. Then plastic blunting ahead of a crack tip and the controlling rate of work-hardening in the plastic zone, giving the characteristic fractographic observation of striation formation under reversed stresses, is replaced by a situation in which "it is now convenient to consider the fatigue specimen as a tensile test-piece with a slowly moving Griffith crack".

Beardmore and Feltner (1969) investigating the cyclic stress response of a low carbon, low alloy martensitic steel, showed that at low amplitudes (Δ_p = 0.0194, 0.0096) the stability of the transformation induced substructure was minimal, and specimens softened rapidly. Cyclic stress-strain curves fell below the monotonic curve. It was noted that the effect of substructure was to restrict the work-hardening capacity of the material and hence the cyclic elongation to fracture. The surface observations of small cracks forming at 45° to the tensile axis on fatigue in tension-compression, correlate well with those observed in iron in bending. The cracks followed intense slip lines as in stage 1 growth in f.c.c. materials; fracture was therefore theorised to initiate at geometrical discontinuities in the structure such as carbide, inclusion or prior austenite grain boundary interfaces, as the matrix could not otherwise be induced to rupture. The propagation in stage II was considered to be independent of such inhomogenieties (but see the discussion).

McGrath and Bratina (1970) examined iron-copper alloys with non-coherent particles of copper of 75Å or 240Å diameter. After fatigue in

tension-compression at medium plastic strain amplitudes such materials cyclically hardened, the fine dispersion more rapidly than the coarse dispersion. No apparent particle cutting to a reversion size was detected by TEM, cell structures build up, particularly at grain boundaries; at early stages of fatigue, the heavily jogged networks formed suggested that the configuration was controlled by the particle distribution, and hardened by accumulation rather than shearing processes.

2.5 Conclusions

It becomes apparent from the literature that the dislocation substructures developed in fatigue of both f.c.c. and b.c.c. materials are similar, and that at the saturation condition , such substructures are inherently unstable, in the sense that they propagate along local, rather than uniformly distributed paths, and are thus vulnerable to overstrain. It is further evident that in two-phase iron base materials the influence of carbides and carbon in solution is complex, and that further pertinent experimental data in a simpler system, such as iron-iron carbide would be of great value in assessing suitability of important commercial steels such as ausforming and High Strength Low Alloy (HSLA) steels for fatigue duty, particularly in relation to resistance to fatigue crack propagation.

The present investigation will attempt to analyse:

(i) the influence of particle size and distribution upon the growth of instabilities in cyclic plastic deformation.

(ii) the effectiveness of thermal mechanical treatment in increasing the stability of the substructure.

Quench-aged low carbon iron is used to facilitate comparison of observations with those of previous investigators.

CHAPTER 3

EXPERIMENTAL PROCEDURE

3.1 Introduction

The experimental scheme consisted of thermal or thermal-mechanical pre-treatment of the material to produce different dispersions of carbide in ferrite. Machined and polished specimens were fatigued in tension-compression under strain amplitude control, and their cyclic stress response measured. Supplementary tensile tests were also made.

The observed mechanical properties were correlated with substructural changes revealed by transmission electron microscopy. Optical metallography of polished and etched sections, and of surface replicas and direct surface fields was used in conjunction with scanning electron microscopy and replica electron microscopy to provide supplementary information.

3.2 Preparation of Material

The material used was Armco Iron, supplied by Corey Steel Co. of Chicago. A full analysis of the composition is given in Table 1. The iron was initially in the form of rod stock in two sizes 0.750" (19.05 mm) in diameter and 0.500" (12.70 mm) in diameter, in the fully annealed condition.

X-ray back-reflection polycrystalline patterns, using unfiltered tungsten radiation, revealed a marked texture in the as-received material. This texture was not removed by any of the heat-treatments subsequently employed.

The cleanliness of the material was assessed by optical metallography of sections parallel and perpendicular to the rod drawing direction; apart from minor constituents, the principal inclusions of metallurgical significance in this investigation were stringers elongated parallel to the drawing axis. These inclusions were determined to be manganese sulphide by electron-probe microanalysis.

Preliminary heat treatments were made at different austenitizing temperatures to determine a treatment which adequately solutionized the material, yet gave a reproducible medium grain size. Specimens were quenched to retain carbon in solution, then aged, either at 60°C for five days, 100°C for three days, or 240°C for five hours, to determine the approximate ageing behaviour and the morphologies involved. The ageing process was followed using Rockwell hardness measurements and transmission electron microscopy (TEM) of thin foils.

From the preliminary investigation three types of material treatment were established:

(a) Austenitize at 850°C for two hours, quench directly into water at ambient temperature. Age five days at 60°C or five hours at 240°C.

(b) Austenitize at 850°C for two hours, cool slowly through the austenite-ferrite transformation and water quench from 725°C. Age five days at 60°C, five hours at 240°C or three weeks to one month at room temperature 23-28°C.

(c) Austenitize at 850°C for two hours, water quench, swage in two passes from 0.615" (15.62 mm) diameter to 0.565" (14.17mm) diameter, and age five days at 60°C or five hours at 240°C. For this thermal-mechanical process the larger diameter stock was turned down to the requisite diameter prior to austenitizing. TEM of this material revealed that the swaging reduction of 8% in diameter

(equivalent to approximately 20% in tension) produced a well-developed cell-structure, suitable for the experiment.

The prepared material was then machined into specimens for fatigue testing, to the dimensions shown in Figure 1(a). A gauge section aspect ratio of 2:1 minimized the risk of buckling, but gave sufficient surface area for replication.

Machined specimens were chemically or electro-polished to obtain a surface free of optically observable defects. A better overall finish was obtained using a chemical polish consisting of 80% H_2O_2, 5% HF and 15% H_2O then by cold electropolishing in an acetic acid - 5% perchloric acid electrolyte using a stainless steel cathode; with an inclusion content such as the material possessed, surface pitting was minimised, but could not be avoided. During surface preparation the threaded portions and shoulders of the specimens were protected with microstop lacquer; at the end of the preparation the lacquer was removed in acetone, and the whole specimen lightly polished, washed in water then dry ethanol and stored in a dessicator prior to testing. This procedure ensured clean, deburred threads for accurate mounting of the specimen for testing, and a suitable gauge section for surface replication and for reproducible fatigue resistance.

To check for possible deleterious effects during machining, X-ray back reflexion photographs of the gauge section surface of the specimen, were taken before, and after, the removal of various depths of material by chemical polishing. The depth of damage by the lathe tool, and emery grind was thus determined and the polishing procedure calibrated to ensure the removal of the damaged layer from each specimen. As a further check, a proportion of all the specimens was prepared by machining the stock, and then heat treating the machined specimen, in a vertical shaft vacuum furnace operating at 10^{-5} torr. No significant variation in results, within

experimental scatter, was recorded for such specimens, compared with specimens heat-treated, then machined. The swaged material could not, of course, be prepared in this manner.

A further proportion of the specimens were produced with fine ground parallel flats along the gauge section, to assist replication and direct surface observations. In addition a series of reduced section parallel gauge length tensile specimens of approximately rectangular section [0.250" x 0.100" (6.35 mm. x 2.54 mm)] with ground surfaces were polished and used for slip line studies.

A complete tabulation of specimens identities, together with the treatments given in preparation is presented in Table 2. The table also gives the tests performed on each specimen.

3.3 Mechanical Testing

Apart from some tensile tests which were carried out in a floor model Instron machine with one rigid, and one hemispherically seated alignment, threaded grip, with an open cage, all the testing was completed using a closed-loop electrohydraulic testing rig, manufactured by the M. T. S. division of Research Inc.

High precision, rapid response, controlled parameter testing is the main feature of this facility. A pre-set electrical signal, applied to a hydraulic actuator, operates a moving ram against a specimen attached to the moving ram, and to a fixed ram. A suitable transducer records the output due to the specimen or ram response, and transmits a signal to a comparitor, which modifies continually the input signal to the actuator to maintain the set point. The equipment is capable of simple sequences of programmed commands and possesses multiple output capacity for recording devices and for calibration. In addition, error detection devices are provided.

For the purposes of the present investigation, a linear variable differential transducer (L. V. D. T.) was used to monitor the movement of the ram, which for rigid systems closely approaches the total extension in the specimen. This parameter was therefore controlled during fatigue to well within the manufacturers stated accuracy of $\pm$ 2%. During fatigue at very low strain amplitudes the L. V. D. T. had to be employed at its lowest total stroke range of $\pm$ 0.25" ($\pm$ 6.35 mm.). Under these conditions the signal to noise ratio may drop to 4:1, according to measurements made with a two-beam oscilloscope, because of the proximity of the hydraulic pumping system, residual mechanical vibration, and other nearby electrically operated equipment. The cyclic stress amplitude and the applied strain amplitude was taken from a filtered output and recorded continuously on a two-pen recorder, but the hysteresis loops, recorded on a separate recorder from an unfiltered output, could not be accurately monitored; a higher resolution L. V. D. T. would be required for the simultaneous recording of the individual parameters and the hysteresis loops.

The fatigue specimens were mounted in an upper rigid threaded grip, and a lower gripping fixture consisting of an internally threaded inner grip cyclinder with a keyed surface, which was embedded in an outer hollow cylindrical grip with a small diametrical clearance, bolted to the moving ram. Woods metal was then cast into the lower grip at 80^{o}C. Specimen cooling was effected using surface evaporation of solvent from a cooling jacket under a compressed air blast. The surface temperature measured by a flat thermocouple attached to the centre of the grip section of a thin specimen never exceeded 45^{o}C. Under peak operating conditions the rig temperature was maintained at a steady 35^{o}C. A perfectly rigid grip was obtained by modifying the design clearance between inner and outer grip cylinders, and by redesigning the keying surfaces of the inner and outer cylinders; the use of a flux prior to casting the Woods metal enhanced wetting of the surface. The specimen was finally secured after solidification of the

solder, by tightening two retaining nuts against each grip. The testing facilitiy is illustrated in Figure 1b. From the available functional relationships between the control parameter and time which could be applied by the signal generator, a sinusoidal wave form supplying a tensile signal followed by a compressive signal was selected. Preliminary tests at various frequencies of cycling were carried out to check for slippage in the gripping system. After careful alignment of the upper and lower ram by adjustment of the bearings supporting the upper ram, an off-axiality of less than 5×10^{-4}" (1.27×10^{-2} mm) measured by a concentricity variation on a dial gauge mounted on the lower ram reading off the upper ram, was obtained. Negligible bending moments were thus induced in the specimens during fatigue, since such misalignments could easily be accommodated by the lower grip clearance, and the relaxed aligned specimen then rigidly held in that position on soldering the lower grip. With this system no slippage was detected either at peak stress or during the change of sign of the stress when cycling about zero mean strain.

The main testing programme was carried out at a total stroke amplitude equivalent to a total strain amplitude of $\Delta\epsilon_t = \pm 0.003$. A cycling frequency of 1 c.p.s. was employed to facilitate the recording of data; the recorder response time was 0.2 seconds. For long life tests ($> 10^5$ cycles) a cycling frequency of 10 c.p.s. was employed in the later stages of the test. The effect of the strain rate change on the peak stress was small, and the transient period was calibrated and allowed to reach completion before a recording was made at 1 c.p.s. after cycling at 10 c.p.s.

Some specimens were overstrained, usually in tension, after a significant fraction of the life. To complete this experiment in the M.T.S. machine, the function was altered to a linear ramp and the specimen overstrained in situ. Other specimens were removed, the gauge section turned down to 0.100" diameter (2.54 mm) and overstrained in the Instron

Dimensions in inches
Double scale
Thread size

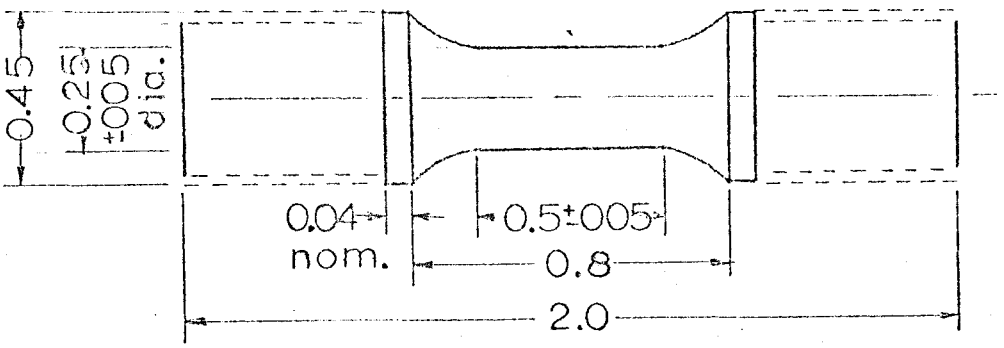

FIG.1.a. SPECIMEN DIMENSIONS

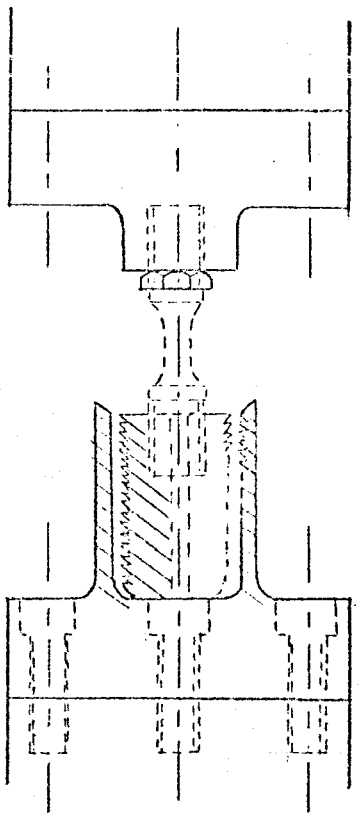

Half scale

FIG.1.b. GRIPPING FIXTURE

machine at the nearest comparable strain rate to the M. T. S. cyclic strain rate (0.03"/"/min) which was 0.04"/"/min. in the Instron.

Cyclic hardening or softening curves were plotted from the peak stress/cycle data for each type of material examined. Tensile data was recorded on virgin specimens and during overstrain. Comparative tests were also made on furnace cooled material. The full testing programme is summarized in Table 2.

3.4 Transmission Electron Microscopy

The majority of the structural data described in this thesis derives from electron microscopy of thin foils. For each of the microstructures prepared, foils were prepared, parallel to, and perpendicular to the tensile axes of the specimen at various stages of fatigue; in addition, the original distributions of particles were observed. The gauge section was cut from the mounted specimen to avoid any risk of overheating during demounting. Thin slices 0.030" - 0.040 (0.85 - 1.33 mm) thick were cut with a jewellers saw, and mechanically ground on fine emery paper to approximately 0.006" (0.17 mm) thickness, by mounting on a rigid block using double-sided linen tape. The mechanically thinned discs were then dismounted and chemically thinned in the chemical polish described in section 3.2, almost to perforation. Final electropolishing by the uniform field method in a 95% CH_3COOH, 5% $HClO_4$ mixture at 10-15^{o}C, washing in clean acetic acid, then dry ethanol gave good foils with extensive thin areas. Evidence of damage during specimen preparation was seldom observed.

All foils were examined at an operating voltage of 100 kV, in a Siemens Elmiskop 1 microscope. A few observations were made using a Phillips EM300 instrument. The Siemens microscope was fitted with a double-tilt stage capable of tilts of $\pm$ 10^{o} about two perpendicular axes.

Various tilting experiments were performed to resolve detailed sub-structural configurations. Kikuchi line shifts were used to measure sub-boundary misorientations in cell-structures. The existing calibrations for (a) the rotation of the image relative to the diffraction pattern and (b) the variation of true magnification with indicated magnification were employed during this investigation.

All plates were analysed emulsion side downwards. Wherever possible, information was derived from as many different areas of the foil as possible, or from more than one foil, in an endeavour to describe representative behaviour.

3.5 Optical Metallography

(a) Surface

Direct surface, and single stage cellulose acetate replica observations were made of the development of slip lines during the fatigue of specimens quenched from the austenite. The replicas were mounted on a reflecting substrate and examined in a Vickers projection microscope.

Direct observations of the surface of polished specimens of each distribution pre-strained by $\epsilon = 0.01$ in tension, were made in a Reichert metallograph fitted with a Nomaski contrast objective. Over-strained specimens were similarly examined.

More detailed information was obtained from tensile specimens pre-strained by $\epsilon = 0.01$ at $-78^{\circ}C$ using two stage replication. Collodian-backed Formvar replicas were used to produce positive carbon replicas which were examined in the electron microscope at 80 kV.

(b) Bulk

Polished sections, etched in 2% nital, were examined to determine the grain size, and grain aspect ratio in two perpendicular sections, after pre-treatment.

Using Fry's reagent (Hahn and Sadey (1966)) the substructure in fatigued specimens was etched up for examination under an immersion lenses. The etchant attacks carbon associated with substructure, and was used in an attempt to obtain overall indications of the extent of the development of the substructure observed in detail by T. E. M. For fine dispersions of carbide the etchant is not effective. Limited resolution is obtainable in such dispersions using a copper deposition etchant, but was found inadequate for the purposes of this investigation.

3.6 Scanning Electron Microscopy

Efforts were made to use the scanning microscope as a high resolution adjunct to the optical microscope. The etchants used did not provide sufficient surface relief for adequate contrast, however.

The microscope was therefore used only for fractographic observations on selected specimens in certain experiments.

3.7 Summary of Schedule

The propensity of the material to age at room temperature required careful scheduling of experiments. Specimens were prepared in batches; because the effects of machining damage could not be accurately assessed in the bulk, and because the average time to obtain machined specimens was one week, it was preferable to heat treat after machining; however considerations of convenience both in the allocation of instrument time, and in the ease of machining (machinability was best after ageing) as well as better control of

microstructural reproducibility obtained by heat-treating bulk material, sometimes required the reversal of this procedure. Mechanical testing and electron microscopy was carried out as quickly as possible after specimen preparation.

The quenched, swaged and aged specimens were tested and examined first, followed by specimens quenched from the austenite field. Finally experiments on specimens quenched from the austenite and ferrite field were carried out. Overstrain tests were made at appropriate points, and other auxiliary observations carried out in sequence. The notched specimen experiment described in Chapter 4 was suggested by the data derived initially in the material in which it was carried out and was not envisaged in the original scheme.

TABLE 1

CHEMICAL COMPOSITION OF MATERIAL

C	P	Mn	S	Si	N	O
0.018		0.037	0.013		0.003	0.072

TABLE 2

SPECIMEN IDENTITIES AND USAGE

Series	No.	Pre-Treatment	Tensile Test	Fatigue Test (Cycles)	Overstrain	TEM	Replica	Optical SEM
QA(γ) 60	1	Quench 850°C		10^5 F		x		
	2	Age 5 days 60°C		6.5×10^4		x	x	x
	3			2.25×10^5 F		x		x
	4			3×10^4		x		
	5		x					
	6			10^5 F				
	7		x					
	8		x					
QA(γ) 240	1	Quench 850°C		10^3		x		
	2	Age 5 hrs. 240°C		1.5×10^4				
	3			4.3×10^4 F		x		
	4			4.5×10^4 F		x		
	5			3.3×10^4				
	6			5.5×10^4 F			x	x
	7			4.5×10^4 F				
	8		x					
QA (γ +∝) 60	2	Furnace cool 850°C - 725°C		10^6F				
	3	Quench, age 3 days 60°C	x					

Table 2 (Cont'd.)

Series	No.	Pre-Treatment	Tensile Test	Fatigue Test (Cycles)	Overstrain	TEM	Replica	Optical	SEM
QA ($\gamma+\alpha$) 25/60	1	Furnace cool 850°C - 725°C Quench age 1 mth. 25°C + 3 days 60°C		1.1×10^6 F		x			
QA($\gamma+\alpha$) 25	1	Furnace cool 850°C-725°C		7.5×10^5 F					x
	2	Quench, age 1 mth.		3×10^5	x				
	3	25°C		7.5×10^4					x
	4		x				x		
	5			Notch $2.5 \times 10^5 \rightarrow 10^6$ F		x		x	x
	6			Notch $.7 \times 10^5$ F	x				
	7			High Amplitude 350F		x			
QA ($\gamma \times \alpha$)240	1	Furnace cool 850°C-725°C		5.5×10^4 F		x	x		
	2	Quench, age 5 hrs.		3.3×10^4	x	x		x	
	3	240°C		3.3×10^4	x	x			
	4		x						
	5			3.5×10^4	x				
	6		x				x		

Table 2 (Cont'd.)

Series	No.	Pre-Treatment	Tensile Test	Fatigue Test (Cycles)	Overstrain	TEM	Replica	Optical	SEM
F. C.	1	Furnace cool from 850°C		3.3×10^4	x				
	2		x				x		
QSA 60	1	Quench 850°C, swage		1.2×10^5 F		x			
	2	8% Red. of Dia. Age		0.9×10^5					
	3	5 Days 60°C	x						
	4			1.5×10^4		x			
QSA 240	1			4×10^4 F		x			
	2			4.6×10^4 F					
	3			1.5×10^4		x			
	4		x						

CHAPTER 4

EXPERIMENTAL RESULTS

4.1 Scheme of Presentation

In section 2, pertinent monotonic and cyclic mechanical property data will be presented. Results obtained by T. E. M. of thin foils will be given in section 3. Finally, ancilliary observations made by optical and scanning electron microscopy, and by surface replication will be described.

Results obtained from specimens quenched from austenite will be given first in each section, followed by results from specimens quenched from the two phase region; the results of thermal-mechanical treatment will be described last.

4.2 Mechanical Response

A complete tabulation of monotonic and cyclic data is recorded in Table 3. The treatments undergone by each specimen are as described in Table 2 of Chapter 3. The principle cause of irreproducibility of properties is the inhomogenieties of quench-aged structures which may be associated with variations in quench rate, quench deformation, and solute segregation, within a single specimen, and from specimen to specimen. In the comparison of cyclic and monotonic properties, the error induced by testing at slightly different strain rates ($\dot{\epsilon}$ = 0.04 in./in./min. in the Instron machine, whilst $\dot{\epsilon}$ = 0.03 in/in/min. in the M. T. S. machine) is not significant. The variation in cross-sectional area of the gauge length of specimens, produced during machining and polishing, may produce an error of $\pm$ 5% in the quoted stresses; the actual errors in the load cell outputs are, of course, appreciably lower ($\pm$ 2%).

All cyclic mechanical data are plotted as the variation of normalised maximum stress amplitude per cycle with the number of cycles to normalise the stress; the stabilized stress amplitude usually achieved after 2-5 cycles is used as the reference level. The problems of setting such levels in materials exhibiting discontinuous yielding will be discussed in Chapter 5.

4.2.1 Series QA (γ)

The cyclic stress response of specimens quenched from the austenite field and aged five days at 60°C or five hours at 240°C is compared in Figure 2. The degree of softening, and the duration of the approach to saturation is reasonably reproducible after ageing at 240°C, as shown in Figure 3. Ageing at 60°C enhanced the life, and did not produce any significant hardening or softening up to failure. Typical mechanical properties of each material in tension are given in Table 3.

4.2.2. Series QA ($\gamma + \alpha$)

Quenching from close to the $(\gamma + \alpha) \rightarrow \alpha$ completion temperature and ageing five hours at 240°C permits fatigue softening of a comparable degree and duration to series QA (γ) 240, as shown in Figure 4. In general the life was of the order of 5×10^4 cycles.

Specimens of this series were also fatigued to approximately 70% of the life to establish the saturation condition, then overstrained in tension. The monotonic response in overstrain is compared with the response of the virgin material in Figure 5. It can be clearly seen that a decrease in the initial rate of work hardening characterizes the fatigued state.

To detect the effect of a carbide dispersion, a comparison was made with furnace cooled Armco iron. The fatigue life of a specimen austenitized two hours at 850°C and furnace cooled was determined at the total strain amplitude used. Specimens were then fatigued to 70% of this

life, corresponding again to saturation, and overstrained. Again, an initially low work-hardening rate is apparent (Figure 6) as a characteristic of the bulk material after fatigue.

Ageing five days at 60°C produced a fairly coarsely dispersed distribution of particles (see section 4.3.2) which was less reproducible than, and of an insufficiently different scale to distributions produced at 240°C. Specimens were therefore fatigue tested after ageing at room temperature for one month, to produce fine dispersions of particles. In Figure 7, such materials can be seen to exhibit only marginal softening, and to give lives up to 7×10^5 cycles. A specimen aged only three days at 60°C gives a slightly coarser dispersion than at room temperature, and responds similarly to a specimen aged one month at room temperature, then three days at 60°C, which gives a coarser particle size but retains a fairly small particle spacing. Both specimens with slightly coarsened distributions relative to QA ($\alpha + \gamma$)25 specimens resist fatigue up to 10^6 cycles, and soften very little (Figure 8).

The tensile properties of these distributions are given in Table 3. An overstrain curve from series QA ($\alpha + \gamma$) 25 is compared with the original tensile curve in Figure 9. The rate of initial work-hardening is diminished after fatigue to 50% of the life.

4.2.3 Series QSA

If a specimen is quenched from austenite at 850°C, swaged to develop a cell structure and subsequently aged, the cold-worked structure, which has little residual work-hardening capacity (Figure 10) may be pinned by the precipitate, and the onset of cyclic softening is retarded. This result of the thermal mechanical treatment is seen in Figure 11 to be more effective after ageing at 60°C for five days than at 240°C for five hours. Once softening is established, however, its extent is great and the saturation state is rapidly approached. The lives obtainable by such treatments do

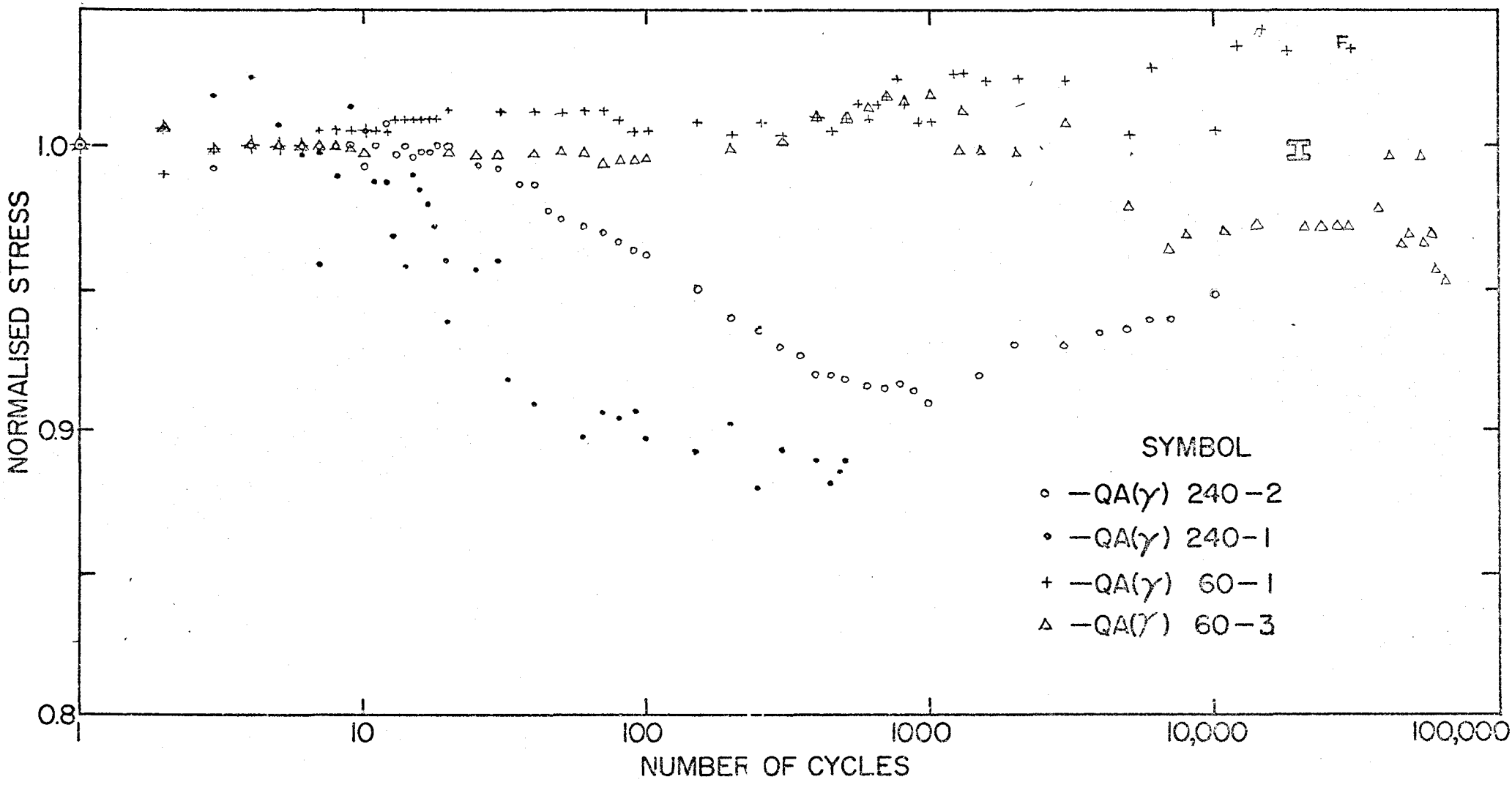

Figure 2. Cyclic stress curves for series QA (γ).

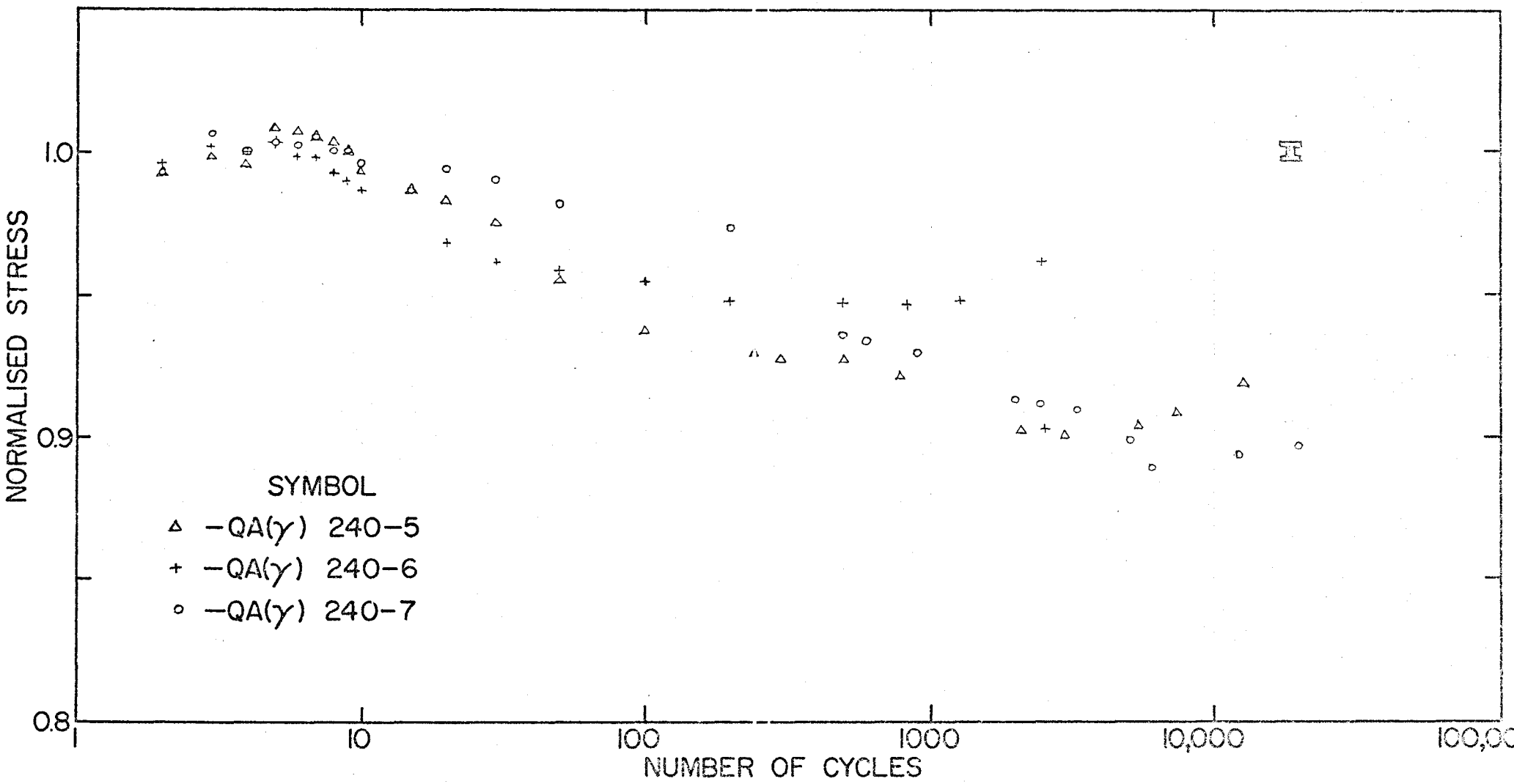

Figure 3. Cyclic stress curves for series QA (γ) 240.

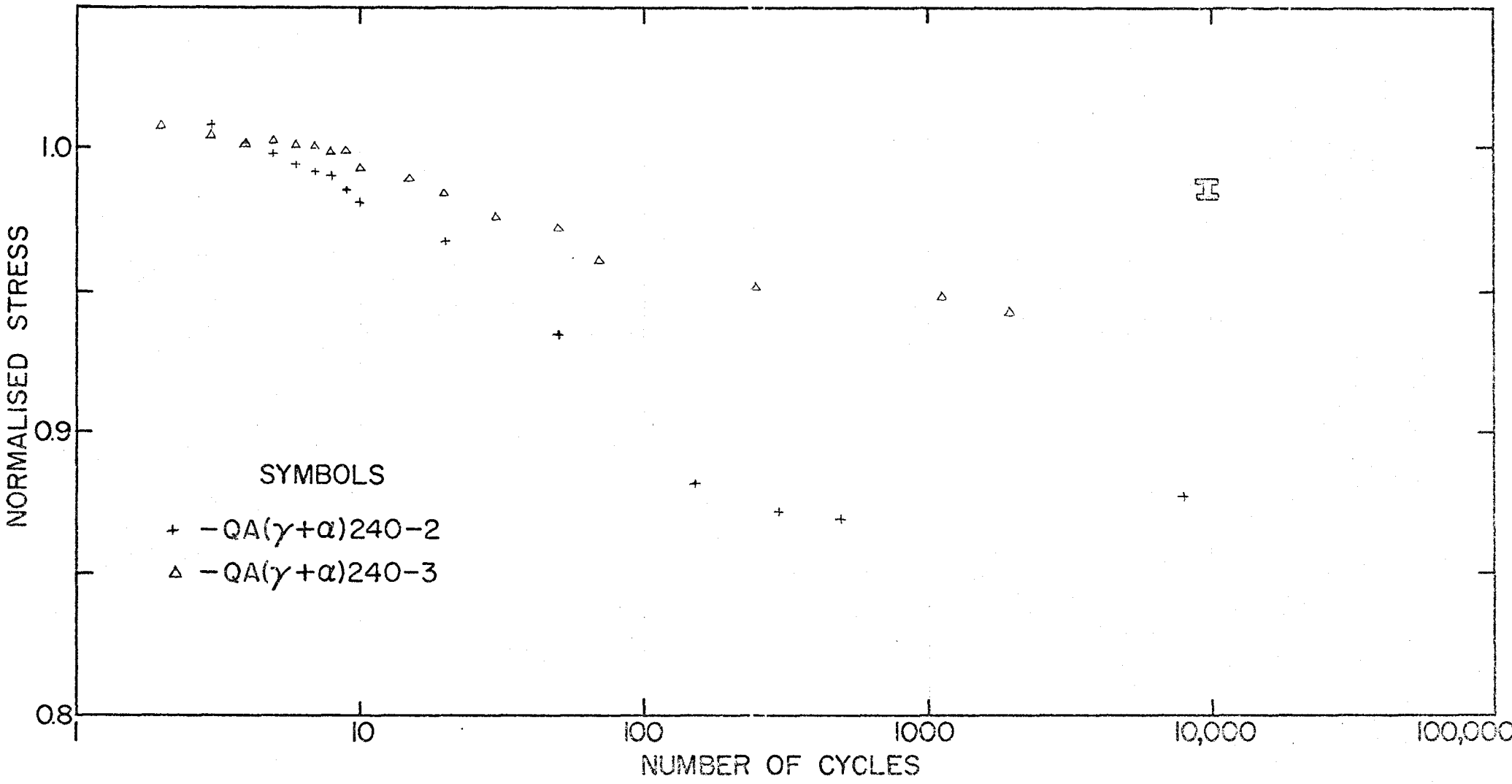

Figure 4. Cycle stress curves for series QA (γ + α) 240.

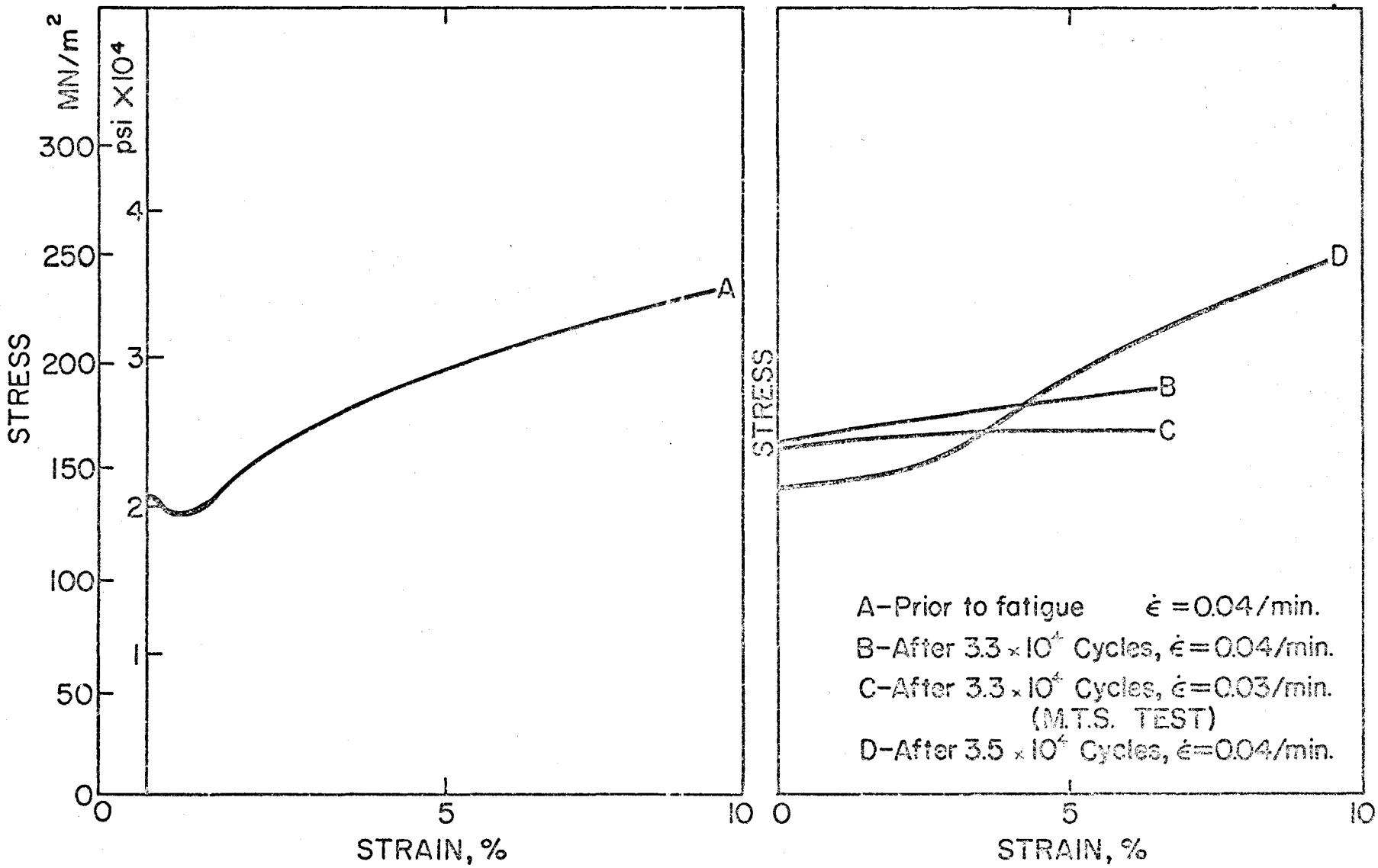

Figure 5. Overstrain of series QA ($\gamma + \alpha$) 240.

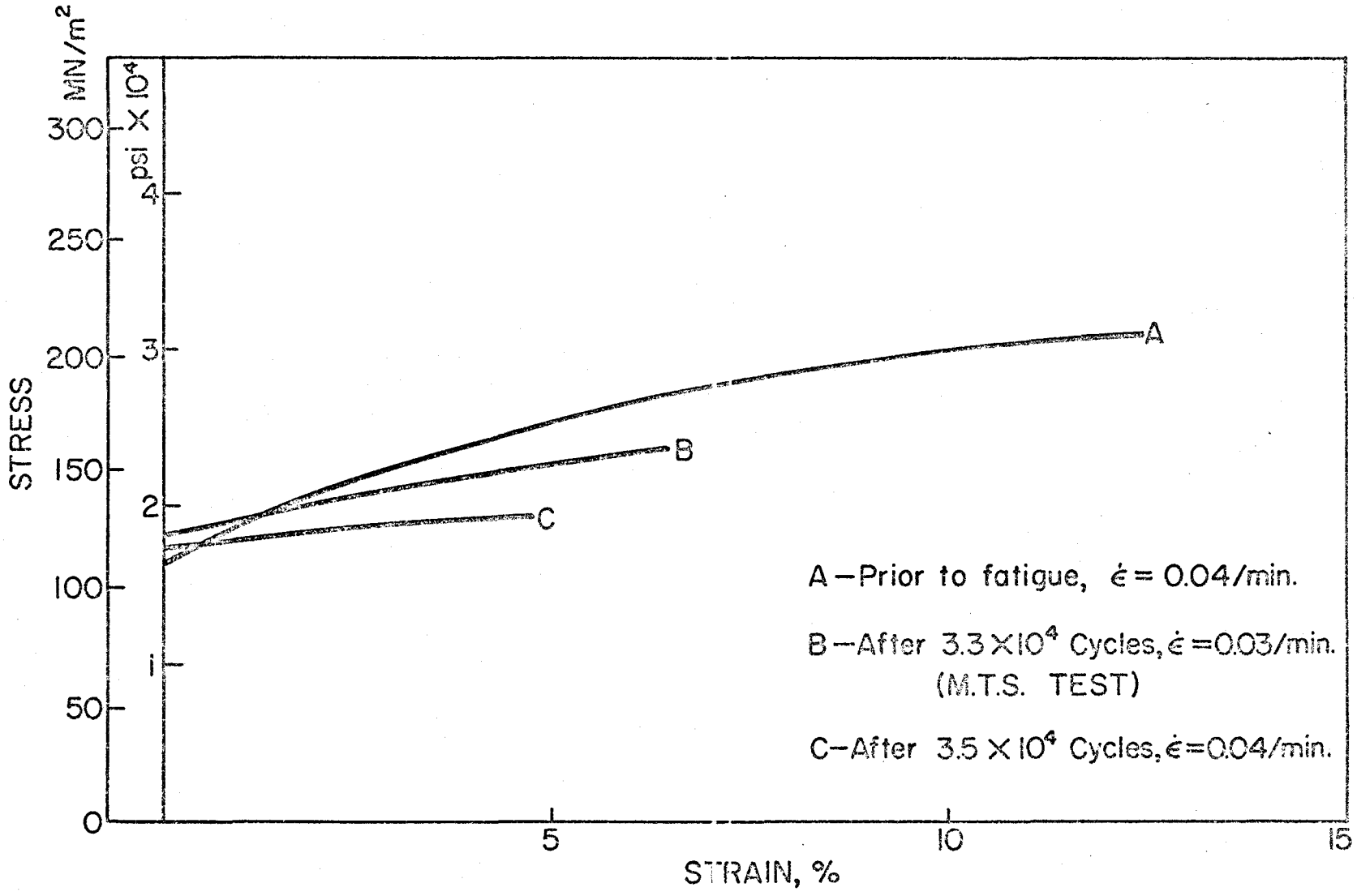

Figure 6. Overstrain of furnace cooled iron.

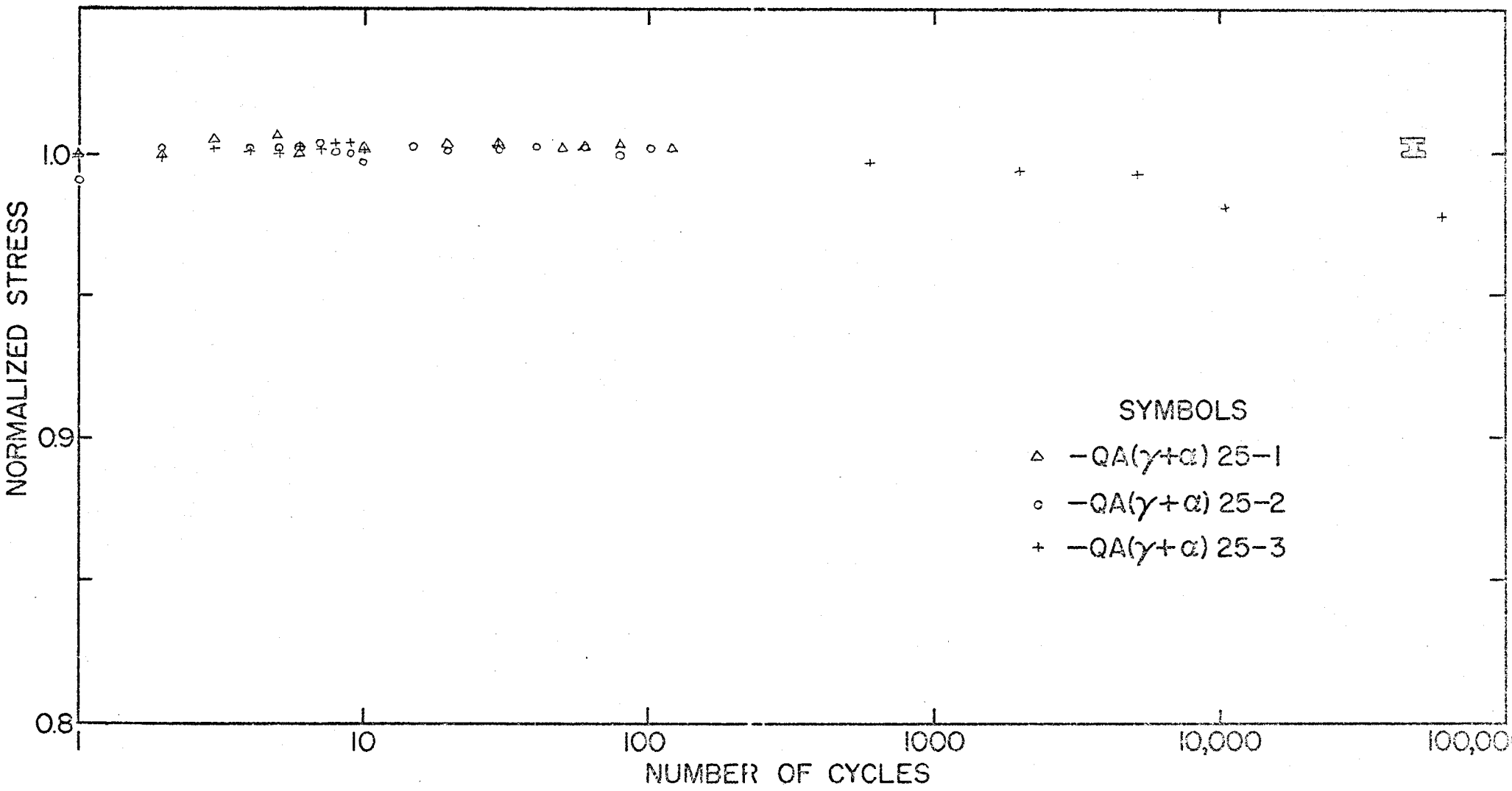

Figure 7. Cyclic stress curves for series QA (γ +α) 25.

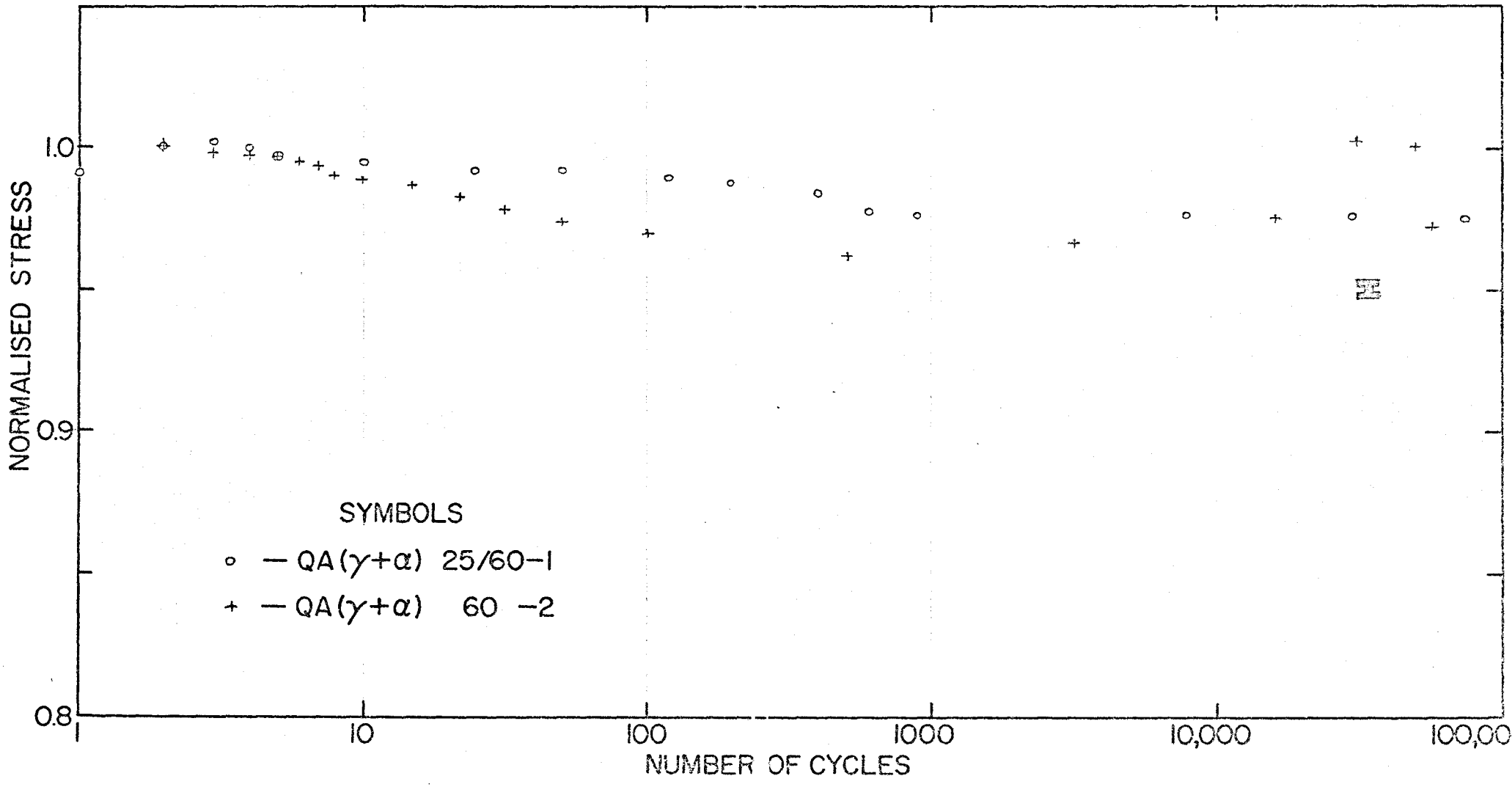

Figure 8. Cyclic stress curves for Series QA (γ+α) 60 and QA (γ+α) 25/60.

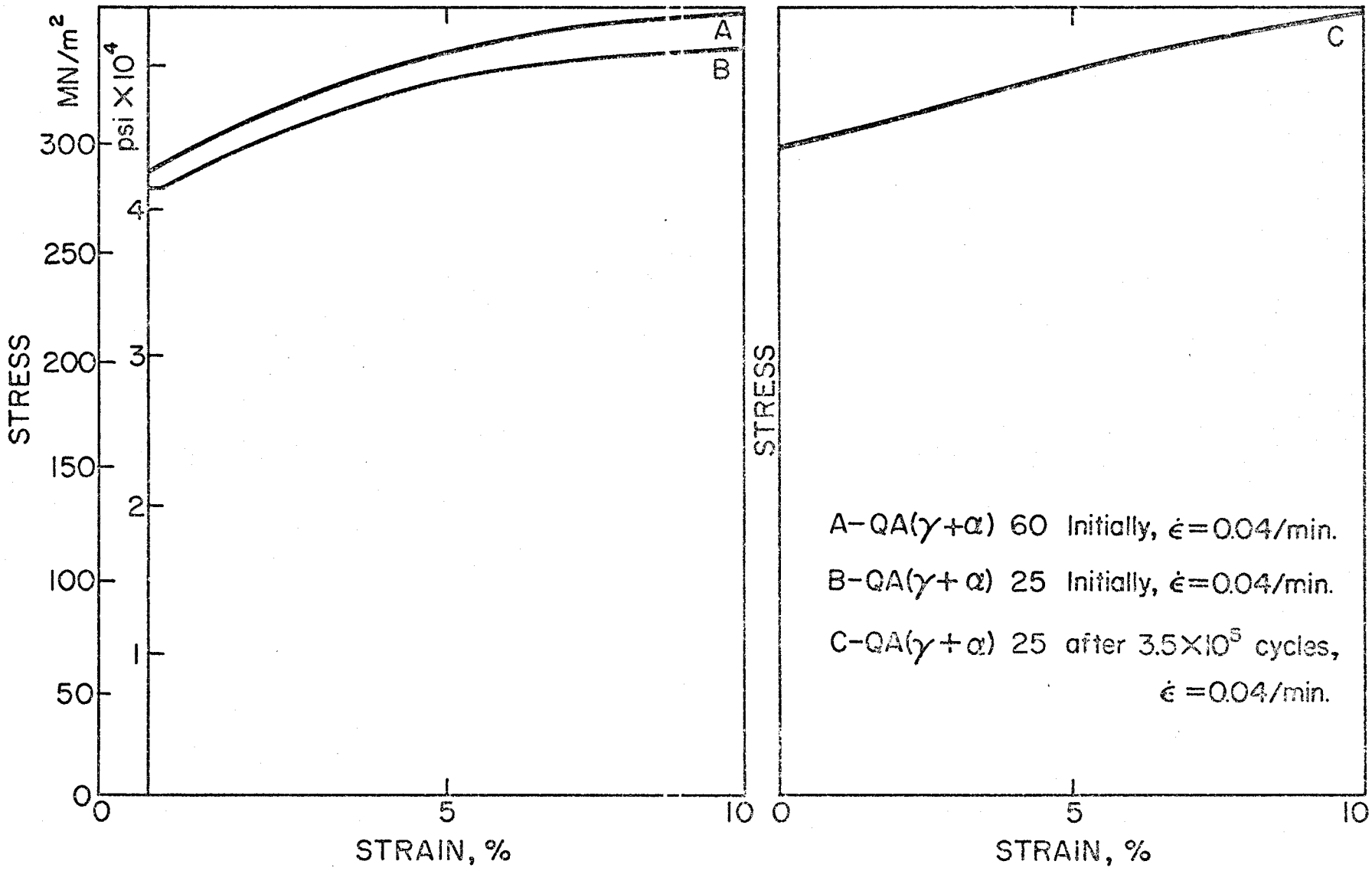

Figure 9. Overstrain of fine dispersions.

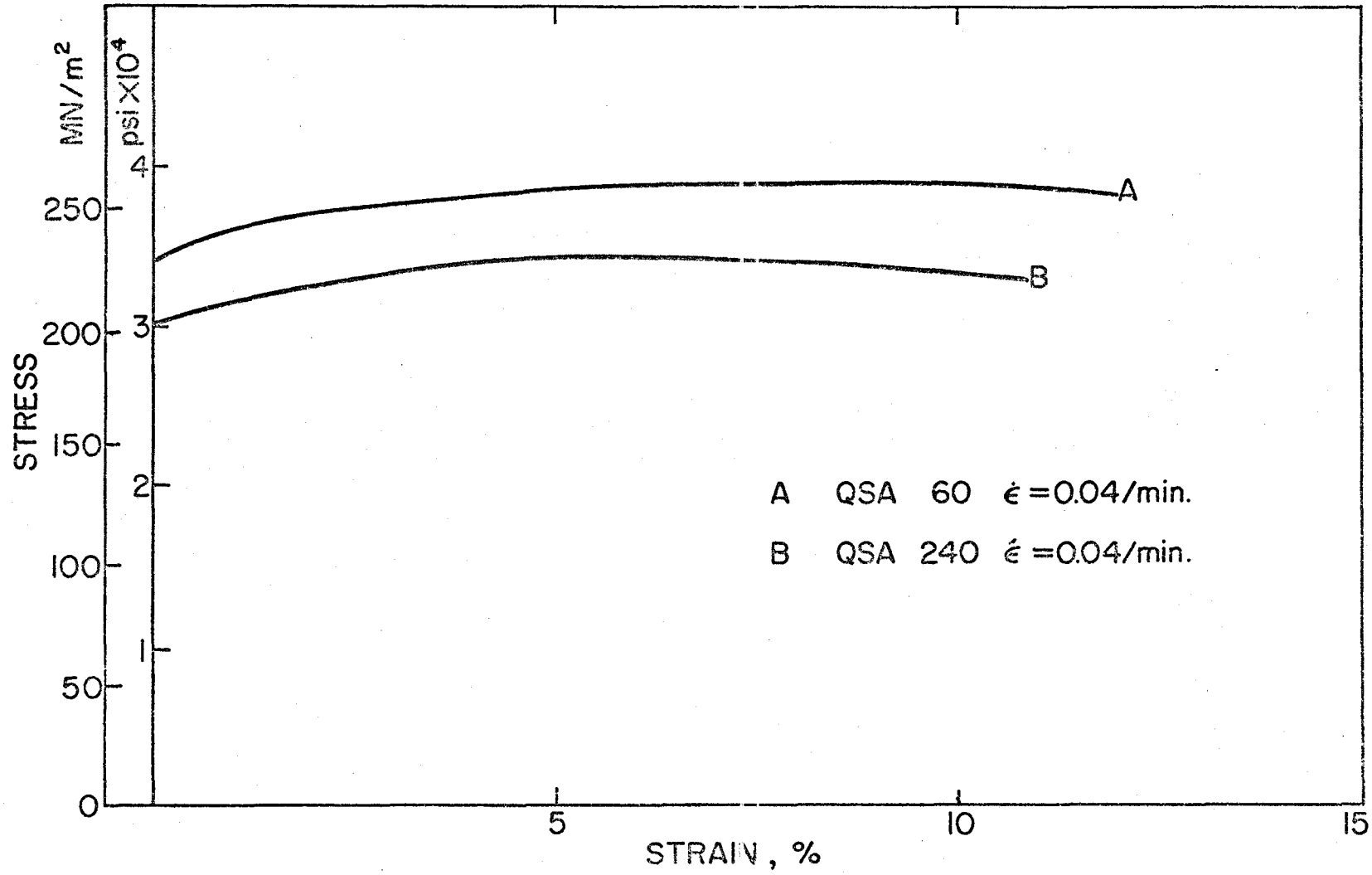

Figure 10. Initial series QSA curves.

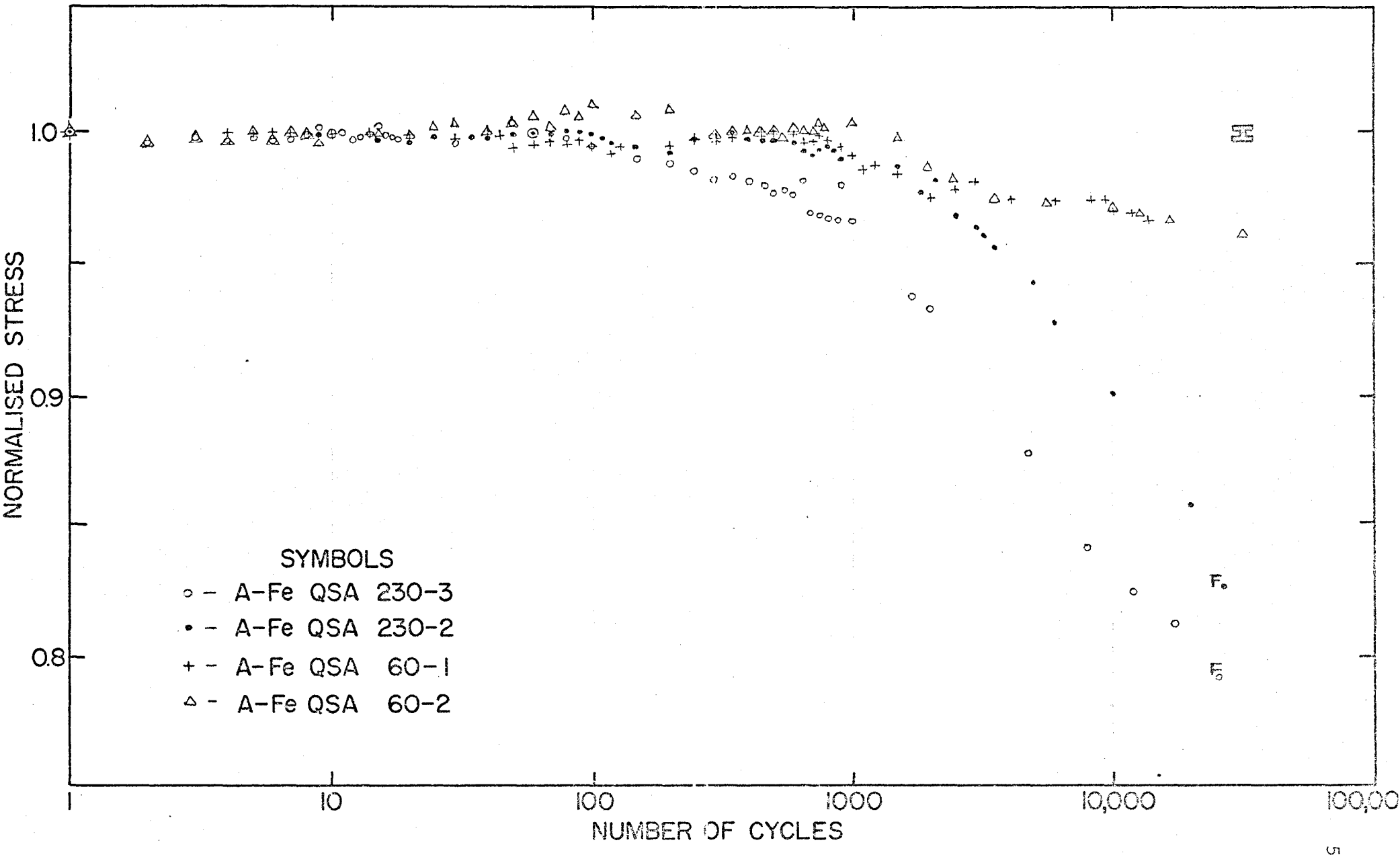

Figure 11. Cyclic stress curves for series QSA.

TABLE 3

MECHANICAL PROPERTIES

(a) Monotonic

Experiment	Yield Point MN/m^2	Luders Strain	U.T.S. MN/m^2	Total Elongation %
QA (γ) 60	217	0.0015	287	40.5
	200	0.002	223	44.1
	233	0.003	345	39.9
QA (γ) 240	129_L	0.01	268	52.6
QA ($\gamma + \alpha$)60	286	0.0016	342	33.4
QA ($\gamma + \alpha$)25	296	0.001	-	-
QA ($\gamma + \alpha$)240	143_U 132_L	0.007	248	53.6
	159_L	0.008	199	-
F.C.	123	None	210	56.0
QSA 60	238	None	290	30.4
QSA 240	217	None	244	31.4

N.B. To convert p.s.i. to SI units multiply by 6.8948×10^3. Units quoted in millions of newtons per square metre.

(b) Cyclic

Experiment		Semi-amplitude of Stress MN/m^2		Softening (-) or Hardening (+) Range	
		Initial Stabilised	Saturation	Cycles	Stress MN/m^2
QA(γ) 60	1	262	283	2.7×10^4	+ 21
	3	269	250	6×10^4	- 19
	6	181	167	6.5×10^4	- 16
QA(γ) 240	1	170	152	10 - 1000	- 18
	2	169	155	20 - 700	- 14
	4	198	156	10 - 10^4	- 22
	5	193	155	10 - 10^4	- 18
	6	232	219	8 - 700	- 13
	7	250	225	8 - 2500	- 25
QA ($\gamma+\alpha$)60	2	224	220	2.4×10^5	- 6
QA ($\gamma+\alpha$)25/60	1	248	238	1.06×10^6	- 10
QA ($\gamma+\alpha$)25	1	302	302		None
	2	285	285		None
	3	269	264	6.5×10^5	- 4
QA($\gamma+\alpha$)240	1	223	231	400 - 5×10^4	+ 8
	2	198	170	6 - 900	- 28
	3	200	187	8 - 1200	- 13
QSA 60	1	240	228	1.2×10^5	- 12
	2	192	178	0.9×10^5	- 14

(b) Cyclic (Cont'd.)

QSA 240	2	224	178	4×10^4	- 48
	3	221	166	4.6×10^4	- 55

not compare favourably with lives obtainable in fine dispersions of particles.

4.3 Electron Microscopy

Photomicrographs obtained by T. E. M. of thin foils are illustrated in plates one to nine. The fields shown are numbered from left to right, top to bottom, and are described in sequence.

4.3.1 Series QA (γ)

Quenching from austenite and ageing at 240°C for five hours, produced a distribution of carbide particles of generally acicular aspect, precipitated on habit planes deduced from their traces in electron diffraction analysis to be $\{110\}$. Electron diffraction patterns were obtainable from the particles but cross-grating patterns which could definitely by analysed to determine the structure of the precipitate could not be obtained. The burden of the literature suggests that under the conditions of ageing used these precipitates should be cementite (see for example Wells and Butler (1966)),or the excellent review of Kelly and Nicholson (1963)). It was difficult to characterize the distribution by numerical measurement of the size or spacing of the particles; the heterogeneity of any distribution produced by quenching and ageing is a consequence of varying local conditions throughout the bulk specimen,and was manifested principally by regions of the crystal containing relatively few precipitates in these specimens; in regions with reasonable densities of precipitates such as illustration 1 of Plate 1, a spacing in the range 1 - 3 μm. with a mean of about 1.5 μm. is typical. The needle size is of the order of 0.5 μm; an appreciable transformation-induced dislocation substructure was present, forming a semi-continuous network linking the particles in regions of uniform density, with fairly extensive tangles of dislocations around particles being present on occasion.

After fatiguing a specimen to the onset of saturation, approximately 10^3 cycles, an irregular cell structure was observed. Field 2 of Plate 1 shows a detail of such a structure. A steeply inclined boundary appears to have formed on a plane containing precipitate particles; the oblique boundaries are not associated with precipitates, nor is their structure very regular. The density of dislocations within the confines of each cell is already very low, however. Fine defects, which could be dislocation loops, and dislocation dipoles, are apparent in the wall structure.

The presence of the transformation induced substructure complicated an understanding of the development of the saturation state and its relation to the particle distribution; although precipitation may then occur on dislocations, no modification was detected in this b.c.c. material comparable to the elimination of one of the three habit planes of θ' precipitates formed in Al-Cu alloys with helical dislocation substructures, as shown by Nicholson (1962). Further study of the saturation substructure was therefore reserved for specimens quenched after slow cooling through the austenite-ferrite transformation range.

Interpretative problems are similarly posed for specimens quenched from austenite and aged five days at 60°C. The aged structure was very inhomogeneous, possessing a considerable quenched-in substructure and evidently precipitated extensively along dislocation lines to form the quasi-regular networks shown in Fields 3 and 4 of Plate 1. The statistically reliable description of such a structure is very difficult to achieve; attempts were made to estimate the distribution of particle sizes using the method of Cahn and Fullman (1956) to calculate the volume fraction distribution from lineal data, making the assumption that the particles precipitate generally as oblate spheroids.

As no identifiable electron diffraction patterns could be obtained the precipitate could not be classified with any certainty. The work of Hale and McClean (1963) showed that metastable ϵ-carbide can precipitate

5 μm

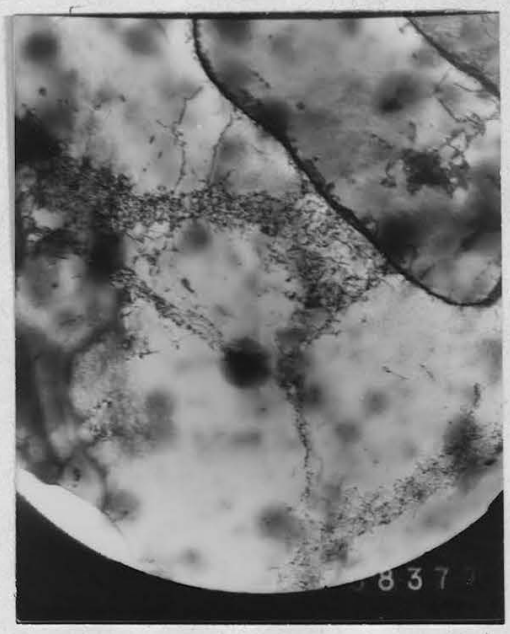

0.5 μm

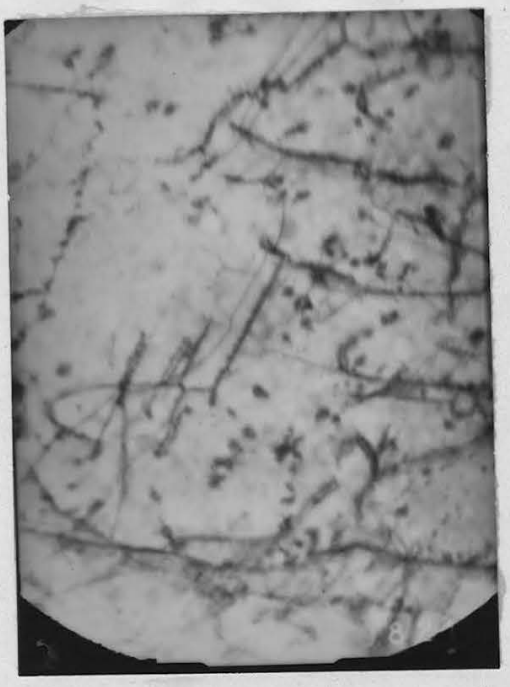

0.5 μm

2 μm

PLATE 1

dendritically as platelets with $\{100\}$ habit planes to form a three-dimensional array with an axial dislocation nucleus. The contrast conditions arising at such a structure vary with tilting of the specimen in such a way as to distort the apparent morphology; for example peripheral contrast in some operating reflexions, possibly arising from solute gradients around particles, masks the true dimensions of the individual platelets. It was quite different therefore to assign intercept limits in a random manner when analysing the overall distribution at low magnification, for off-contrast conditions at local orientation or thickness changes distorted the apparent image size. Only at high magnifications in foils oriented so that the electron beam lay in the habit plane of the particle, could the platelets thickness be seen to be ~ 100Å, and the habit plane $\{100\}$. It is possible therefore that a proportion of the precipitate in these distributions is cementite, rather than metastable ϵ-carbide. The distribution function derived is shown in Figure 14. The dendrite spacing is in the range 0.2 - 1.0 μm with a mean of about 0.4 μm; the dendrite size is typically 0.7 μm long, with platelets of 0.2 μm radius. Few particles not associated with dislocations were observed.

After fatiguing 3×10^4 cycles, no significant changes were observed in foils taken from the specimen. By 6.5×10^4 cycles, however, certain changes had occurred; in Field 1 of Plate 2, taken with the electron beam approximately parallel to $\langle 100 \rangle$ so that background ϵ-carbide platelets are in the plane of the foil, many extensive dendritic structures are observable. No identifiable diffraction patterns could be obtained from these features; Field 2 shows a detail in which a composite of carbide platelets precipitated on a forest dislocation axis is associated with dislocation loops and other configurations. The size of such a feature (> 2 μm long and 1 μm wide) distinguishes it from coarsened carbide dendrites, but there is cause for circumspection in interpreting these

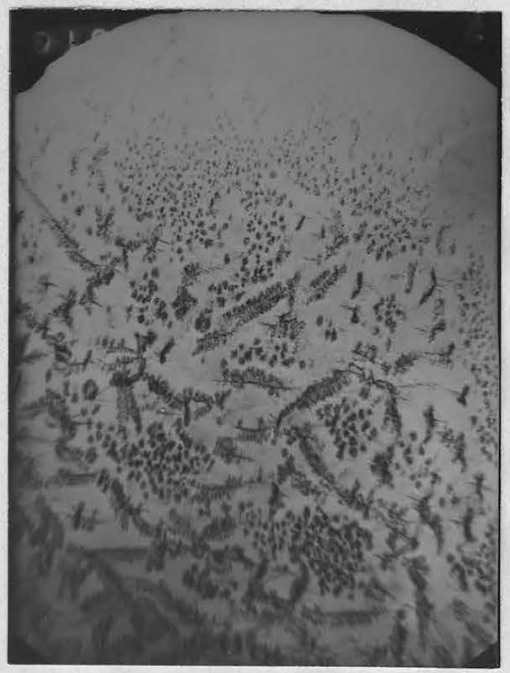

2 μm

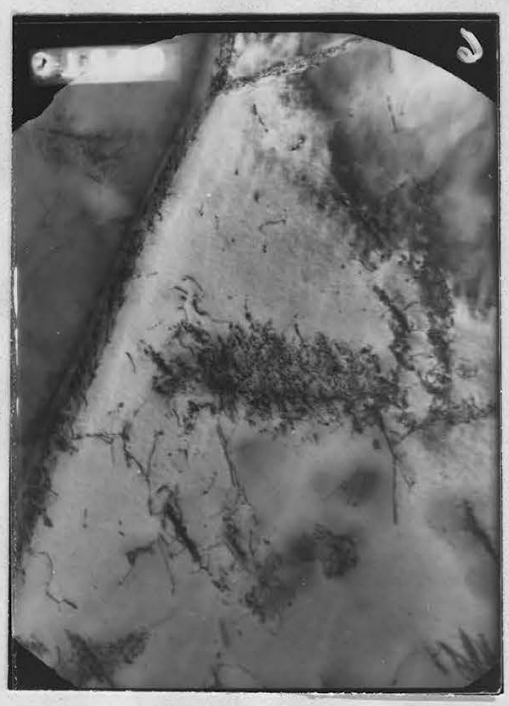

0.3 μm

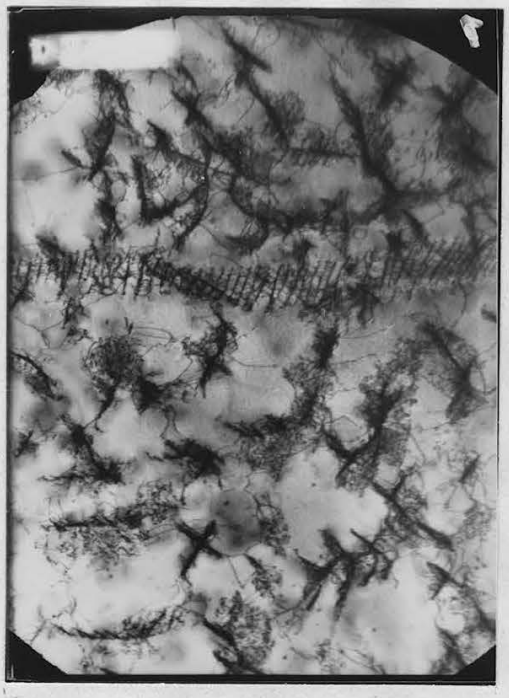

1 μm

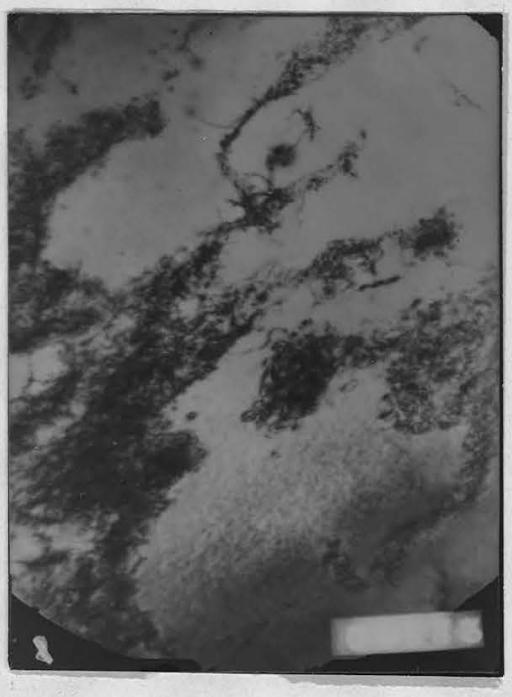

0.5 μm

PLATE 2

structures. The work of Hale and McClean (1963) again shows that precipitation during ageing may occur at more complex substructural arrays such as networks or sub-boundaries formed during transformation; the resulting structures may be very complex. Furthermore, the rig temperature (35°C), and the specimen demounting procedure in this case, both allowed overageing to occur to a limited degree, and so it is not possible to determine if any ageing process enhanced per se by fatigue deformation has occurred. The most reliable observations of the general change accompanying fatigue are shown in Field 3 and clearly illustrate that the formation and development of tangles of dislocation loops thrown around carbide particles, forming a continuous network, accompanied by the production of fine loops resolvable in the low-density enclaves, is the salient feature. There is no evidence that particles are sheared by dislocations.

The specimen from which illustration 4 was taken fractured at 2.25×10^5 cycles. The structure now consists predominantly of large complex tangles. Particle contrast is obscured and the details of the substructure are irresolvable. From a careful examination of many fields of the specimen the scale of this substructure appears to depend strongly on the local original distribution of particles. This is illustrated by the low magnification Field 1 of Plate 3 which is taken slightly off-contrast, and should be compared with the results of McGrath and Bratina (1967, Fig. 7), who attributed the change of scale to a particle shearing process, rather than the accumulation of dislocations around particles. Both from the measured scale of the distribution of tangles and the detailed observations of the tangles, for example in Field 2, where the tangle is 3 μm. long it is quite apparent that particles are not sheared in these materials. A cell structure was never observed to form at the strain amplitude used, but dislocation loop densities appeared to increase throughout the fatigue process.

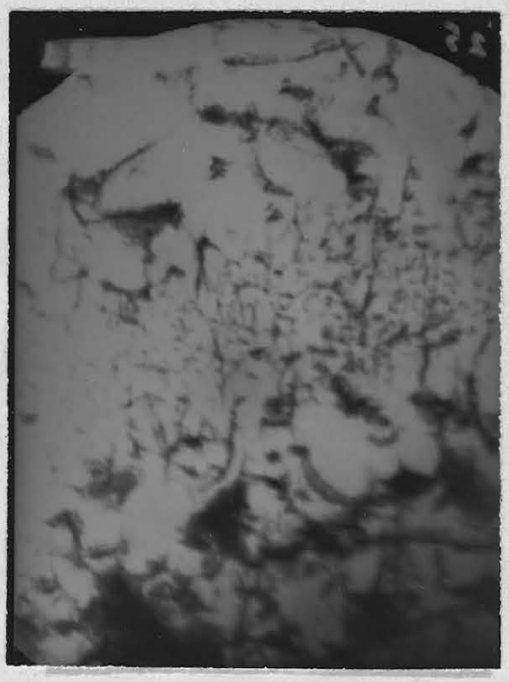

1 μm

1 μm

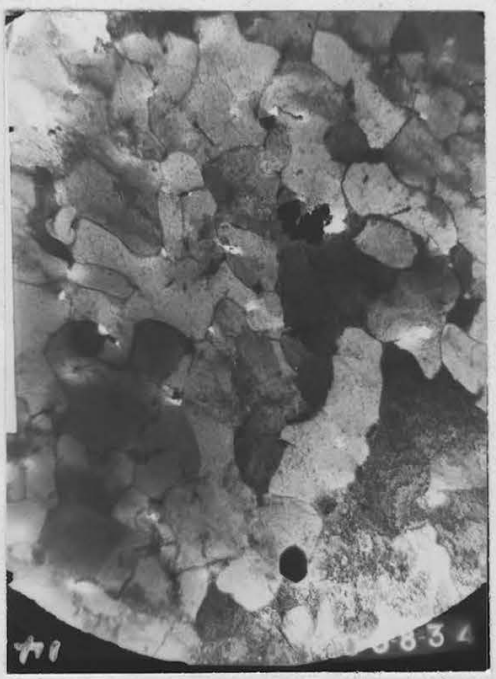

1 μm

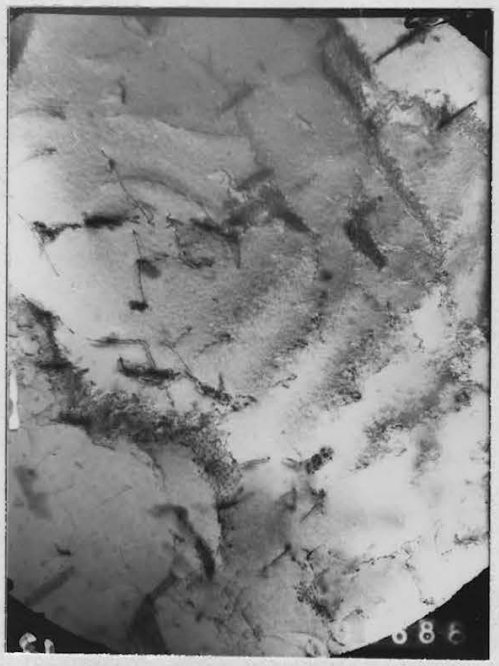

1 μm

PLATE 3

The fields observed in foils from the specimen fatigued 6.5×10^4 cycles were used to derive the distribution function for particles after fatigue. The attendant difficulties were enhanced by the increased substructure, but the resultant distribution is compared with the original distribution, in Figure 14 . The expected volume fraction, calculated from the equilibrium diagram, was approximately 3×10^{-3}, for the equilibrium Fe_3C phase.

4.3.2 Series QA ($\gamma + \alpha$)

The particle distribution formed on ageing five hours at 240°C after slowly cooling through the austenite-ferrite transformation, and quenching from 725°C was very similar to the QA (γ) 240 distribution; the amount of transformation substructure was very much decreased, however and the distribution correspondingly more uniform. Particles were still associated with a forest structure, but the average spacing was slightly larger ($\sim 1.6 \mu m$). Particle sizes were comparable.

At saturation, a cell structure had developed whose scale was similar to that of the QA (γ) 240 series being in the range 0.8 - 1.9 μm with a mean of about 1.5 μm, the detailed configuration being controlled substantially by the carbide distribution. This is shown clearly by Field 3 of Plate 3. The pinning of dislocations in the sub-boundaries by carbide particles is shown in Field 4; details of such cell walls are generally difficult to resolve in this material, but in Field 4 two sets of parallel dislocations forming a network can be seen.

Although it was not possible to carry out Burgers vector determination on the cell wall components, other measurements were obtained. Using foils of different orientations, the plane of the cell wall was determined by stereographic projection of the traces of walls intersecting reciprocal lattice sections, to establish the pole of a suitable habit plane. Since the

cell geometry is often dependent on the particle geometry, and may also be strongly dependent on the segregated solute concentration, certain simplifications in indexing the traces were made so that only low index directions were analysed. The results are displayed in Figure 12; the cell walls appear to be more frequently on $\{112\}$ slip planes than $\{110\}$ planes in the foils considered.

Further, the misorientations acorss various types of cell boundary were measured using shifts in the Kikuchi line patterns obtained from thicker regions of the foil (Hirsch et al. (1965)). These misorientations were generally small; in Figure 13, a field including seven cells was examined in detail. The misorientations are quoted as rotations, about low-index axes comprising the major component of the displacement of the pattern; their magnitude is typically one-tenth to one-half of a degree. It is interesting to note from Figure 13 that the misorientations as measured are self-cancelling over distances of the order of 5 μm, corresponding to four cell diameters.

In plate 4, Fields 1 and 2, the effect of overstraining the saturation cell structure by $\epsilon = 0.01$ in tension is displayed for the QA $(\gamma + \alpha')$ 240 material fatigued 3.3×10^4 cycles. In an attempt to pin the structure in the stress-applied state after overstraining, in a manner similar to the irradiation pinning technique used by Mughrabi (1968) the specimen was aged under stress at 130°C for three hours; the amount of stress relaxation observed was not greater than 15% indicating that no significant recovery of the structure occurred. Michalak and Paxton (1961) analysed similar recovery of the flow stress and found significant recovery to occur after comparable times only above 300°C. The micrographs indicate that sufficient carbon was available still in solution to produce a fine precipitate. The overstrained structure therefore appears in the stress-applied state; the effectiveness of particles in retaining the cell structure during overstrain is clearly limited by their spacing. In Field 1 segments of dislocation line

Recip. Latt. Section	Prominent Trace Normals	No. of Fields
100	⟨110⟩ ⟨310⟩ ⟨200⟩	4
120	⟨123⟩ ⟨112⟩ ⟨200⟩⟨210⟩	2
110	⟨112⟩ ⟨111⟩ ⟨110⟩	1

KEY

1	⟨110⟩	IN (100)	7	⟨123⟩	IN(120)
2	⟨310⟩		8	⟨112⟩	
3	⟨200⟩		9	⟨200⟩	
4	⟨112⟩	IN (110)	10	⟨210⟩	
5	⟨111⟩				
6	⟨110⟩				

o 112 TYPE

× 123 TYPE

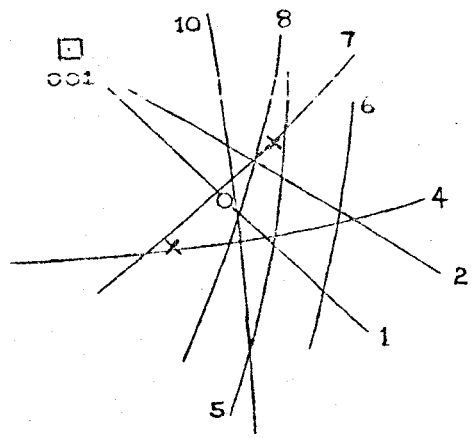

FIG. 12. TRACE ANALYSIS OF CELL BOUNDARIES IN SERIES QA(δ+∝)240

BOUNDARY	TRACE OF KIKUCHI SHIFT	ROTATIONAL MISORIENTATION RADIANS ($\times 10^{-2}$)
1-2	[002]	1.92
2-3		0.38
1-3		1.79
1-4		0.38
3-4		2.05
4-5		0.51
5-6		0.26
4-6		0.13
6-7		0.26
1-7		0.26
4-7		1.94
2-7		0.38
1-2	$[2\bar{1}3]$	0.29
2-3		0.29
1-3		0.15
1-4		0.45
3-4		0.45
4-5		0.95
5-6		0.63
4-6		1.50

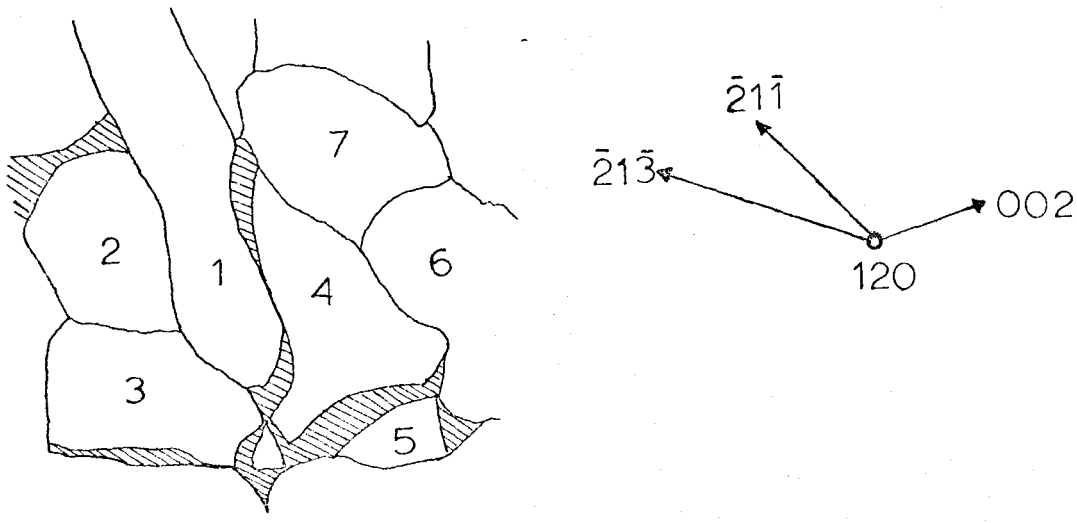

FIG. 13. KIKUCHI LINE ANALYSIS

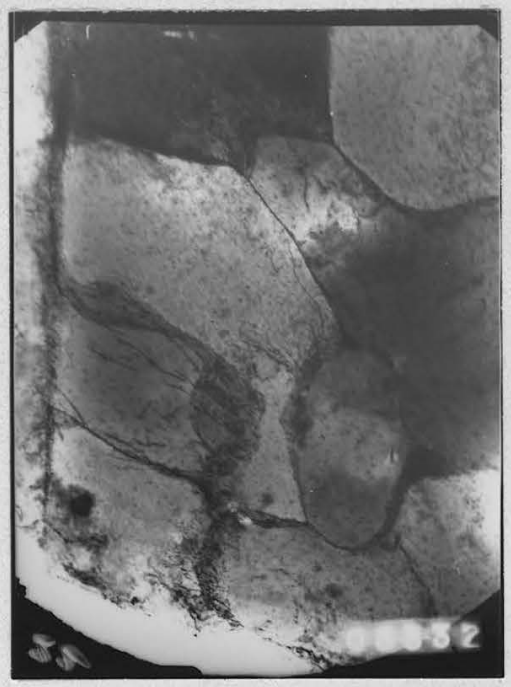

1 μm

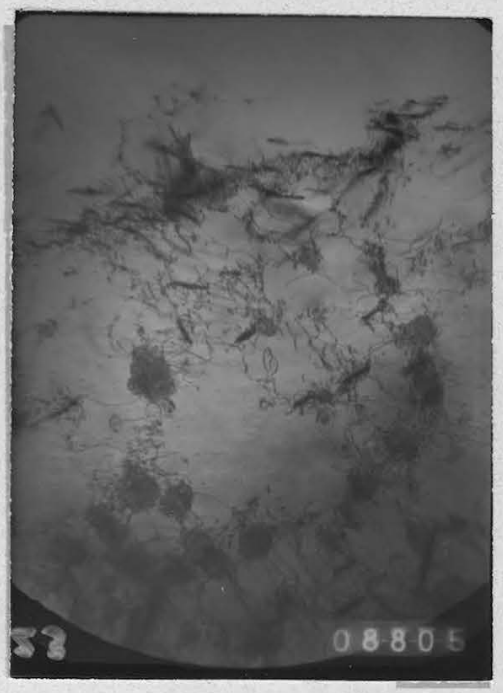

1 μm

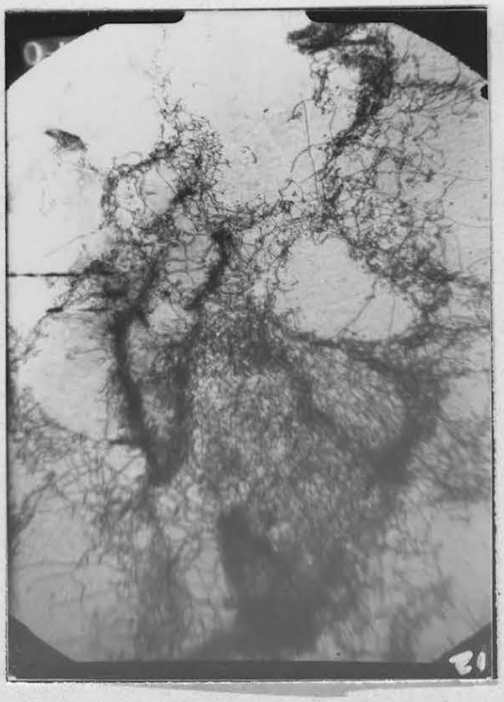

1 μm

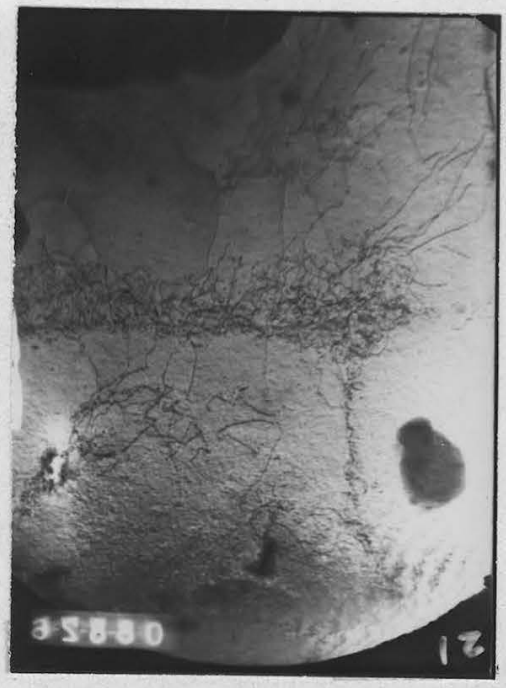

1 μm

PLATE 4

have bowed out in the slip plane to accommodate the applied overstrain; where the number of particles is sparse large segments of the cell walls are destroyed by overstrain. Around carbide particles dislocation tangles are retained, much as they are accumulated prior to saturation, in a random configuration. This can be seen in Field 2. The breakdown of the structure is confirmed by observations in overstrained but unpinned specimens; the cell structure is locally destroyed but the detailed nature of the breakdown, the bowing out of dislocations from pinning points in the wall, cannot be clearly seen in the relaxed state.

The breakdown of the substructure in overstrain was more clearly seen in a furnace cooled specimen, austenitized two hours at 850°C. Sufficient carbon is apparently available to pin the structure in the stress applied state however, and Field 3 shows that the cell structure is not very resistant to small overstrains; the original cell structure is apparent but the constituent wall networks are disturbed. Much of the wall debris of loops and dipoles is visible in the breakdown structure of Field 4.

In plate 5, Field 1, a typical distribution formed by ageing five days at 60°C after quenching from 725°C subsequent to slow cooling from 850°C, is shown. The size and spacing of the particles was insufficiently different from the (cementite) distributions produced at 240°C for the purposes of this investigation. The contrast effects observed at these particles and the traces of their habit planes correlates closely with observations of ϵ - carbide made by several investigations (see Kelly and Nicholson (loc. cit.)). Distributions after ageing at 25°C for one month consist of very much finer particles, visible only by strain-field contrast at higher magnifications; the precipitates can be resolved as platelets in suitable reflexions at high magnifications. The platelet diameter is 400Å and the thickness much less than 100Å, compared to platelets of up to 0.5 μm in diameter after ageing at 60°C; no interface interference fringe contrast

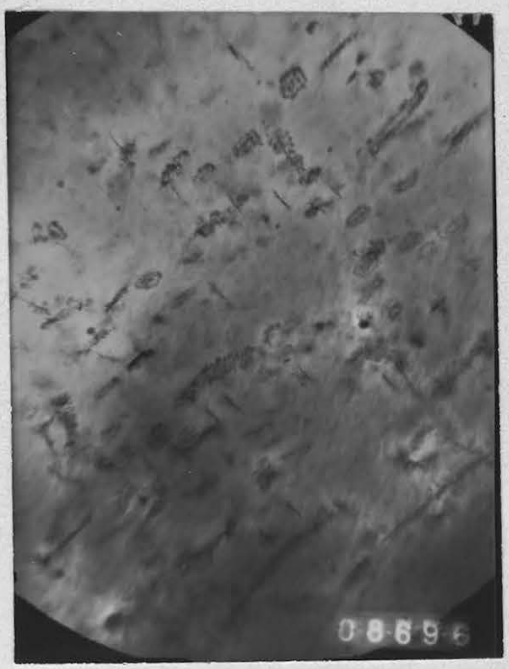

2 μm

0.5 μm

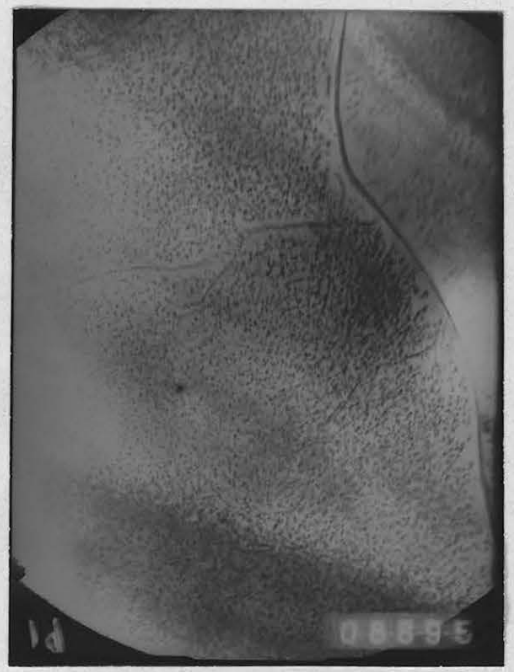

2 μm

2 μm

PLATE 5

can be obtained, but displacements in the line of no contrast across extinction contours in the foil are observable. The strain-field contrast was not analysed in detail, for example with respect to the position of the particle in the foil thickness, as the tilting angles on the Siemens microscope are limited. The true thickness of the particles is therefore undetermined. The particle spacing is slightly larger than the particle size, being typically 500Å.

Such distributions are very resistant to fatigue. Illustration 3 was taken after 1.1×10^6 cycles, and apart from isolated simple sub-boundaries, which may form during transformation, as they possess denuded zones, the substructure is restricted to very fine scale networks of dislocations linking particles, visible only at higher magnifications.

The paucity of observed slip activity led to the design of three experiments to determine the details of substructural development in fine dispersions during fatigue, and to obtain correlation with some of the observations present in the literature. In the first of these experiments a specimen aged at 25°C was subsequently aged for three days at 60°C; this treatment coarsened the precipitate size to about 600Å and generally increases the spacing to about 800-1000Å. After 10^6 cycles a recognisable fatigue sub-structure can be generated. Field 4 of Plate 5 shows a simple geometrical cell structure based on H-junctions. The network of dislocations connecting matrix particles is better defined in Plate 6; here the sub-boundaries have simple structures consisting of sets of parallel dislocations. The misorientations across these walls, indicated by changes in contrast conditions across the foil, do not appear to be large. Plate 6 was taken in an $01\bar{1}$ operating reflexion; since the set of dislocations in best contrast in the walls is also visible in a $\bar{1}12$ reflexion, then a consistent scheme would give a Burgers vector of $a/2\ [111]$ to the set. A second set, perpendicular to the first, and almost invisible in $01\bar{1}$, is best resolved in 130 reflexions of the same scheme, whence the Burgers vector would be

PLATE 6

$a/2\ [\bar{1}11]$. This determination is not unambiguous however, but the assigned Burgers vectors correspond to a screw dislocation network.

The second experiment was designed to generate larger scale features such as those described by McGrath and Bratina (loc. cit.) and Wilson and Tromans (1970) as channels of localized slip. Such observations have been made principally in reversed bending tests, in which gradients of strain amplitude are maintained. To duplicate this condition a specimen aged at $25^{o}C$ for one month was fatigued to 30% of the life (3×10^{5} cycles) in an attempt to suitably increase the mobile dislocation density, notched circumferentially at its mid-section in situ, and fatigued to fracture, which occurred at 7×10^{5} cycles compared with 10^{6} cycles in the un-notched specimen. In plate 7, micrographs of foils prepared by single-sided polishing of samples cut directly below the fracture surface are displayed. In the presence of the gradient of strain produced between the stress concentration at the crack tip and the bulk of the specimen, slip activity has apparently localised into channels, the traces of which correspond to a $\{110\}$ slip plane in the case of Field 1. The interior of the channel is out of contrast but it does contain dislocations; the peripheral contrast is remeniscent of carbide precipitation at a boundary, but no discernable electron diffraction patterns could be identified, nor could misorientations be measured; resolution of the tangled dislocations at the boundary was not possible, similarly, because the quality of foils prepared close to the fracture surface is necessarily inferior to those prepared from the bulk. Other important observations were made, however. In several regions considerable alignment of dislocations into parallel arrays frequently piled up against an inclusion were seen. At what is possibly a later, but still embrionic stage of channelling of slip, dislocation boundaries of braids of dislocations and extensively aligned monopoles delineate small misorientations across the crystal as shown by Field 2. These embryo channels are by no means either precipitate or

dislocation free, but the added complexity of poorer definition in fracture surface foils restricted a detailed investigation of all the possible effects obtainable from the channels. It was noted that the channels frequently began or ended at inclusion sites, however, and it was quite apparent in the examination of fracture surface foils that the channels were not precipitate free; in some reflexions precipitates could be brought into contrast throughout regions which in other reflexions showed black-white contrast suggestive of denuding within a channel, particularly in a second specimen prepared similarly to the first and thinned as before. The third experiment was therefore designed to determine the detailed structure of the channels; on the premise that the structure was actually a function of the local strain amplitude, rather than the local gradient of strain, a specimen aged at 25°C was fatigued at a total strain amplitude of $\Delta\epsilon_t = \pm 0.018$, which was six times the level employed in all other tests.

The material developed extensive channels and was examined after fracture, which occurred at 350 cycles. There were seldom more than three channels per grain, and not every grain exhibited channels; in some grains, channels on two intersecting systems were observed. The channel contrast frequently diminished and eventually vanished within a grain. Two important observations were made; firstly the detailed nature of interaction between matrix particles and dislocations is a tangling process, not a shearing process, as previously speculated by several authors, and is exactly the same in fine dispersions of carbides which are probably metastable, as in coarse dispersions of stable cementite. Only the spacing of the particles prevents a cell structure from forming; in general a simpler network of dislocations is formed. Secondly from Fields 3 and 4 of Plate 7 it is obvious that misorientations are present between the channels and the matrix and that apparent denuding within the channels has occurred. It is necessary to examine the channels at high magnfication to determine, as is shown in the detail of Field 1 of Plate 8, that if the interior of the channel

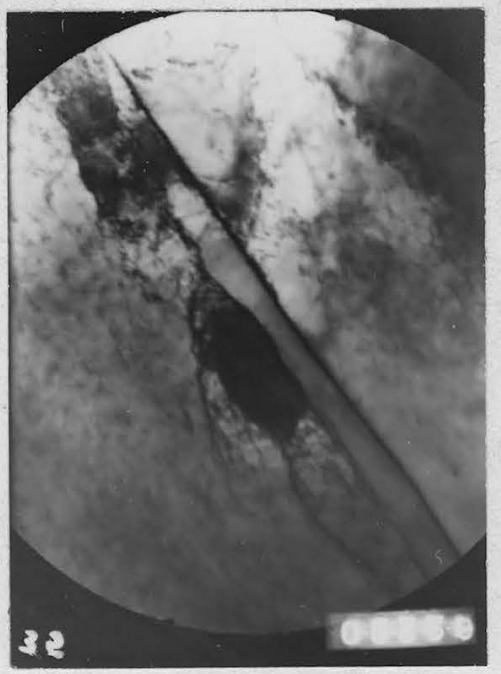

0.5 μm

1 μm

2 μm

2 μm

PLATE 7

is tilted into contrast then it can be seen to contain a high density of dislocations and debris. Since the projected width of the channel in a foil of $\{100\}$ orientation is about 1200Å, then in a material with a particle spacing in that plane of 800Å, and particles whose resolution is primarily a function of their strain fields, it is unwise to describe these channels as slip paths devoid of particles, as the extent of contrast at a particle on either side of the channel, i. e. a particle acting as a pinning point for the zig-zag dislocation boundary shown in Field 2 (compare Field 2 of plate 7), can locally reduce the apparent channel width to the interparticle spacing. Furthermore, when the slip plane is only partly out of contrast, and the surrounding matrix is in contrast, precipitates above and below the slip plane are visible, and the channel may completely vanish. It is concluded therefore that the observed contrast in a channel is determined by the Bragg conditions necessary to obtain diffraction images from dislocations in the plane of the channel, and not by absorption contrast in the absence of a second phase; i. e. this is an orientation contrast effect.

One further observation (Field 3) was the initiation of a simple cell structure at a grain boundary in addition to dislocation tangling around particles in the matrix. From Field 1 the network of dislocations can be seen to closely follow the geometry of the particles, in that in local regions dislocation networks with spacings between quadropoles of the order of the particle spacing have been established; since furthermore we see a region with a well defined network of two sets of dislocations spaced only about 300Å apart, which corresponds closely to the spacing of dislocations in cell walls formed at saturation in coarsely dispersed specimens, the tangling and tidying process seems to be confirmed as the mechanism of substructural development in fatigue of iron-iron carbide composites regardless of the distribution.

0.1 μm

0.5 μm

0.5 μm

PLATE 8

4.3.3. Series QSA

Plate 9, Field 1, illustrates the rough cell structure produced by swageing, and Field 2, the structure after ageing five days at 60°C. The precipitate morphology is not clear; precipitation must primarily have occurred on the cell boundaries. There also appears to be some precipitation within the cells, although this type of contrast can arise from dislocation loops, produced during deformation, which did not anneal out on ageing.

After 1.5×10^4 cycles, very little change in the structure is observed (Field 3). After a similar number of cycles, a specimen of series QSA 240 (aged at 240°C for five hours after swageing) begins to develop a well defined cell structure, amongst the swaged irregular network, apparently initiated at a grain boundary. We may conclude that ageing at the lower temperature pins the swaged structure more effectively than high temperature precipitation, from this observation (Field 4).

The initial QSA 240 structure does not differ markedly from the QSA 60 structure, except that the cell interiors are free of precipitates. Diffraction patterns can be obtained from cell walls suggesting cementite precipitates are present on the walls. The structure is shown in Field 1 of Plate 10. At fracture (10^5 cycles), the structure has reverted to a fairly regular cell structure, very similar in its scale and dependence on carbide particle spacing to the saturation structure in both series QA(γ) 240 and QA ($\gamma + \alpha$) 240. This is apparent in Field 2, though regions remain that have not completely tidied, as can be seen in Field 3. A further feature of interest (Field 4) is the nature of the cell wall junctions and the long continuous cells whose traces are those of slip planes of both $\{110\}$ or $\{112\}$ type from electron diffraction patterns from such regions.

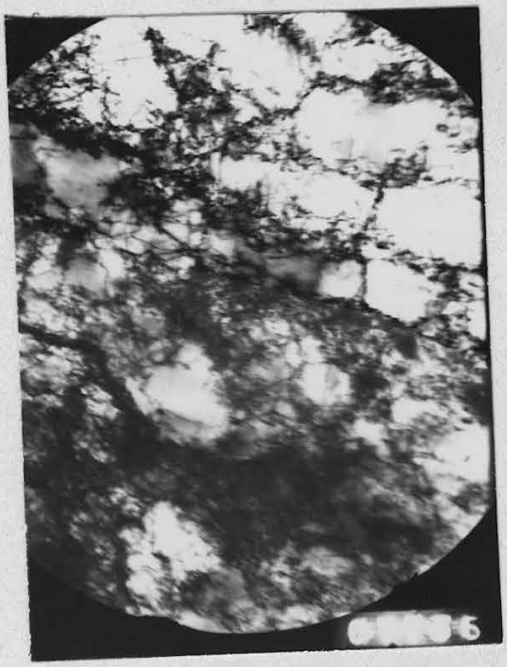

1 μm

0.5 μm

1 μm

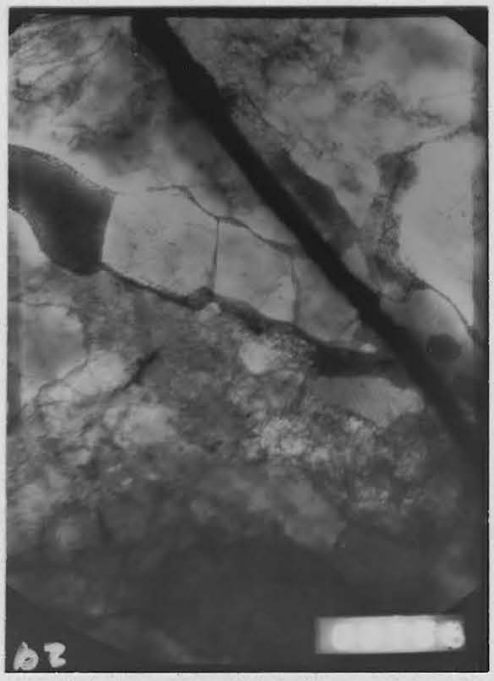

1 μm

PLATE 9

0.3 μm

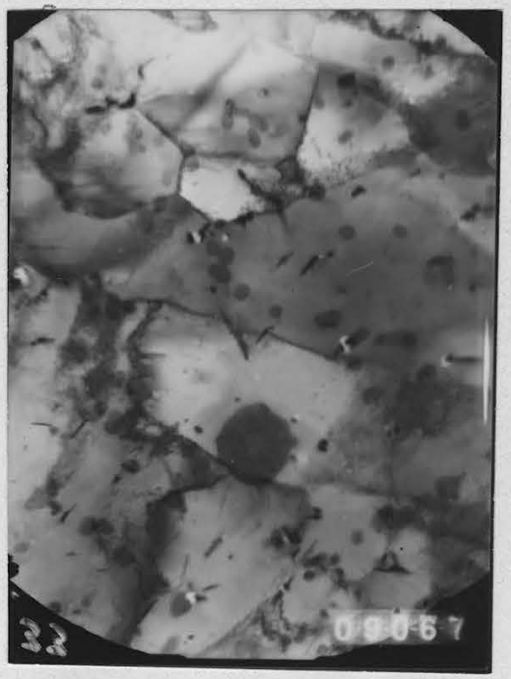

1 μm

1 μm

1 μm

PLATE 10

4.4 Ancilliary Observations

4.4.1 Optical Metallography

The limitations of electron microscopy in producing results representative of the bulk behaviour have been widely debated. In any process of localized deformation, any technique which provides a more macroscopic view of the extent of deformation constitutes a valuable means of checking the reproducibility and applicability of microscopic observations. High resolution optical metallography of polished sections, etched with suitable reagents, was therefore used wherever details of the substructure were large enough to be resolved by oil-immersion lenses. In practice, this meant that cell structures could be observed directly and the process of fatigue substructural development could be followed quite readily.

For both series QA (γ) 240 and QA (γ +) 240 the build-up of the cell structure was observed to occur gradually through the softening process, and to be initiated at an inhomogeniety such as a grain boundary or an inclusion interface. Measurements of the cell size observed optically correlated well with T.E.M. observations; at saturation the cell structure extended across the entire transverse section of the specimen, the cell size being about 1.5 μm. Occasionally slip band cracks formed at the surface could be correlated with the saturation cell structure.

As an adjunct to understanding the fatigue process in Series QA (γ) 60, sections were carefully examined after preparation by mechanical polishing and etching for a fixed period (40 seconds), in Fry's reagent, before fatigue, and after 6.5×10^4 cycles. It was found possible to distinguish several different etching effects which could be related to electron microscope images; a histogram of the number of fields displaying each feature before and after fatigue is presented, with a description of each feature, in Figure 14. The change in the distribution of features indicated by the histograms may be compared with the distribution functions for particle or particle-substructure composites derived from electron micrographs both before and after fatigue described in section 4.3.2. While this data could be interpreted as an

Etch features occurring in the histograms of Figure 14.

1. Fine features $< 0.2\ \mu m$. in diameter.
2. Dendritic features corresponding to original distribution $< 0.4 \mu m$ in diameter.
3. Coarser dendritic or acicular features $> 0.4\ \mu m$ in diameter.
4. Coarser features associated with substructural networks, as in original distribution.
5. Large dendritic composites observed near interfaces or grain boundaries.
6. Fatigue tangle-shaped features.
7. Cellular networks of comparable scale to type 4 features.

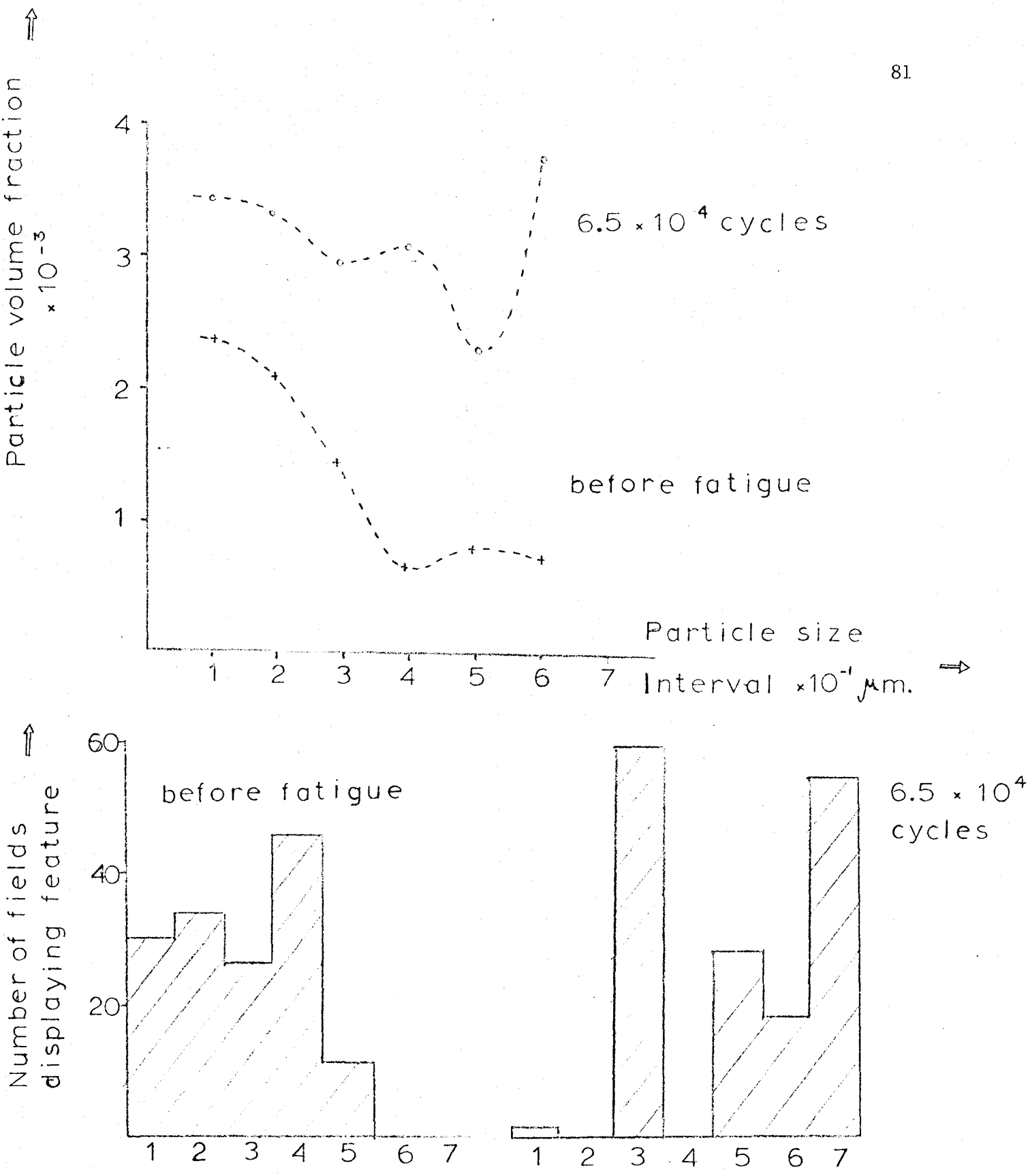

FIG 14. DISTRIBUTION CHANGE IN FATIGUE

indication of carbon redistribution during fatigue, it suffers from limitations in the accuracy of its acquisition, firstly because of the problems of interpretation and secondly in the lower-bound resolution cut-off, which limitations are statistically indeterminate.

No images either on transverse or longitudinal sections, even at the fracture surfaces could be resolved in the QA ($\gamma + \alpha$) 25 specimens in which the scale of the structure or its response to the etchant evidently render it irresolvable.

The austenitizing treatment gave a grain size of approximately 40 μm. diameter in all specimens; the aspect ratio was close to unity for transverse to longitudinal sections, but some grains were elongated in the rod-drawing direction, and a considerable range of diameters could be found in any one specimen.

4.4.2 Scanning electron microscopy

A considerable amount of scatter is to be expected in the duration of the fatigue life in different specimens. In the fine dispersion QA ($\gamma + \alpha$) 25 series this scatter was an order of magnitude, however, and the cause of failure was therefore investigated in two specimens, one of which failed at 7.5×10^4 cycles and the other at 5×10^5 cycles, using fractography in the scanning electron microscope. In Plate 11, Fields 1 and 2 the cause of premature failure at 7.5×10^4 cycles is assigned to an interfacial fracture mode initiated at inclusions producing straight boundary cleavage facets. The normal wavy matrix striations are shown in Field 3.

The fracture surface of a specimen notched during fatigue to promote a strain gradient was examined similarly, and at higher magnifications fine side branching cracks were observed, as in Field 4.

50 µm

10 µm

100 µm

2 µm

PLATE 11

4.4.3 Surface observations

Cellulose acetate replicas were used to monitor the development of surface slip during the fatigue of series QA (γ). Specimens aged at 60°C with a life of 2.2×10^5 cycles showed no resolvable slip activity until 5000 cycles, when a few grains began to display fairly straight slip lines, some of which extended across a whole grain. Subsequently there was little surface development, but by 6.5×10^4 cycles most grains exhibited surface slip. In contrast, slip lines were first resolved in specimens aged at 240°C after 1000 cycles and by 5000 cycles nearly every grain had slipped. The slip lines possessed quite large offsets, were fairly straight and mostly propagated right through the grains. By 15000 cycles a pattern of fissures or microcracks at approximately 45° to the specimen axis had developed, apparently along active slip bands as well as grain boundaries; the feature is shown in Field 1 of Plate 12. At higher magnification, direct surface observations with an oil immersion lens revealed that the slip lines consisted of short wavy segments deviating in direction of distances of the order of 2 μm, which is comparable in scale to the periodicity of the saturation structure, or, of course the particle spacing. In Field 2 a detail (x3300) is shown. A few observations on specimens repolished lightly after replicating at saturation, indicated that on overstraining many slip lines followed the paths of the original fatigue slip bands.

The resolution of the above method is not sufficiently high for the reliable comparison of the influence of the various particles distributions on basic slip processes to be assessed. The mode of slip in a fine (QA ($\gamma + \alpha$) 25) and a coarse (QA ($\gamma + \alpha$)240) distribution during tensile pre-strain to $\epsilon = 0.01$ was therefore examined in detail using two-stage replication, the final carbon positive being examined in the electron microscope. Field 3 shows that the slip lines formed at -78°C in series QA ($\gamma + \alpha$)240 were short and apparently limited by the particle distribution, frequently changing direction. In Field 4, slip lines in the fine dispersion QA ($\gamma + \alpha$)25 are shown; although in general

50 μm

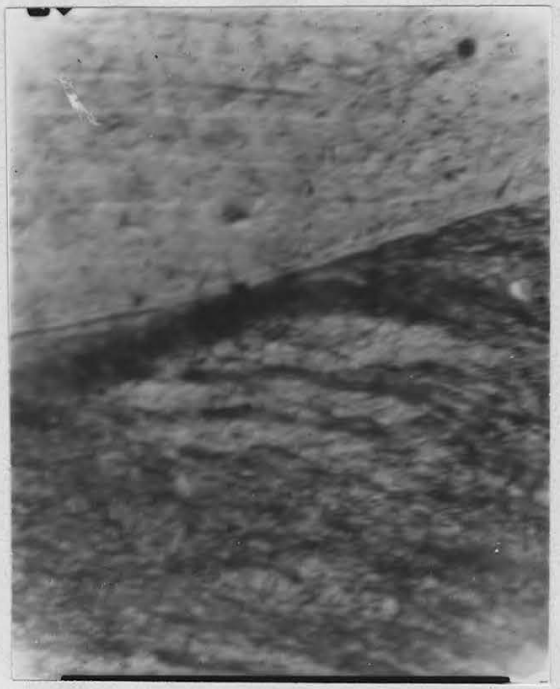

2 μm

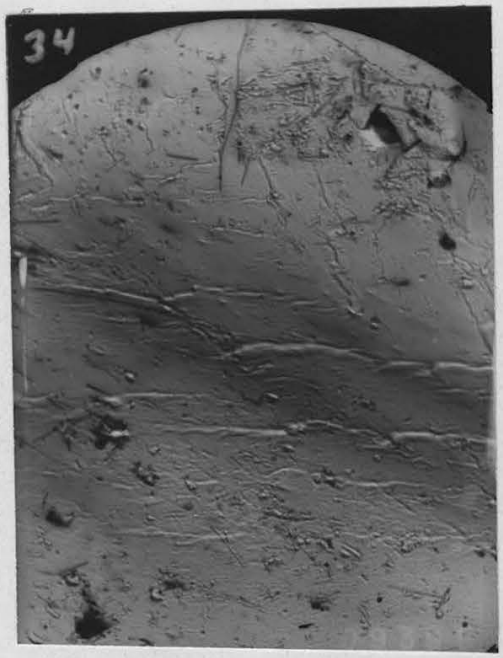

5 μm

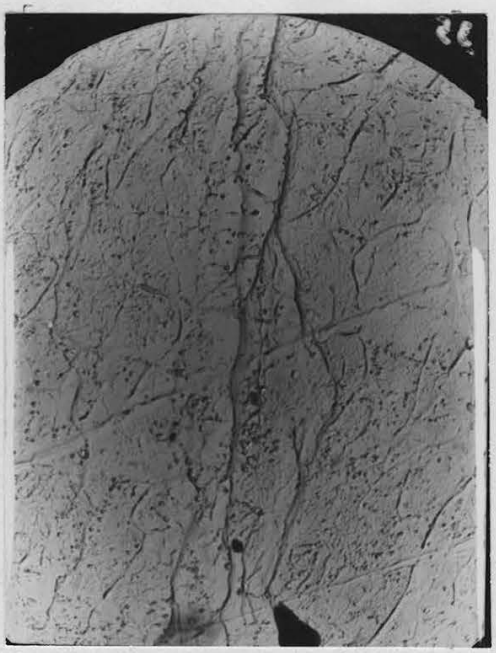

5 μm

PLATE 12

slip lines appear to be longer they are still wavy and constrained locally by the distribution; no evidence for shearing of particles could be obtained, the slip lines always being wavy at -78°C.

4.5 Summary

1. During the fatigue of age hardened low carbon iron alloys containing dispersions of carbides of various sizes and interparticle spacings, dislocations are accumulated around particles, regardless of their size, spacing or structure. No evidence of shearing of particles by glide dislocations could be detected in this investigation.

2. In general cyclic softening is associated with the formation of a saturation cell structure. The influence of particles of a second phase on the resultant geometry of the cell structure is marked. Fine particles tend to restrict the development of dislocation networks at the cyclic total strain amplitude used, unless this amplitude is raised appreciably. Coarsening dispersions permits cell structures of decreasing regularity to develop .

3. When the scale of particles is very fine, localised deformation may occur, the conditions for which are sensitively dependent on the local strain amplitude, producing intensive slip channels during cyclic softening.

4. Thermal mechanical treatments described in this thesis act to enhance fatigue resistance by retarding the development of cyclic softening by the pinning of the cold-worked structure by precipitates.

5. The saturation cell structure exhibits a lower rate of work hardening under tensile overstrain than during prestrain of the virgin material.

Evidence is presented suggesting that the substructure is unstable on a local scale in subsequent tensile deformation.

CHAPTER 5

DISCUSSION OF RESULTS

5.1 Introduction

It is possible to discuss substructural observations both in regard to the mechanisms of development, and in terms of the subsequent stability of the dislocation arrangements. In the present investigation, emphasis has been placed upon the latter consideration, and this will be reflected in the discussion. The correlation between the substructural changes observed to accompany fatigue, and the initiation and propagation of fracture, must be facilitated by any investigation which seeks to determine the criteria under which instabilities occur, and thence the definition and prevention of instability in the structure.

The properties of the dislocation sub-structure are nevertheless a consequence of the manner of its formation, and particularly when considering the constraints imposed upon the observed sub-structure by particles of a second phase, during fatigue, it is important to recognise the possible mechanisms of the transient processes of hardening and softening in the matrix. Only then can a model for the influence of particle distributions upon the substructural development be formulated. In Section 2, a rationale will be proposed to describe this influence; the stability of the resulting substructures will then be assessed, with special reference to the uniformity of strain distribution in the material, and to the efficiency of the thermal-mechanical treatment tested in this investigation.

The discussion of the observations of low initial rates of work hardening, observed on overstraining fatigued specimens, will be based on the conclusions of Section 2. Suitable mechanisms leading to this behaviour

will be presented and discussed in Section 3.

Finally, the applicability of generalised models of fatigue to the description of experimental data will be reviewed to assess the relationship between macroscopic models of unstable plastic flow and the mechanisms propounded in the present investigation.

Before passing to the main body of the discussion we should note that even in the overaged specimens used in this investigation, sufficient carbon was apparently left in solution for extensive fine precipitation to occur on low-temperature ageing treatments used to pin substructures in the stress-applied state. Since there is, therefore, likely to be sufficient carbon in solution in most specimens during the fatigue process for strain ageing or further precipitation to occur, a brief consideration of some of the effects of solute carbon concentration and redistribution during fatigue is in order. The detection of such effects requires the use of experimental techniques beyond the scope of this thesis, but certain indirect observations indicative of solute redistribution have been observed in the present work, and should be related to the literature to assess their importance.

Considerable evidence is available for cyclic strain ageing, although the interpretative prerogatives seem to have been widely asserted, for example by Sanders and Hempel (1952) who reported observations of reprecipitation in slip bands. However De Foucquet (1961) detected changes in solute carbon concentration in quenched iron during fatigue, using internal friction measurements. At higher cyclic strain amplitudes evidence of dissolution-atmosphere formation-dissolution mechanisms was obtained with resting data which correlated with the known precipitation kinetics of carbides in ferrite. If such processes do occur, then knowing the constraining effects of continuous precipitation are similar to those of pre-existing precipitates, according to the substructural observations of Wilson and Tromans (1970), we may well attribute fatigue strengthening in

iron, defined as a resistance to extensive partitioning of strain amplitude or strain rate, to two active components, fine initial precipitation, and subsequent continuous strain-ageing, following Wilson (1970). Certainly the stability of the large fatigued tangles observed in series QA (γ) 60 in the present investigation would be enhanced by pinning by a solute atmosphere, and the difficulties in obtaining good diffraction contrast in T. E. M. of these tangles could be partly attributed to the presence of solute carbon atmospheres.

Other authors have attempted to analyse S-N data to determine if accelerated ageing is a consequence of fatigue deformation in steels. Yamakazi (1970) applied a damage criterion and ideal ageing kinetics for the total precipitation in an alloy steel fatigued in the ageing temperature regime, but the assumptions of the model were crude; the rate was observed to be accelerated but the rate equation took no account of sub-structural modification. The source model of Kawasaki et. Al (1967) is more interesting, being based on the premise that damage will not occur if the rate of source generation $\geq$ rate of pinning by strain-ageing. It suffers in detail from its simplifications.

Apart from basic modifications to slip processes by solute carbon concentration variations, the other effect of interest lies in the interaction of solute carbon with other point defects manufactured in fatigue. There is evidence, for example,that radiation induced defects generally nucleate ϵ-carbide precipitates, although the exact nature of the defect is not known with any certainty (Hull and Mogford (1961)) . Vacancy-interstitial pairs have been detected by resistivity measurements by Fujita and Damask (1964), and grow under similar kinetics to ϵ -carbide (Arndt and Damask (1964)). Such a defect may be important in diffusional processes (Homan (1964)). The interpretation of damping and resistivity data is so complex, however that at the present time it is not possible to assess the mobility of such defects as distinct from their influence on nucleation frequency.

5.2 The Stability and Influence of a Second Phase

The accumulation of dislocations by coarse cementite particles and the influence of the particles on the local geometry of cell structures developed at saturation, in both series QA (γ) 240 and QA ($\gamma + \alpha$) 240, together with the absence of any evidence of shearing of the particles, suggests that the material is plastically inhomogeneous according to the definition of Ashby (1970). The particles are thus effectively rigid and non-deformable.

The experimental observations of the influence of particle size on the substructure developed under cyclic strain may be summarized thus: very fine particles accumulate dislocations locally, and require high strain amplitudes to be applied in order to develop a recognizable cell structure, or sub-boundaries. Increasing the particle size and spacing, however, permits the dislocation substructure to develop a regular cell structure or a large scale localized structure, such as the clusters of dislocations observed in series QA (γ) 60, even at low strain amplitudes.

It is possible to rationalize these observations by considering how the particle size and the applied strain amplitude affect the method of storage of dislocations in the deformed material. Dislocations can accumulate to accommodate shear deformation of the matrix and maintain continuity at a particle-matrix interface in two ways (Figure 15); shear loops can accumulate around the particle according to the simple model of Fisher et Al. (1953) producing a heavily polarized structure and a back stress on the primary system, or prismatic dislocation loops may be generated. In the former case the substructure can be detected by a Bauschinger effect; this point is fully developed in the Appendix. The latter type of slip will tend to be activated once the component of the back stress due to shear loop build up, exceeds the critical value on the secondary slip systems. Once prismatic glide is facilitated the model of Fisher et Al. breaks down and the situation is best described by Ashby's model, in which

Fig. 3

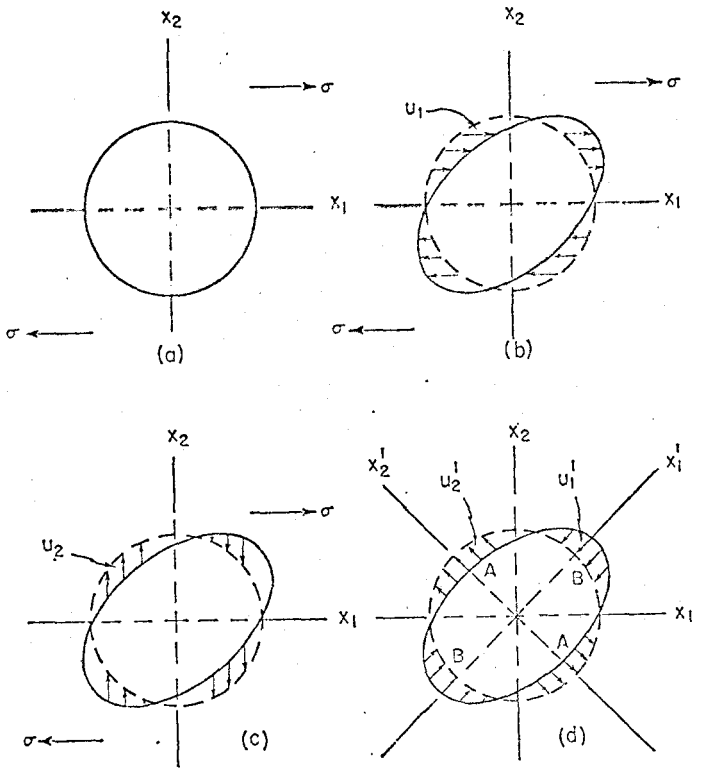

(*a*) A hard particle in a plastic matrix. (*b*) When the particle is removed from its hole, and the matrix undergoes a uniform primary shear displacement $u_1 = \alpha x_2$, the hole is distorted as shown. (*c*) To replace the particle in its hole, a secondary *shear* displacement $u_2 = cx_1$ at the particle-matrix interface is first needed if the particle is to be elastically distorted only. (*d*) Alternatively, the matrix can be displaced by prismatic punching to give displacements u_1' and u_2' parallel to new axes x_1' and x_2'. (For clarity, diagram (*b*) shows a large shear strain of 0·5. In consequence, a subsequent *uniform* secondary shear $u_2 = cx_1$ would not restore the hole to a sphere. When strains are small, or are applied simultaneously, a *uniform* shear u_2 restores the ellipsoid to a sphere.)

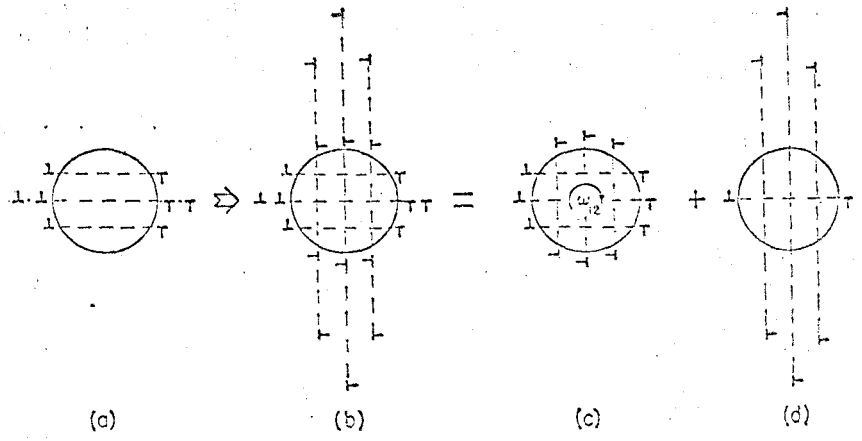

The dislocation analogue of fig. 3 (*c*). At (*a*), shear in the primary slip system has left N primary loops round the particle. At (*b*) secondary slip has occurred by the nucleation and movement of *glide* loops. The complex pattern of (*b*) is the superposition of the low energy arrangement shown giving a rotation ω_{12} shown at (*c*), plus the residual loops shown at (*d*). The residual loops at (*d*) will cause work hardening.

Fig. 5

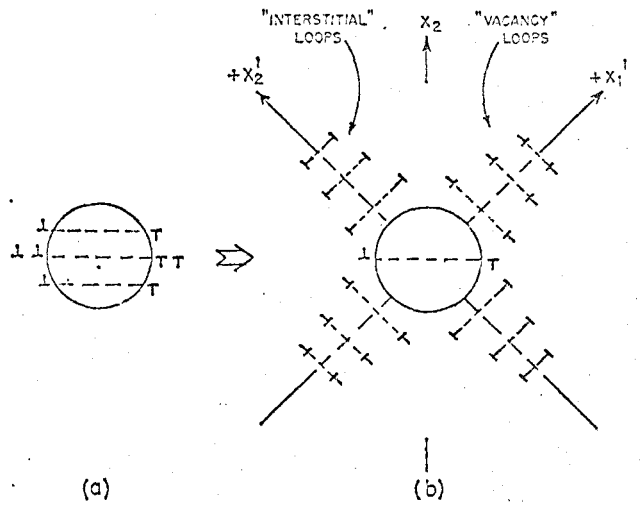

The dislocation analogue of fig. 3 (*d*). At (*a*) shear in the primary slip system has left N loops round the particle. At (*b*) secondary slip has occurred by the nucleation and glide of secondary *prismatic* loops, leading to a complex but low energy arrangement of loops at the interface plus residual prismatic loops shown at (*b*) which will contribute to work hardening.

Figure 15. Maintenance of continuity of matrix-particle interface during deformation (after Ashby (1966)).

the activation of secondary slip produces the characteristic work-hardening of two-phase plastically inhomogeneous materials.

The applicability of Ashby's theory has been successfully tested experimentally; Russell and Ashby (1970), have deformed single crystals of aged Al-Cu alloys containing incoherent θ' platelets, in tension. They found that geometrical storage of dislocations at particle interfaces, either as shear loops of the same sign or dipoles or prismatic loops dominated the observed density of dislocations. Now the system tested by these authors was probably the most complex case which could be completely analysed, yet it was exceedingly simple compared to the system treated in the present investigation. In a polycrystal, five independent slip systems must operate just to maintain the continuity of the material at grain boundary interfaces; however they need not all operate throughout the grain, if the grain size is suitably large. Nevertheless, we cannot completely separate the effect of a second phase particle from matrix constraints on dislocation storage, particularly when examining the resultant misorientation across cell boundaries such as those formed in fatigue. It is possible to say from observations such as those of Plate 2 , that from a qualitative viewpoint, considerable similarities exist between dislocation accumulation in iron-iron carbide after fatigue and the simple Al-Cu system analysed by Russell and Ashby.

The total cyclic strain amplitude employed in the present investigation was $\frac{\Delta \epsilon}{2}$ (total) = 0.003; this is a lower strain than that corresponding to the critical stress for activation of secondary slip, calculated by Ashby to be $\epsilon \simeq 0.02$. Particles may therefore accumulate shear loops in the manner proposed by Fisher et Al. over the first few cycles, until the secondary system is activated, unless dislocations are able to cross-slip around the obstacles. According to the observations of Boyd et Al. (1969) of slip lines in iron at room temperature unidirectional deformation, wavy slip, indicative of cross-slip processes, occurs in sub-bands 200-400Å

apart. If we assign 300Å as an average cross-slip offset, then particles with diameters < 600Å might not act as obstacles to slip at low strain amplitudes. The absence of slip activity observed in series QA ($\gamma + \alpha$) 25 in the present investigation is therefore attributed to cross-slip around particles occurring, rather than any accumulation of dislocations developing. To obtain activation of secondary slip it is necessary to either coarsen the particle size or increase the macroscopic applied strain amplitude. Both these changes were observed to produce cyclic softening and the development of a cell structure in the present work; increasing the particle size from 500Å to 800Å resulted (in series QA ($\gamma + \alpha$) 25/60) in a regular cell structure, and raising the amplitude to $\frac{\Delta \epsilon}{2}$ (Total) = 0.02 i.e. the limit of the Fisher et Al. treatment produced embryo networks and extensive accumulation.

All the coarsely dispersed materials softened cyclically after a brief initial hardening period, the mechanism of which is obscured because the material was then being cycled in the Lüders region of strain. According to the Fisher et Al. theory the number of shear loops which can accommodate strain has a maximum value inversely proportional to the radius of the particle. Coarser particles should therefore more readily permit activation of secondary slip. However in order to understand more of how the cell structure actually develops, a review of observations of softening and the concommitant detailed mechanisms proposed in the literature of single phase materials is essential.

The detailed mechanism of the reduction of the flow stress is generally assigned to the production of dislocation dipole arrays from the existing structure. Such arrays have negligible long-range internal stress fields, as the individual fields are almost self-cancelling for pairs of dislocations of opposite signs. The increase of the primary dipole density thus decreases the sum of the contributions to the flow stress. Apart from direct

observations of increased dipole densities during fatigue softening (Huggard (1970)), it is interesting to note that their production may be assisted simply by the release of the applied stress. Mughrabi (1968) observed no primary dipoles in unidirectionally strained copper single crystals irradiated in the stress-applied state to pin the substructure for examination. On this basis cyclic strain will inevitably produce dipole configurations, and the fundamental substructures in fatigue should be dipole-based. Two mechanisms have been proposed for dipole formation. The first (Gilman (1962)) requires the jogging of a screw dislocation at an obstacle; the jog is sessile and continued movement of the screw, followed by constriction, for example prior to cross-slip, would produce a pair of edge dipole loops. Pairs of dipoles are not generally observed however, and the second mechanism, due to Tetelman (1962) is much more attractive. It involves the re-orientation of lengths of two non-colinear glide dislocations on parallel glide planes, along a common direction, followed by pinching-off. Only one mixed dipole is produced by this process, which can readily occur in reversed strain, and, according to Bullough and Sharp (1965), not only is the force perpendicular to the glide plane for the initial configuration quite appreciable, but the component in the cross-slip plane, required for constriction, is significant. The process should be easier in f.c.c. materials rather than b.c.c. materials according to these authors because the ratio of the area of potential cross-slip plane to the area of glide plane is greater in the former lattice.

In the present two-phase system dipoles may easily be generated on the primary system from the shear loops, which will either be annihilated, by loops of opposite sign, or repelled and distended in the glide plane by loops of the same sign. To what extent dipoles would be produced by distension of prismatic loops on secondary systems is not clear. It is possible that interactions with forest obstacles would be weak; Huggard did observe an

unchanged secondary (forest) density during fatigue softening.

It is instructive to examine the resulting cell-wall structure and to compare the properties of cyclically formed cells with those of cells produced by unidirectional deformation. The principal habit plane of the cell walls determined in this investigation was the $\{112\}$ plane. The details of the wall structures are strikingly similar to those obtained from analyses of stable networks. Li (1963) has determined that fourteen of the eighteen stable networks formed in b.c.c. metals have $\{112\}$ habit planes, although only two of these are of twist configuration. The overall rotation axes determined for these configurations could not be correlated with the present measurements which are unlikely to represent stable networks, but typical angles of tilt or twist measured are of the same order as the values calculated from Li's expressions for two orthogonal sets of dislocations of the experimentally observed dislocation-dislocation spacing. If $\theta = \sqrt{k_1 a_o / k_2 h_2}$ where a_o = lattice parameter of iron

h_2 = spacing of second set of dislocations

k_1, k_2 are constants

then for $h = 300\text{Å}$, θ is typically 4×10^{-3} radians for a twist wall. The observed misorientations are very much smaller than in cell structures produced in unidirectional deformation, at least for dislocations of the same net sign, such as were determined by Steeds (1966) during stage III hardening of copper single crystals. In the absence of particles of a second phase, the obstacles promoting both cyclic hardening and unidirectional hardening appear to be similar, according to the activation volume measurements of Kettunen and Kochs (1969). Such obstacles, described as forest obstacles by Steeds, are any dislocations threading the glide plane. Consequently as the secondary dislocation density in a single crystal increases the unidirectional hardening increases. In cyclic deformation, however,

the formation of a cell structure from primary dipoles can occur without hardening, because the magnitude of the associated secondary density is fundamentally different from that of cells formed in unidirectional deformation, being much lower.

The dislocations accumulate to form cell structures with approximately self-cancelling misorientations, at least over a small number of cell diameters in either type of deformation. Whilst in single phase materials this can be accomplished by obstacles of opposite sign, since by stage III the secondary slip distance is small (Steeds, loc. cit.), in two phase materials the continuity requirement ensures that once a cell builds up from geometrically necessary dislocations that region of the crystal becomes effectively dead, and further cell formation produces a compatible opposite rotation of the lattice. This has been demonstrated to be true by Russell and Ashby (loc. cit.) in Al-Cu at higher unidirectional strains. One further observation is of interest here; the cell structures formed in monotonic deformation of iron single crystals contain internal misorientations within the walls, according to Ikeda (1970), between a core multipole network, and an outer tangled periphery, containing a high density of active primary edge dislocations. This type of structure could continue to grow, and would usefully represent the intermediate structures observed in the present investigation of series QA (γ) 60, where large tangles rather than cells developed into saturation, with little cyclic softening, but exhibiting no net lattice rotation across the crystal. Such a structure might require stabilising by local constraints such as strain-ageing, which would also explain the lack of cyclic softening associated with its formation.

Although no explicit account may be given for the kinetics of cyclic softening from the present results, a basis for the influence of particles of a second phase on the initiation of softening is established. To initiate the process of dipole formation the particles must be large enough, or the strain amplitude sufficiently high to activate slip systems irreversibly, generating dislocation structures with negligible long range stresses. To outline

generally the influence of particle spacing is more difficult; if secondary slip is initiated, then according to the Ashby model the amount of cyclic softening should increase as the particle spacing increases, just as in monotonic deformation the work-hardening decreases. On this basis the particle spacing determines the local constraint on the substructural build-up, limiting the slip distance, and hence the scale of the structure. Hence in a fine dispersion, less cyclic softening is expected; the extreme regularity of the cell structure observed in series QA ($\gamma + \alpha$) 25/60 of the present investigation is an indication of such a constraint. In the extreme case, series QA ($\gamma + \alpha$) 25, not only is it necessary to raise the strain amplitude to initiate the processes of softening, but the constraints are apparently so severe that the networks that do form are very closely related to the particle morphology indeed.

Fatigue data in very simple systems obeying the criteria of the Ashby model is scarce. As shown by Woo et Al. (1970), however, in more ideal cases, such as copper-alumina alloys containing a fine dispersion of incoherent particles, fatigue hardening is possible at low strain amplitudes. The rate of hardening is significantly lower than for pure copper during unidirectional hardening. It is not possible to compare the observations in detail with the present results, not only because of the single crystal technique used by Woo et Al, but also because the internal oxidation technique used by these authors resulted in a bimodal particle distribution. In single crystals and polycrystals of Al-Cu, precipitation hardened to give particles of differing sizes, spacings and coherency, Park et Al. (1970) have observed a similar influence of particle size and spacing on cell formation in fatigue to the present investigation, but considered only the effects on fatigue life, and then principally in terms of interfacial coherency strains; the fatigue life diminished as the coherency decreased, but increased again for fully incoherent precipitates observed to constrain the cell structure as in the

present investigation.

When the quenched material was aged after swageing it did not begin to soften as rapidly during subsequent fatigue as material simply quenched and aged. The effect was more marked on ageing at a low temperature than at a high temperature. This retardation of softening is attributed to pinning of the swaged substructure, either by discrete precipitation or a semi-continuous atmosphere of solute atoms associated with the three-dimensional dislocation array. No significant difference in the rate of softening relative to the rate in quench-aged materials was detected, and the eventual saturation condition occurred at a stress amplitude within the range of saturation values observed. In the absence of a detailed understanding of the kinetics of softening, it is pointless to speculate upon the differences between rates of softening in series QSA 240 and series QSA 60 except to indicate that strain ageing processes may be important. Feltner and Laird (1967) have used strain-rate sensitivity measurements in copper and Cu-7.5% Al to derive activation volumes in an attempt to distinguish the rate controlling process for each mode of slip, but the problem in analysing differing systems such as these is to make measurements of modifications to similar initial substructures. Because the deformed pre-strain structures were not similar in the two materials these results are not reliable.

In the present investigation, the nature of the initial unpinning may be important in determining the efficiency of thermal-mechanical pre-treatment. In the investigations of Neumann (1969), pre-strained copper single crystals subjected to a controlled, increasing cyclic applied stress amplitude, responded with bursts of cyclic strain of increasing amplitude occurring at regular intervals. This behaviour, of cyclic softening in bursts, the author attributed to catastrophic unpinning of dislocations on a local scale, but simultaneously throughout the crystal in regions of analogous dislocation configuration (and hence flow stress). Cyclic softening of a pre-strained

substructure could then depend sensitively on the pinning strength of the structure, in terms of its orientation and the density of defects in its vicinity. The onset of discernible softening in a material would then depend on the distribution of pinning strengths in the material. This description complicates interpretation of the initial hardening response frequently observed in the present investigation particularly when the pre-strained structure is exhausted of work-hardening capacity; for this reason, and because of delays in the initial response of the recording device, the stabilized stress amplitude used for normalising data was taken at the end of the initial transient.

One further important observation in the present work was of the conditions governing the uniformity of strain distribution within the structure. It was apparent that in the very finest distributions of particles regions of intensive slip activity could be induced, but only by local or macroscopic increases in the strain amplitude. These regions, described in the literature as channels, were observed by T. E. M. to consist probably of glide planes containing fairly large active densities of dislocations, and are rotationally misoriented about two parallel sub-boundaries formed by the braiding of dislocations about consecutive particles lying along the boundaries. The projected dimensions of the channels were not significantly different from the interparticle spacing in the glide plane, so there is little justification for assigning the observed contrast to an absorption effect, i. e. to the denuding of the glide plane of particles. The misorientations could not be detected by selected area diffraction with the diffraction apertures available, but would be self-compensating. The contrast would then be due to an orientation effect, and the thin platelets of carbide immediately above and below the bundle of active glide planes would be out of contrast in some reflexions permitting resolution of the glide dislocation structure, since unless the particles are at oblique angles to the foil normal they are visible only by strain field contrast, rather

than absorption contrast. In other reflexions, contrast in the channels could in fact be weakly resolved, coming from both particles and dislocations.

The embryo structures observed below the fracture surface then represent the build-up of the misorientation, i.e. of the sub-boundaries. Once the material begins to cyclically soften in such a region, slip will be enhanced on slip planes contained in the regions of misorientation, and the length of the region will increase to assume the aspect ratio with the lowest associated back-stress, the lateral extent only being constrained by the interparticle spacing. It will thus appear elongated and narrow, like a small twin. Following Friedel (1964), the back stress in the centre of a platelet of thickness t, and diameter D, deformed to a shear strain γ is

$$\tau = \frac{\mu \gamma t}{2D}$$ where μ is the shear modulus.

If $t = 0.1\,\mu m$. and $D = 40\,\mu m$, then even if all the shear strain is confined to these regions ($\gamma = 0.02$ in the high amplitide experiment), $\tau \sim$ 300 psi (2×10^{-1} MN/m^2) which is hardly sufficient to explain the observed softening of 10% of the original flow stress.

It is concluded from the foregoing that the description of cyclic softening in terms of channel formation by the shearing and reversion of precipitates, due to McGrath and Bratina (1967) is inapplicable to iron-iron carbide in fatigue. No evidence of shearing of particles could be obtained in the present investigation, and there appears to be no valid reason why particles should accumulate dislocations in one region of the crystal, yet be sheared sufficiently to redissolve in another. Furthermore, McGrath and Bratina (1970) failed to detect channel formation in an iron-copper alloy containing copper rich zones, fatigued at a suitably high strain amplitude; nor did they find any evidence of shearing of particles. Channel formation

is therefore believed to require initial dislocation accumulation in a finely distributed material. Hence low amplitude tests failed to produce detectable channels in series QA $(\gamma + \infty)25$ in the present investigation. The introduction of a strain gradient ahead of a crack, or a macroscopic strain amplitude increase was required to produce such localization of substructural development.

5.3 Response Under Overstrain

The instability of a fatigued cell-substructure under tensile overstrain has been related in this thesis to the breakdown of the structure beyond the original imposed units of cyclic strain amplitude. This results in a period of low initial work-hardening and is directly analogous to the observations of Basinski et Al. (1969) who observed long straight slip lines propagating across the surface of an overstrained copper single crystal fatigued to develop a localized cell-like substructure, and to the results of Neumann (1969), who, by interrupting an increasing-stress fatigue test and overstraining the crystal at any point just prior to the next strain burst response, obtained similarly, long straight slip lines and very low rates of work hardening over strains of up to five percent.

To account for the low rate of work hardening and the localization of strain observed in the present investigation, two general types of model may be considered. The first type requires that some additional obstacle be produced during fatigue which suppresses the rate of work-hardening such as point defects, which contribute significantly to the thermal component of the flow stress. If, following Friedel ((1964) p. 274) the defect concentration is described by $C \sim 10^{-4} \epsilon^{2}$, where ϵ is the plastic strain amplitude used then $C \sim 10^{-10}$ defects/atomic volume, corresponding to a mean spacing of $\sim 10^{-5}$ cm between defects in iron in the present experiments. Foreman (1968) computed that the interaction between rigid obstacles randomly

distributed, and a glide dislocation would be

$$\tau_H \simeq \frac{\mu b}{1.75L}$$ where L is the obstacle spacing, provided the obstacle radius $V < L$.

whence as an upper bound limit of the present case $\tau_H \sim 7 \times 10^3$ p.s.i. (50 MN/m^2) if no defects collapse and coalesce as loops, and the defects are rigid and immobile. In a more realistic estimate, for a cell wall of 0.5^o twist misorientation, the shear strain accommodated, $\gamma \sim 0.009^c$ requires a dislocation spacing h in the wall of b/γ, where b is the Burgers vector of the constituent dislocations, so that $h \sim 3 \times 10^{-6}$ cm., as is observed by T.E.M. If we use the appropriate expression for the passing stress at an obstacle

$$\tau_H \simeq \frac{\mu b}{2\pi h} \sim 5 \times 10^3 \text{ p.s.i. } (35 \text{ MN/m}^2)$$

Regardless of the detailed nature of the obstacle, therefore, its attrition would significantly reduce the hardening; furthermore cyclic softening could be produced by the destruction of such obstacles progressively. Indeed, Makin (1967) has explained cyclic softening in neutron-irradiated copper single crystals by the destruction of defects in localized channels.

The second type of model depends on the saturation substructure being intrinsically unstable to overstrain. To model this instability in a polycrystal would require an accurate knowledge of the distribution of Burgers vectors in the cell structure; clearly during polyslip it would be very difficult to describe the process. The model outlined below is developed qualitatively therefore for a simplified cell wall geometry, but should be capable of verfication by observation of the overstrain response of fatigued single crystals. It is based on the well documented evidence that whereas in unidirectional deformation in stages II and III dislocations of opposite sign accumulate only over appreciable distances, so that primary arrays give rise

to observable X-ray asterism or misorientation contrast in TEM, in fatigue they tend to pair up at the local level, to form enhanced primary dipole densities. There is considerable ancilliary and indirect evidence to support TEM observations in the latter case. Huggard (1970) detected a decrease in Laue asterism accompanying cyclic softening of fatigued pre-strained single crystals of copper. Stored energy measurements made by Halford (1966) revealed a decrease in stored energy immediately upon reversal of plastic strain during each cycle of fatigue softening of cold-worked copper. In recovery experiments after large tensile and small reversed strains, Hargreaves et Al. (1963) detected decreases of up to 50% in the stored energy after reversal of strain. Although these results could be interpreted in terms of defect annihilation, concommitant density changes observed in the latter case might be better attributed to total core volume changes produced by dislocation substructural modifications. The dipole based model does explain the stored energy decrease qualitatively.

Following Li (1963) a simple twist boundary of a cross grid of screw dislocations is unstable mechanically by the pulling out of one screw dislocation, for which the stress perpendicular to the boundary is required to be at most $\frac{\mu b}{2h}$ where h is the spacing of the dislocations, or by the emission of a single loop of dislocation form intersectional pinning points; again the required stress is $\sim \mu b/2h$. Neither event would result in catastrophic destruction of the boundary or deformation of the boundary as a whole.

The only other mode of instability is disintegration by self-elimination of each set of dislocation composing it; if the boundary is thermally stable this is unlikely. The fatigued boundary is likely to consist of crossed grids of dipoles, however. The stability of the boundary, now consisting of pairs of dislocations of opposite sign in close proximity is then severely reduced with respect to stresses on the slip plane, according to Li (1964). He considers the simple case of a screw dipole, and shows that two interior

dislocations moving against each arm of the dipole will always exert a force on the dipole sufficient to decompose it, and reform as two widely separated dipoles. There is thus no equilibrium configuration, i.e. of maximum attractive force or minimum Gibbs free energy, for two dipoles on parallel planes. Computer calculations for the stability of an individual dipole in an infinite dipole array, and for edge dipoles in similar arrays reveal that the introduction of additional dislocations always results in the stress required to decompose the dipoles being less than $\frac{\mu b}{2h}$ by a factor proportional to cosh $\frac{2\pi y}{x}$ where y is the separation of the slip planes and x the interaction distance. Hence as y becomes small the approach distance x of a dislocation emitted by some source within the confines of a cell, and required to initiate decomposition of the wall increases. Thus for fatigue dipole arrays where y is quite small the activation of a source during overstrain may quite readily produce an instability of the type described by Neumann (1969) as the passing stress may decrease to a few percent of the value $\mu b/2h$ required for arrays of the same sign; after breaking down the wall dislocations are more randomly distributed so that a large series of local events will produce considerable extensions, with very little associated work-hardening occurring. The regime of reduced work hardening rate at low temperatures, observed by Keh and Weissman (1962) in iron, displays an analogous break-down process; cell structures formed at room temperature in unidirectional behaviour modify in subsequent low temperature deformation apparently by unpinning of wall segments. Neumann, loc. cit., depicted the process more as a series of local events rather than Luders instabilities even in single crystals with no second phase obstacles. The observed geometry of cell walls is certainly suitable for this process; for a dislocation spacing of y = 300Å in the plane of the cell wall, the spacing of dislocations perpendicular to the plane of the wall is probably similar as the dipole is stable in a 45^{o} configuration. According to Li's calculation for the interaction of two screw dipoles the force on the dipole tending to split it is $> \frac{\mu b^2}{4\pi y}$ for spacings

perpendicular to the plane of $< 1200\text{Å}$. The walls should thus easily decompose once a source is activated, for little contribution from the applied stress would even be required. The proposed configuration used in the model and the variation of the force on the dipole with the dipole width (after Li (1964)) is shown in Figure 16.

To test the dominance of either an obstacle or saturation dislocation network instability, in the reduction of work-hardening capacity after fatigue, strain rate change tests over one decade were carried out before fatigue, and after fatigue during overstrain through the low work-hardening regime, in furnace cooled specimens. The strain rate sensitivity, $(\frac{\Delta \ln \dot{\gamma}}{\Delta \ln \tau})$ increased only slightly from 0.96 to 0.97. Here τ was the flow stress, and $\dot{\gamma}$ the applied strain rate. Clearly such a difference is not significant and suggests that there is little contribution to the thermal component of the flow stress during the overstrain process, from easily activated obstacles such as point defects, clusters or fine loops, produced during fatigue. We are therefore justified accordingly in considering in detail alternative processes, and the model described above is not only suited to the overstrain case but also to modifications to the cell size by strain amplitude changes during saturation. It may also indicate the mesh length, activated during reversible non-linear elastic bowing of dislications, to accommodate strain during fatigue deformation, although in this case it must be necessary to estimate the effects of local pinning at wall intersections or by solute or after defect configurations. A simplistic calculation of the average distance $\bar{x}$ moved by a dislocation in a wall network to accommodate an applied shear strain $\gamma = 0.003$ in the present investigation where p, the dislocation density equals $3.6 \times 10^{14}/\text{cm}^3$ (resulting from a simple cubic cell structure consisting of walls of two perpendicular sets of dislocations of the experimentally observed spacing (300Å)) gives $\bar{x} = \gamma/pb \sim 3 \times 10^{-2}$ Å which is clearly ridiculous. Obviously, if this mechanism is to be applicable a smaller proportion of sources must be activated at any given stress level. Even in

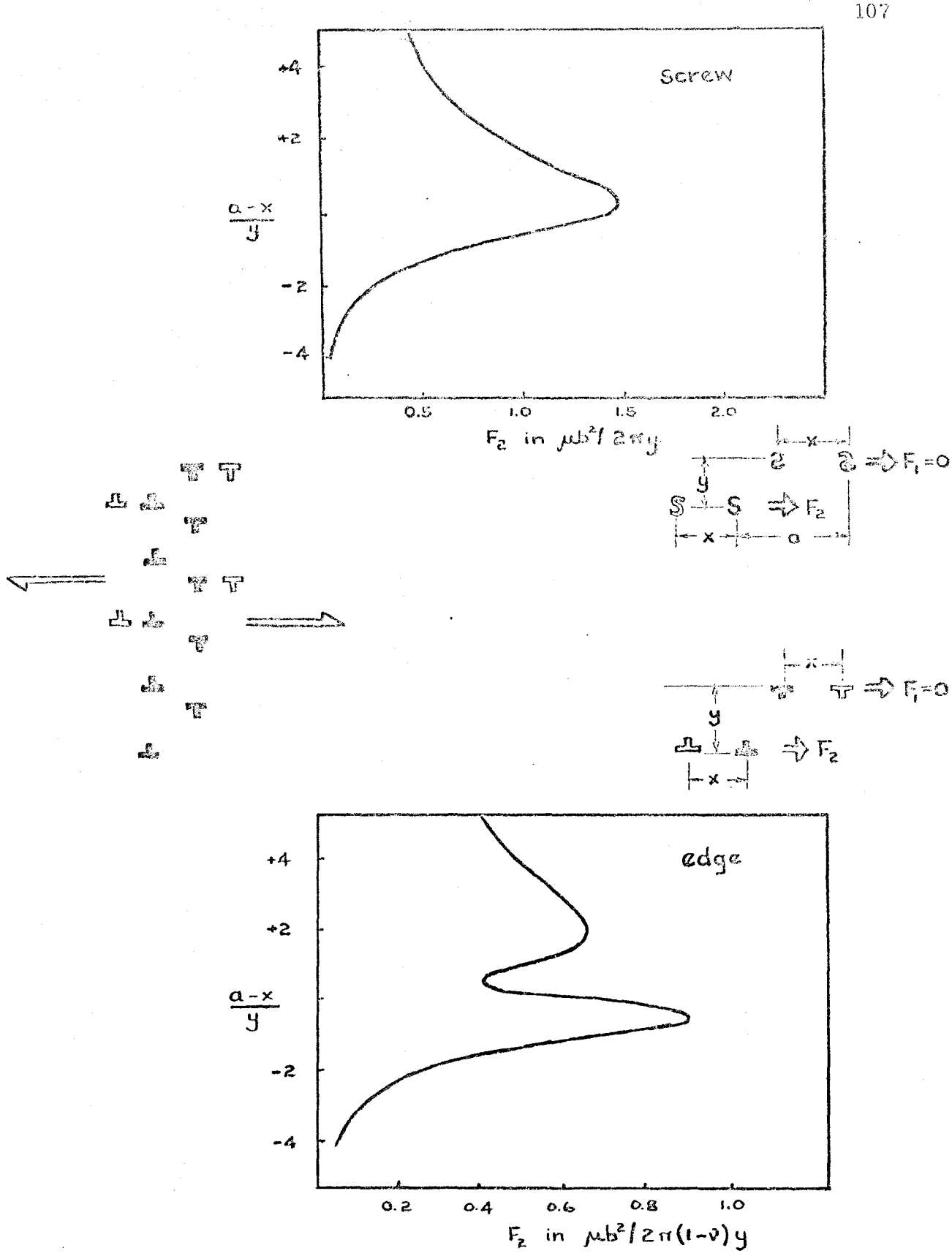

Figure 16. Breakdown of a dipole array (after Li (1964)).

overstrain however, strain can easily be borne by movements of dislocations over distances less than the cell dimensions, as the number of potential sources is evidently adequately high.

5.4 Macroscopic Descriptions

By considering a system consisting of two elements of different areas in series (so that the load on each element is equal), McClintock (1963) has shown that during cycling at constant total strain amplitude, the difference in strain borne between each element tends to increase exponentially as cyclic straining continues. The system had a simple invariant work-hardening coefficient h, producing linear hardening, and a constant Bauschinger effect ratio b. At stress levels $S \geq h$ necking instability occurs: if $S > \sqrt{h(h-b)}$ the fractional increase in strain differences per cycle $\frac{1}{\delta\epsilon} \cdot \frac{d\delta\epsilon}{dn} = \frac{[S^2 - h(h-b)]}{h^2 - S^2}$ is very large whilst even at lower stress levels $S < \sqrt{h(h-b)}$ deformation is still unstable as $\frac{1}{\delta\epsilon} \cdot \frac{d\delta\epsilon}{dn} = \frac{2\epsilon_a \cdot S(h-b)}{h(h-b) - S^2}$ is still increasing. In a real material fatigued at low stress or strain amplitude the rate of strain hardening is not constant but decreases towards the Bauschinger coefficient value; the third expression is applicable in the present investigation, and as an indication of the inevitability of instability propagation we will consider typical data for the furnace cooled condition. Here h decreases from an initial value of $\sim 5.8 \times 10^5$ psi to $\sim 4 \times 10^4$ psi after fatigue. Taking b constant and equal to 1.5×10^5 psi, the value of $\sqrt{h(h-b)}$ drops from $\sim 5 \times 10^5$ psi to $\sim 7 \times 10^4$ psi. Under these conditions the stress $S < \sqrt{h(h-b)}$ but the difference of the squares is decreasing. One description of fatigue softening is therefore the growth of an instability defined as the difference in strain between elements of the material.

McClintock's model is of course only qualitative and applicable only to macroscopic sources of instability progressing right through the material,

in particular to the plastic zone ahead of a growing fatigue crack. Nevertheless, it delineates elegantly the basic fact that any material which possesses little strain hardening capacity will not resist fatigue crack propagation adequately, without resorting to detailed dislocation substructural models.

Experimental evidence for the fundamental importance of work-hardening capacity has been obtained by Klesnil and Lukas (1967), in annealed low carbon steels, who discovered that an empirical description of the initial cyclic softening under stress amplitude control, in terms of the spreading of plastic zones through the specimen below the macroscopic yield point, could also be accurately applied to subsequent cyclic hardening to saturation. Since their description was based on a linear activation of plastic sources but also on an exponential development of slip with cycling within each plastic zone, it was equivalent to the description of McClintock, albeit for control of stress rather than strain amplitude.

There is good reason, therefore, to investigate source models of transient fatigue processes, saturation and residual work-hardening, since a basic microscale instability developed at many points in the crystal should according to the above considerations be capable of producing macroscopic instability by simple geometrical spreading, in materials possessing insufficient strain-hardening capacity to dissipate local partitioning of strain. Thus crack propagation by side branching under stress intensification in shear bands should, in principle, be controlled by the work hardening during shear deformation, as can be seen by the development of the Coffin-Manson law given by Tomkins (1968) in terms of fundamental material parameters.

CHAPTER 6

CONCLUSIONS

6.1 Summary

From a study of polycrystalline iron, containing various distributions of carbide particles, subjected to controlled low-amplitude cyclic straining, it was determined that the effect of particle size upon the development of fatigue substructures lay in the influence of particles of a second phase on the accumulation of dislocations. A qualitative description of this influence, and of the influence of the magnitude of the applied strain amplitude has been developed to explain the occurrence of cyclic softening in these materials based on the requirements of continuity in plastically inhomogeneous materials. No detailed model of the softening process itself could be proposed from the present results, though an effect of particle spacing was observed.

Comparisons of the observed saturation substructures were made with unidirectional structures of corresponding scale, in terms of the detailed configuration and the associated lattice rotations. It was concluded that the characteristic simplicity of the cyclic structure was a consequence of the high primary dipole density, compared with the low secondary and forest density, producing very much lower rates of work-hardening in a fatigued structure than during the original unidirectional deformation of the material. As the polycrystalline case is complex, it was not possible to separate the contribution of second phase particles to the observed accumulation of dislocations at saturation, from the overall matrix continuity requirements.

By considering macroscopic instability criteria in conjunction with observations of the stability of the fatigued structure during tensile

overstrain, a model describing micro-scale instabilities as the activation of potentially unstable dislocation sources in the saturation substructure has been proposed consistent with the present and other results.

Further observations have been made of the efficiency of thermal-mechanical pre-treatment in retarding cyclic softening of deformed substructures subjected to fatigue. These results have been interpreted in terms of precipitate constraints. Some evidence of strain ageing as a contribution to local constraints of the substructure has been detected, but the relative importance of this effect, and its distinction from normal ageing processes could not be assessed.

6.2 Recommendations for Future Work

The results of the present investigation suggest strongly that finely dispersed particle distributions, with small particle sizes and small interparticle spacings resist the development of fatigue substructures which characteristically partition the bearing of strain into active and dead regions, permitting cyclic softening to occur. This is particularly apparent in coarse distributions which soften readily and allow cell structures to build up. The resistance of any particle distribution is however sensitively dependent on the applied strain amplitude, and local instabilities can still arise, such as the slip channels observed in the present investigation.

Evidently, thermal-mechanical working offers considerable opportunity, for example in ausforming, to produce strong, pinned substructures. Equally, materials such as TRIP steels capable of crack-blunting, should dissipate localized dislocation substructural development by phase transformation. Certainly, HSLA and ferritic stainless steels should be examined in a similar manner to the present investigation to determine the optimum carbide morphologies for fatigue resistance.

There are several critical experiments, however, which should be attempted, preferably in single-phase, single crystals, to test some of the predictions arising from the present work.

(1) To determine the saturation strain bearing mechanism, a single crystal, fatigued to saturation, could be irradiated to produce a high concentration of defects, and then fatigued a further half cycle. Examination by T.E.M. should reveal which dislocations move, and by how much, as moving dislocations annihilate irradiation induced defects, and would hence leave denuded traces.

(2) A similar experiment could be performed for tensile overstrain to assess the validity of the source model, which cannot be readily correlated with surface slip observations except in single crystals.

Two phase single crystals would be most suitable for examination of the softening process in detail, particularly in the determination of the dipole formation and the development of cell structures in the content of secondary slip.

In general, further investigation of polycrystalline iron with finally dispersed carbides is required, in order to:

(i) determine whether overstrain of such dispersions results in channel formation once dislocation accumulation has been initiated.

(ii) determine if softening can be induced in very fine dispersions by suppressing cross-slip by fatigue at low temperatures.

Techniques for more detailed examination of the plastic zone ahead of a growing fatigue crack should be developed, such as etch-pitting; materials resisting fatigue crack propagation could then be more fundamentally assessed.

BIBLIOGRAPHY

Adamson, R.B. (1968), Phil. Mag. 17, 681.

Argon, A.S. (1969), The Physics of Strength and Plasticity, ed. Argon, p. 217, M.I.T. Press, Cambridge.

Arndt, D. and Damasic, A. (1964), Acta Met. 12, 341.

Ashby, M.F. (1966), Phil. Mag. 15, 1157.

Ashby, M.F. (1970), Acta. Met. 21, 399.

Avery, D.H., and Backofen, W.A. (1963), Acta. Met. 11, 653.

Basinski, Z.A., Basinski, S. and Howie, A. (1969), Phil. Mag. 19, 899.

Beardmore, P. and Feltner, C.E. (1969), Proc. Int. Conf. on Fracture, p. 607, Brighton.

Bowden, P.B. (1970), Phil. Mag. 21, 455.

Broom, T. and Ham, R.K. (1957), Proc. Royal Soc. A 242, 166.

Bullough, R. and Sharp, J.V. (1965), Phil. Mag. 11, 605.

Cahn, J.W. and Fullman, R.L. (1956), Trans. AIME, 206, 610.

Clarebrough, L.M., Hargreaves, M.E., West, G.W. and Head, A.K. (1957), Proc. Royal Soc. A 242, 161.

De Foucquet, J. (1961), Mem. Sci. Rev. Met. 58, 129.

Eckert, D. (1958), A.S.T.M. Special Technical Publication No. 216, p. 21.

Feltner, C.E. (1966), Phil. Mag. 14, 1219.

Feltner, C.E. and Laird, C. (1967a), Acta. Met. 15, 1621.

Feltner, C.E. and Laird, C. (1967b), Acta. Met. 15, 1633.

Feltner, C.E. and Laird, C. (1968), Ford Motor Co. Publication 25-11-68.

Ferro, A. and Montalenti, G. (1962), Phil. Mag. 8, 105.

Foreman, A.J.E. (1968), Phil. Mag. 17, 353.

Forsyth, P.J.E. and Stubbington, C.A. (1961), J. Inst. Met. 90, 347.

Friedel, J. (1964), Dislocations, Addison-Wesley, New York.

Fujita, K. and Damask, A. (1964), Acta Met. 12, 331.

Gilman, J.J. (1962), J. App. Phys. 33, 2703.

Grosskreutz, J.C., and Waldon, P., (1963), Acta. Met. 11, 717.

Hahn, G.T., and Sadey, D. (1966), Trans. Quart. A.S.M., 59, 16.

Hale, K.F., and McClean, D. (1963), J. Iron and Steel Inst. 201, 337.

Halford, G.R. (1969), Ph.D. Thesis University of Illinois, Urbana.

Hancock, P., and Grosskreutz, J.C., (1967), Air Force Publication AFML TR 67-203.

Hargreaves, M.E., Loretto, P.E., Clarebrough, L.M., and Segall, R.L., (1963), N.P.L. Symposium on the Relation Between the Structure and Mechanical Properties of Materials, No. 15, H.M.S.O., London.

Hirsch, P.B., Howie, A., Nicholson, R.B., Pashley, D.W. and Whelan, M.J., (1965), Electron Microscopy of Thin Crystals, p.522, Butterworth, London.

Hirsch, P.B. and Mitchell, T. (1967), Can. J. Phys. 45, 663.

Homan, P. (1964), Acta Met. 12, 1071.

Huggard, D. (1970), M.Sc. Thesis, McMaster University, Hamilton.

Hull, D. and Mogford, I.L. (1961), Phil. Mag. 6, 535.

Ikeda, S. (1970), Proc. Int. Conf. On Science and Technology of Iron and Steel, Iron and Steel Inst. of Japan, Tokyo.

Kawasaici, T., Izumi, H. and Sawaki, Y. (1967), Trans. Quart. A.S.M., 60, 707.

Keh, A.S. and Weissman, S. (1963), Electron Microscopy and the Strength of Crystals, p.231, ed. Thomas, Interscience, New York.

Kelly, A. and Nicholson, R.B. (1963), Progress in Materials Science 10.

Kemsley, D. (1958), J. Inst. Met. 87, 10.

Kettunen, P. and Kochs, U.F. (1969), Czech. J. Phys. B19, 299.

Klesnil, M. and Lukas, P. (1965), J. Iron and Steel Inst. 203, 1043.

Klesnil, M. and Lukas, P. (1967), J. Iron and Steel Inst. 205, 746.

Klesnil, M., Holzmann, D., Lukas, P. and Rys. P., (1965), J. Iron and Steel Inst. 203, 47.

Kuhlmann-Wilsdorf, D. and Nine, H. D. (1967), J. App. Phys. 38, 1683.

Laufer, E. E. (1969), Czech. J. Phys. B19, 333.

Laufer, E. E. and Roberts, (1966), Phil. Mag. 14, 65.

Lawrence, F. V., and Jones, K. (1970), Met. Trans. A.I.M.E. 1, 367.

Li, J. C. M. (1963), Aust. J. Metals 8, 206.

Lukas, P., Klesnil, M. and Rys, P. (1965), Z. Metallk. 56, 109.

Lukas, P., Klesnil, M., Krejci, J. and Rys, P. (1966), Physica, Stat. Sol. 15, 71.

Makin, M. J. (1969), Phil. Mag. 19, 931.

McGrath, J. T., and Bratina, W. J. (1965a), Phil. Mag. 11, 429.

McGrath, J. T. and Bratina, W. J. (1965b), Phil. Mag. 12, 1293.

McGrath, J. T. and Bratina, W. J. (1967), Acta. Met. 15, 329.

McGrath, J. T., and Bratina, W. J. (1969), Czech. J. Phys. B19, 284.

McGrath, J. T. and Bratina, W. J. (1970), Phil. Mag. 20, 1087.

McClintock, F. (1963), Fracture in Solids, p. 65, eds. Drucker and Gilman, Gordon and Breach, New York.

McEvily, A. J., and Boettner, R. C. (1963), Acta. Met. 11, 725.

Michalak, A., and Paxton, H. W. (1961), Trans. A.I.M.E. 221, 850.

Mintz, B. and Wilson, D. V. (1965), Acta. Met. 13, 947.

Morrow, J. (1965), Theoretical and Applied Mechanics Report No. 277, Univ. of Illinois, Urbana.

Morrow, J., Halford, G. R. and Millan, J. F. (1966), Theoretical and Applied Mechanics Report No. 288., University of Illinois, Urbana.

Mughrabi, H. (1968), Phil. Mag., 18, 1127.

Nicholson, R. B. (1962), Electron Microscopy and the Strength of Crystals, ed. Thomas, Interscience, New York.

Neumann, P. (1969), Acta. Met. 17, 1219.

Oates, D. and Wilson, D. V. (1964), Acta Met. 12, 21.

Park, B.K., Greenhut, V., and Weissmann, S. (1970), Proc. 2nd Conf. and Strength of Metals and Alloys, Asilomar, p.664.

Pratt, J.E. (1967), Acta. Met. 15, 319.

Russell, K. and Ashby, M.F. (1970), Acta. Met. 18, 891.

Sanders, D., and Hempel, M. (1952), Arch. Eisenhuttenw. 23, 383.

Shinozaki, D., and Embury, J.D. (1969), Metal Science J. 3, 147.

Tetelman, A. (1962), Acta. Met. 10, 813.

Tomkins, R. (1968), Phil. Mag. 18, 1041.

Wadsworth, D., and Hutchings, K. (1964), Phil. Mag. 9, 195.

Watt, D. (1971), Private Communication.

Watt, D., Embury, J.D., and Ham, R.K. (1968), Phil. Mag. 17, 199.

Wei, R.P., and Baker, A.J. (1965a), Phil. Mag. 11, 1087.

Wei, R.P., and Baker, A.J. (1965b), Phil. Mag. 12, 1005.

Weissman, S., Shrier, A., and Greenhut, V. (1966), Trans. Quart. A.S.M. 59, 709.

Wells, M.G.H. and Butler, J.F. (1966), Trans. Quart. A.S.M. 59, 427.

Wilson, D.V. (1970), Phil. Mag. 22, 643.

Wilson, D.V. and Russell, B. (1960), Acta. Met. 8, 36.

Wilson, D.V. and Tromans, R. (1970), Acta. Met. 18, 1197.

Woo, O.T., Kupcis, O.A., Ramaswami, B., and McGrath, J.T. (1970), Proc. 2nd Conf. on Strength of Metals and Alloys, Asilomar, p.659.

Wood, W.A. (1962-3), J. Inst. Met. 91, 193.

Yamakazi, M. (1970, Proc. Int. Conf. on Science and Technology of Iron and Steel, p.620, Iron and Steel Inst. of Japan, Tokyo.

APPENDIX

The Bauschinger Effect in Two Phase Materials

A1. Introduction

When a crystalline solid is pre-strained under a particular stress system, and then restrained under a different stress system, the absolute value of the yield stress in the restrained material is reduced. A degree of permanent softening is observed indicating that work-hardening processes are modified in the reverse direction of straining. The effect was first observed by Bauschinger (1886).

Controlled measurements of the effect in single and polycrystals of various materials were obtained by Buckley and Entwhistle (1956) using torsion of thin walled cylinders, which bear approximately uniform cross-sectional strains, after the method of Woolley (1953). By applying a Taylor factor of 3.1 to polycrystalline data, these investigators showed that the greatest Bauschinger effect occurs in single crystals during easy glide, for single phase materials. The textural and grain boundary back-stresses become significant in polycrystals only at higher equivalent strains. The effect was detected according to Woolley's definition of the Bauschinger strain, modified to include the anisotropy of unloading, as the deviation of the reverse shear stress-shear strain curve from the elastic line of the pre-strain curve, at a fixed stress level. Such a definition is unsuited to comparisons of materials of different elastic moduli and does not take explicit account of work-hardening.

Wilson (1965), used a similar experimental technique on single and two-phase materials, but used a definition of the effect based on the

ratio of the flow stresses which designates the work-hardening in the material. He found that the effect saturated above 1 1/2 to 2% reversed strain, having its greatest value in two-phase alloys with high volume fractions of precipitate, particularly if the particle size were small; the effect of particle spacing was much less marked. As a semi-quantitative measurement of the internal strain remaining after reversed straining, the X-ray line peak shifts detected by diffractometry were used to calculate the residual back stress $\tau_x = \epsilon_x \left(\frac{E}{1-\nu}\right)$ where ϵ_x is the residual lattice strain measured by the line shift. This stress was found to be a linear function of the permanent softening stress increment. Furthermore the measured lattice residual strain saturated at a similar pre-strain to the macroscopic Bauschinger effect.

Abel and Ham (1966) investigated the effect in single crystals of Al-4% Cu containing Guinier-Preston zones or θ'' precipitates, using the reverse yield stress in tension-compression tests to measure its magnitude. They found increases in prestrain and decreases in test temperature increased the magnitude of the Bauschinger effect suggesting that cross-slip might be important to the relief of back-stresses built up at second phase obstacles. A decrease in coherency or stacking fault energy also increased the effect.

Numerous investigations of the effect have been carried out in steels, for it is detrimental to the strength of fabricated components. Hoff and Fischer (1958) took specimens from badly bent girders which required cold straightening; they found the effect was highly anisotropic, being detectable on re-straining at small angles to the direction of pre-stress. Kumakura (1968) made similar observations; he also observed that in spheroidized steels the effect was markedly decreased, but that higher annealing temperatures were needed to effectively reduce it than in pearlitic steels. In general, however, recrystallization is necessary to completely remove the Bauschinger effect.

Janiche et al. (1965) found that the annealing kinetics for removal of the effect corresponded to recovery of substructure in steel. They found a larger Bauschinger effect in steels with high pearlite contents than with low pearlite contents, but the effect was independent of the lamellar spacing. Milligan et al. (1966) found the effect more sensitive to morphological changes in bainitic steels than in pearlitic or martensitic steels, using a high stress 4340 material, although the effect always saturated at about 2% pre-strain. Subsequently Milligan and Koo (1968) related the hardening increment σ_{Δ}, equal to the difference between the forward flow stress and the reversed 0.2% offset yield stress, to the hardening stress derived from the theory of Fisher et Al. (1953) for two phase materials (discussed in section A2) and obtained a linear relationship after corrections for hardening in the ferrite matrix had been applied. They used spheroidized steels and lamellar pearlitic steels but did not explicitly test the predictions of the theory outlined in section A2 of this appendix.

The motivation of the present work was to test quantitatively a simple model of the Bauschinger effect in two phase materials to fully assess its physical feasibility.

A2. Theoretical Basis

The problems of analysing the Bauschinger effect have been elegantly described by Orowan (1958). A real solid does not exhibit true Voigt behaviour, i.e. the stress components are not linear functions of strain: instead of relaxing homogeneously and elastically with time a stress applied to a real solid deforms it inhomogeneously, and subsequent relaxation of the stress will include a component of non-linear relaxation, termed anelasticity by Zener (1948). Typical inhomogenieties result from the anistropy of

individual crystals in a polycrystal with respect to orientation and yield strength, from the restriction of deformation to slip bands, and from plastic inhomogeniety in two-phase materials. Each of these inhomogenieties is a source of internal stress, which on removal of the applied stress will generate an anisotropy with respect to stress reversal, and there is no sharp distinction between such sources, whether they be of macroscopic or microscopic scale. The main requirement of a theory of the Bauschinger effect is the ability to distinguish which source is most important.

Back stress hardening at a barrier in a Taylor lattice should give symmetrical unloading, because of the symmetry of the network, and hence no Bauschinger effect. Similarly, most hardening, in which Lomer-Cottrell locks prevent reversible slip, would result, under stress reversal, in the destruction of the network by source generation, by the Frank-Read mechanism. The presence of the effect even in single crystals suggests that Heyn stresses are unimportant; more crucially, the difficulty in annealing out the Bauschinger effect suggests that fairly large scale inhomogenieties, such as those between a slip band and the undeformed matrix, or Luders instability in a polycrystal cannot be critical to the effect, as they should be thermally sensitive.

The origin of the strain-hardening is therefore important. A back-stress model provides for permanent softening, i.e. reversed flow at a stress consistently less than in the initial direction, by the supplementing of the reversed stress by the polarised back stress, but does not provide for an intrinsic Bauschinger effect on unloading, as is observed. Obstacle hardening theories are better, but the degree of irreversibility obtainable is restrictive, since persistent hardening of the structure by intersecting slip processes can only be maintained at the expense of irreversibility.

Orowan therefore invoked his loop-hardening theory. A rather specific obstacle distribution, with regions of both high and low obstacle density will accumulate dislocation loops on stressing in one direction. On

removing the stress, local readjustment takes place, so that on reapplying the stress in the reversed direction segments are propelled under both the back stress of the loop accumulations, and the applied stress, which will therefore be lower than in the forward direction. The build up of loops around obstacles results in continued hardening, but at a lower rate than for simple barrier hardening. The Bauschinger effect should then saturate at some finite glide strain where the availability of slip plane for reversed glide at a reduced stress begins to be outweighed by the distribution of loop hardening.

The work hardening problem has been treated for a simple case, that of a random distribution of rigid obstacles of circular section, in two dimensions, by Fisher et Al. (1953). To sum the self energies of dislocation loops accumulating about these particles an analogy with the magnetic field of a thin wire conductor was used, the strain due to a derived distribution of loop radii was related to the energy sum, and minimised to give the optimum annular radius, which was not a function of the number of loops. Assuming the spacing of dislocation sources to be large compared to the spacing of accumulated loops, a uniform distribution of particles was shown to give rise to a hardening stress increment

$$\tau_H = 3\frac{N}{R} f^{3/2} \quad \text{where } N = \text{number of loops/particle}, \; R = \text{particle radius}$$

If we now consider the flow stress to consist of two components,

$$\tau_{\text{Forward Flow}} = \tau_o + \tau_H \quad .$$

and $$\tau_{\text{Reverse Yield}} = \tau_o - \tau_H$$

if we allow kinematric reversibility. Then

$$\tau_{\text{Forward Flow}} - \tau_{\text{Reverse Yield}} = 2\tau_H \qquad (1)$$

This hardening stress contained a contribution from the single phase matrix,

and should be corrected for this. Thus if we approximate the average shear strain due to the loops of dislocation built up at the second phase particles by

$$\gamma = \frac{1}{2} N \frac{b}{r} \quad \text{for N loops of mean radius r, of Burgers vector b}$$

then $$\tau_H = 3 \frac{N}{r} f^{3/2} \text{ Gb in absolute units}$$

$$= 6 G \gamma f^{3/2} \qquad (2)$$

At any fixed strain γ the relationship between the corrected hardening stress measured as in equation (1) above, and (volume fraction of second phase)$^{3/2}$ should be linear, with a gradient of 12 Gγ.

The model is clearly restricted, both in the allowed geometry of the second phase distribution and in the specific mechanism of work-hardening used. In real materials, the saturation of the Bauschinger effect after a few percent deformation can be explained by the breakdown of the mechanism, or more specifically, its reversibility, a problem analysed by Ashby (1970) in his theory of work-hardening in plastically inhomogeneous materials. By considering the continuity requirements in the material Ashby showed that activation of secondary slip systems was geometrically necessary beyond certain limiting strains. Further analysis of the Bauschinger effect is however not required since the internal stresses producing it, arising from shear loop arrays derived according to the Fisher et Al. model, do not contribute further to work-hardening. The effect saturates when the glide dislocation-obstacle or glide dislocation-prismatic loop interaction stresses are no longer screened by the long-range stresses of the loop arrays; Ashby estimates the limiting strain to be of the order of 2%.

A3. Results

To test the predictions of the Fisher et Al. model developed in Section A2, data supplied by the Steel Company of Canada Ltd., for a range of carbon and high strength, low alloy (HSLA) steels with lamellar pearlite morphlogies was re-analysed. Most of the materials were as rolled (A.R.), but some were normalized for one hour at 1850°F or 2000°F. All had fine grain sizes and approximately similar carbon contents; the pearlite content was modified by the high manganese and small alloy additions. For further details on the experimental arrangement and analyses of the materials, the reader is referred to Jamieson and Hood (1971).

The data was originally acquired in the form of a ratio

$$\frac{\tau_1 - \tau_2}{\tau_1}$$

where τ_1 = original flow stress at the pre strain γ

τ_2 = 0.2% offset yield stress in reversed strain

termed the Bauschinger Effect Factor (BEF). The saturation of the effect with increased pre-strain is shown in Figure A1, for plain carbon (P.C.) and Vanadium (V) steels, and in Niobium (Nb) steels in Figure A2. Saturation occurs around prestrains of 0.02.

The product of the BEF and the original flow stress was plotted as the uncorrected hardening stress versus the volume fraction of second phase (cementite) calculated from equilibrium concentrations, to the power 3/2. Figure A3 shows the results for P.C. and V steels, and Figure A4 results for Nb and V steels. The vanadium HSLA steel data fits best with the other HSLA Nb steel data, as the points for this alloy (shown in parentheses) indicated. Each line is shown for a constant initial pre-strain γ.

Reasonable linearity is obtained, considering that the data is not corrected for hardening in the pure material. The hardening stresses quoted are double their true values, as can be seen from equation (1) of

Section A2.

The data of Hoff and Fischer (1958) was similarly reanalysed and in Figure A5 a plot of the hardening stress vs. $f^{3/2}$ is shown for a range of P. C. steels. Linearity is obtained with the small number of points used.

A4. Discussion and Conclusions

At low applied strains the model of Fisher et Al. appears to provide a reasonable description of the Bauschinger effect in terms of the accumulation of dislocations at particles of a second phase, producing kinematically reversible stress fields which assist reversed flow. Beyond the limits of strain acceptable for this simple model, the effect saturates as secondary slip systems become activated at the particle matrix interfaces.

The model has been crudely applied in what is essentially a preliminary investigation. The distribution of the second phase in a pearlitic steel is somwhat remote from the idealized distribution of the model. It would appear that the manner of accumulation of dislocations at the interface is the important process, so that providing the spacing of second phase particles is sufficiently small for the gradients of strain at each interface to overlap and contribute to low amplitude reversibility of dislocation motion little effect of interparticle spacing is to be expected as observed by Janiche et Al. (loc. cit.). Spheroidized structures, approaching the ideal distribution more closely, should show strain limits at saturation corresponding to the theoretical limit for activation of secondary slip, if the particles are completely incoherent. Milligan and Koo (loc. cit.) found that the linear relationship of the observed hardening stress to that predicted by the Fisher et Al. model held up to pre-strains of 4%, suggesting that dislocation accumulation is more ideal in spheroidized structures.

Measurements of the gradients of the plots of τ_H vs. $f^{3/2}$ gave values of G from 5×10^6 to 8.5×10^6 p.s.i., and the gradients of the BEF saturation curves at various strains gave suitable values of the hardening stresses, showing that the physical basis of the model is quite consistent. The magnitude of the observed back stresses is of the order of 25% of the flow stress at most; the calculations of the stress fields of various ideal dislocation pile-ups, made by Mitchell (1964) suggest that a suitable internal stress field of this magnitude could be exerted over distances twice as large as the dimensions of pile-ups in the primary plane. Secondary slip systems could only be activated in regions of dimensions about half those of the pile-up. Obstacles in general are better represented as providing a resistance to further slip which varies with the distance from it, than as unsurmountable obstacles, as in the long-range stress theory of the Stuttgart school; this type of description is well suited to an explanation of the saturation of the Bauschinger effect in general.

Bibliography

Abel and Ham, R.K. (1966), Acta Met., 14, 1489.

Ashby, M. F. (1968), Harvard University Technical Report No. 579.

Bauschinger, J. (1886), Mitt. Mech-Tech. Lab., Munchen, H13.

Buckley and Entwhistle (1956), Act. Met. 4, 352.

Fisher, J. C., Hart, E. W. and Pry, R. (1953) Acta Met. 1, 336.

Hoff and Fischer, (1958) Stahl Und Eisen 78, 1313. →

Jamieson, R. and Hood, J. (1971), J. Iron and Steel Inst. 209, 46.

Janiche, Stolte, and Kugler (1965), Tech. Mitt. Krupp, Forschungbereits 23, 117.

Kumakura (1968), Bulletin Jap. Soc. Mech. Eng. 11, 427.

Milligan R. V., Koo and Davidson (1966), Trans. A. I. M. E.

Milligan, R. V. and Koo (1968), Trans. Jap. Inst. Metals. 9, 895.

Mitchell, T. E. (1964), Phil. Mag. 10, 301.

Orowan, E. (1958), Symposium on Internal Stresses and Fatigue in Metals, Eds. Rassweiler and Grube, p. 78, Elsevier, New York.

Wilson, D. V. (1965), Acta. Met. 13, 1489.

Woolley (1953), Phil. Mag. 44, 597.

Zener, C. (1948), Elasticity and Anelasticity of Metals, Wiley, New York.

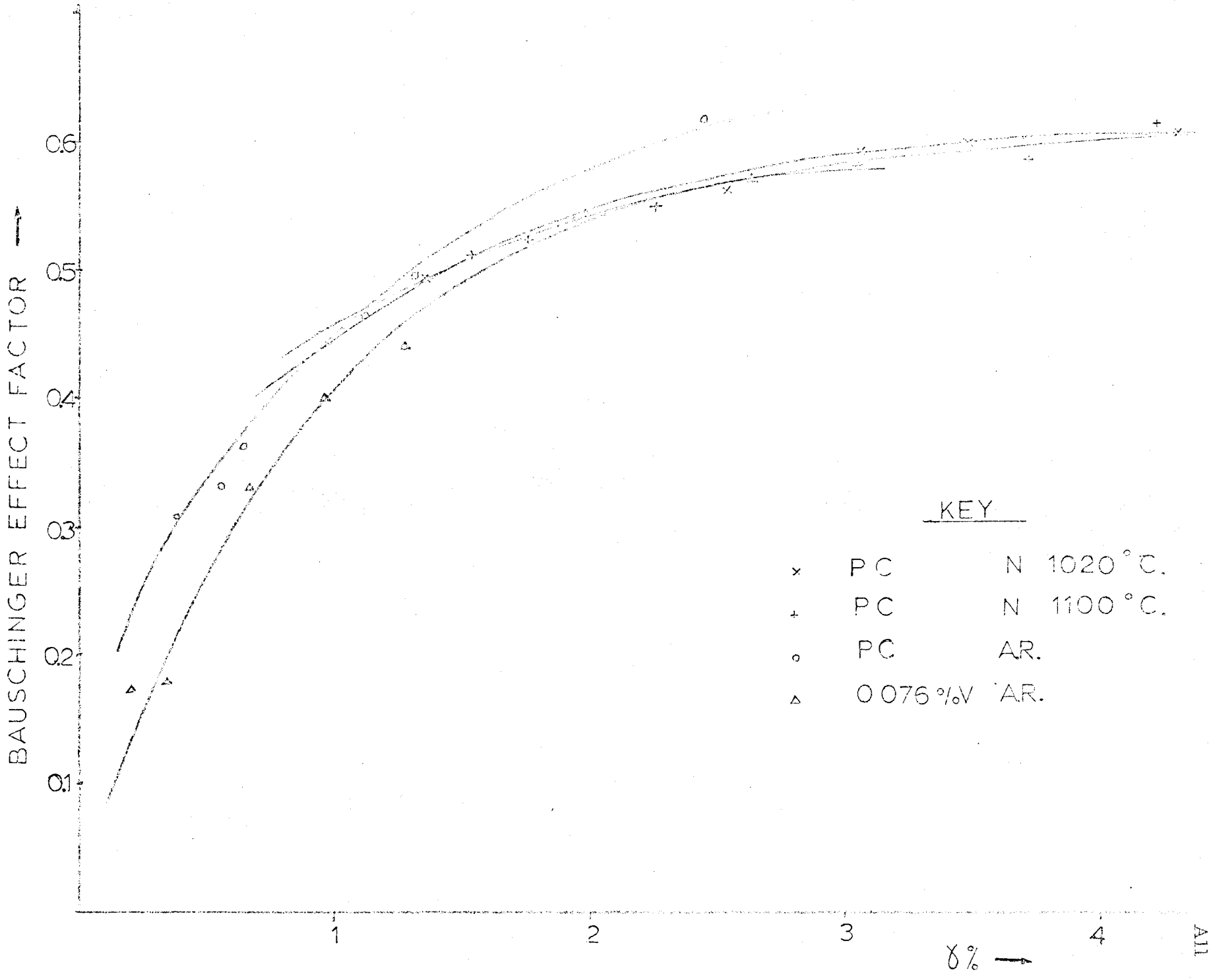
BAUSCHINGER EFFECT FACTOR →
0.6
0.5
0.4
0.3
0.2
0.1
1
2
3
4
γ% →
KEY
× P C N 1020 °C.
+ P C N 1100 °C.
○ P C A.R.
△ 0 076 %V A.R.
A11

FIG. A1.

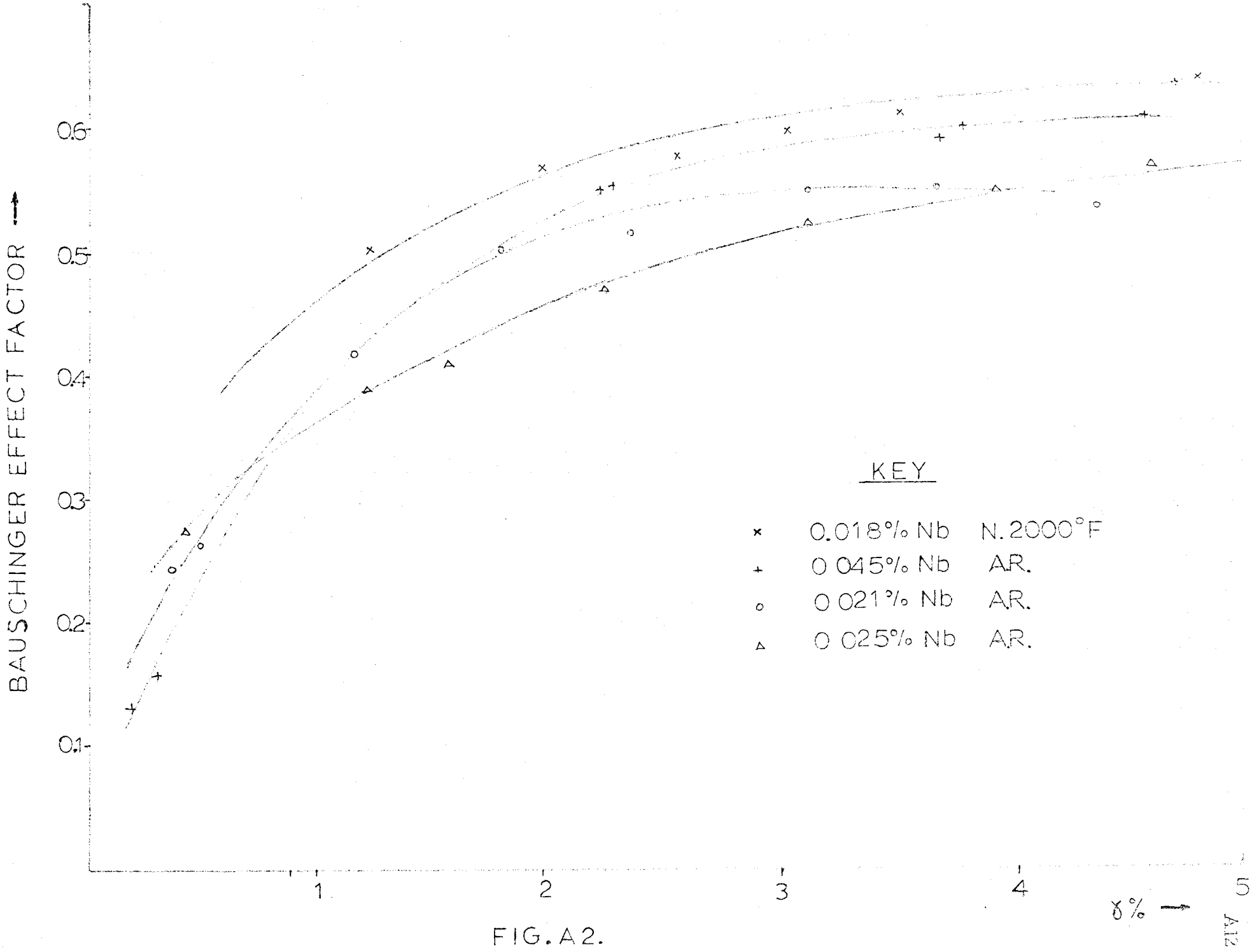
BAUSCHINGER EFFECT FACTOR →
0.6
0.5
0.4
0.3
0.2
0.1
1
2
3
4
5
δ% →
KEY
× 0.018% Nb N. 2000°F
+ 0 045% Nb AR.
o 0 021% Nb AR.
△ 0 025% Nb AR.
A12

FIG. A2.

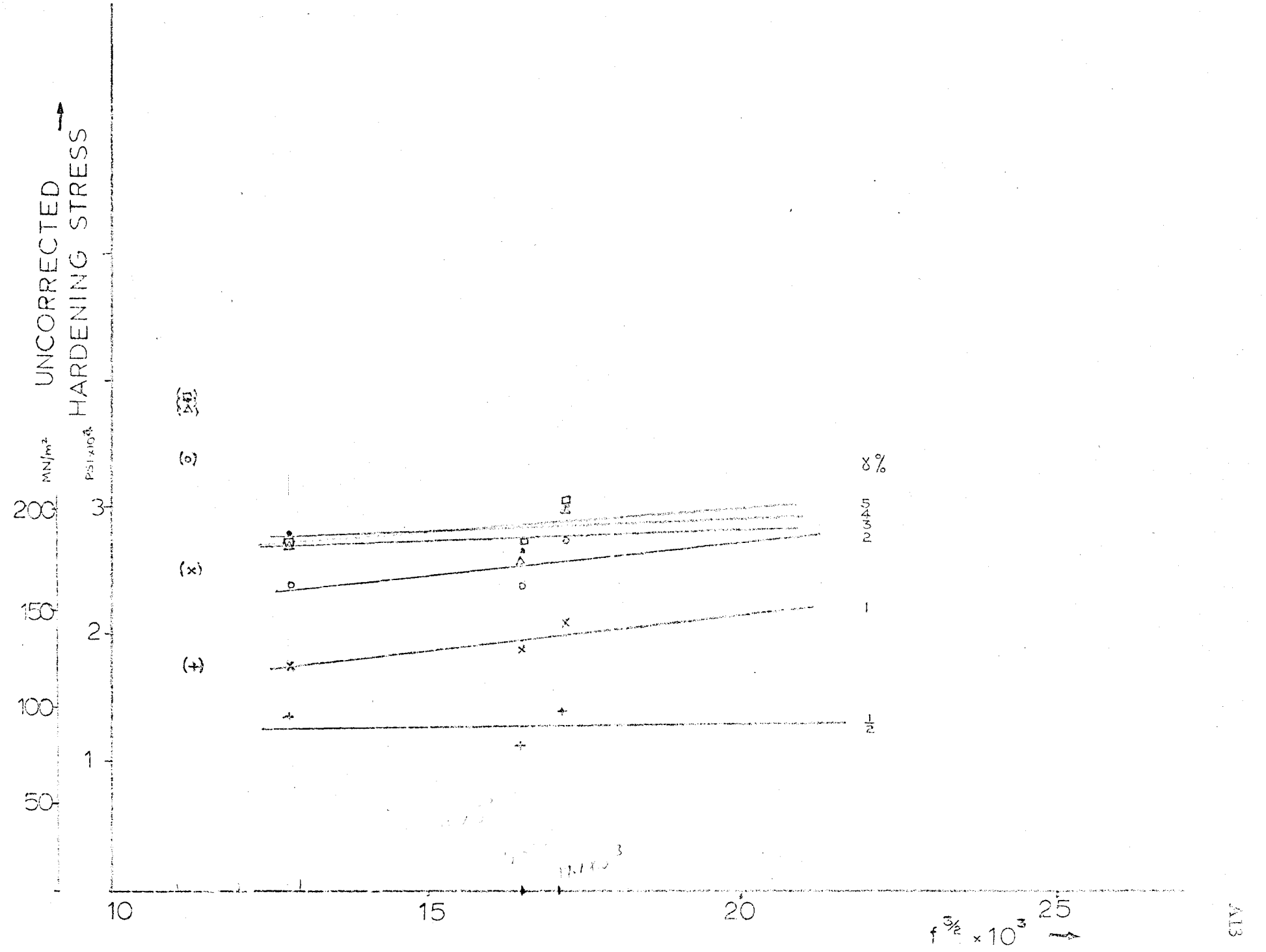

FIG. A3: PLAIN CARBON & VANADIUM STEELS

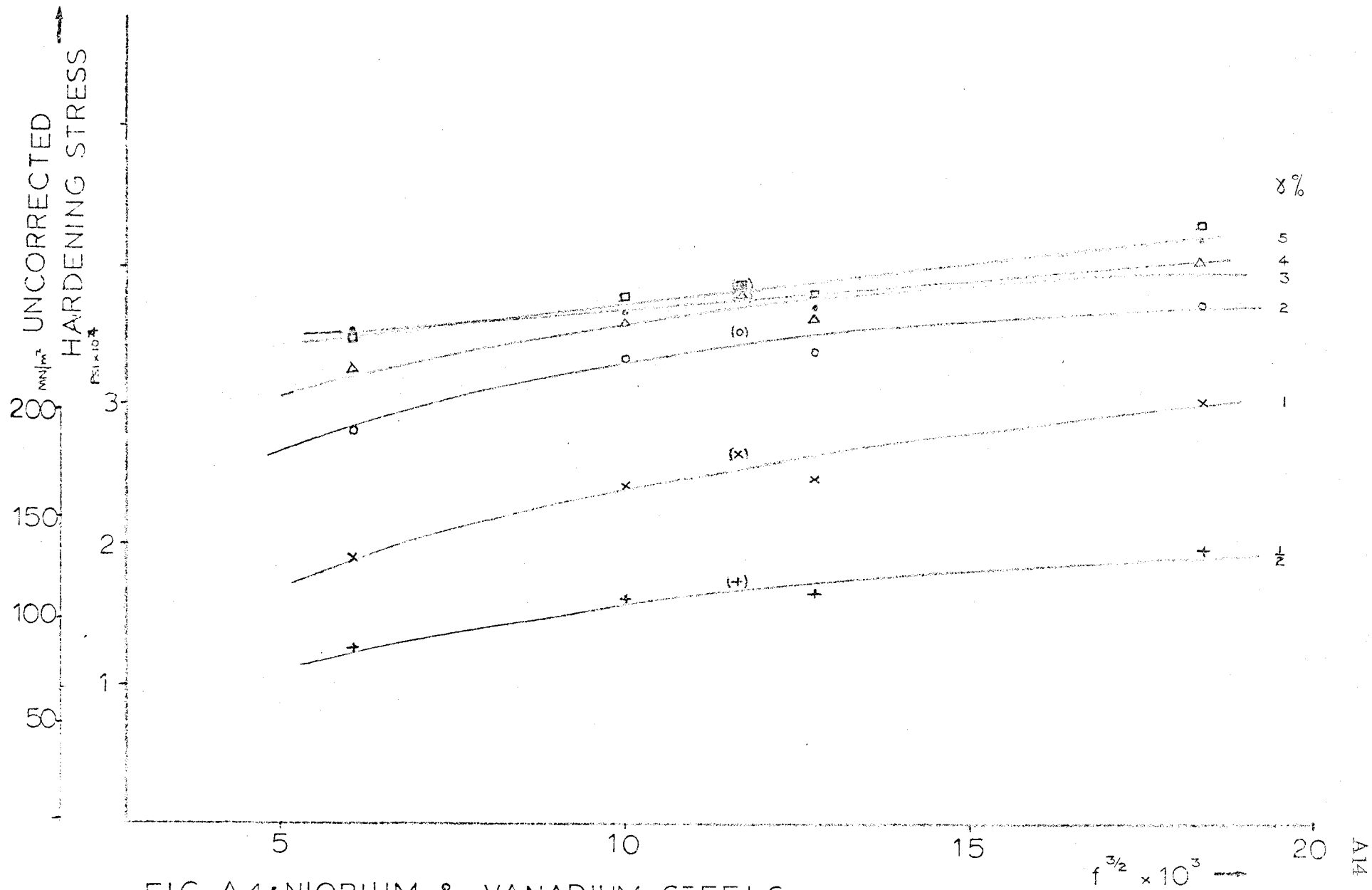

FIG. A4: NIOBIUM & VANADIUM STEELS

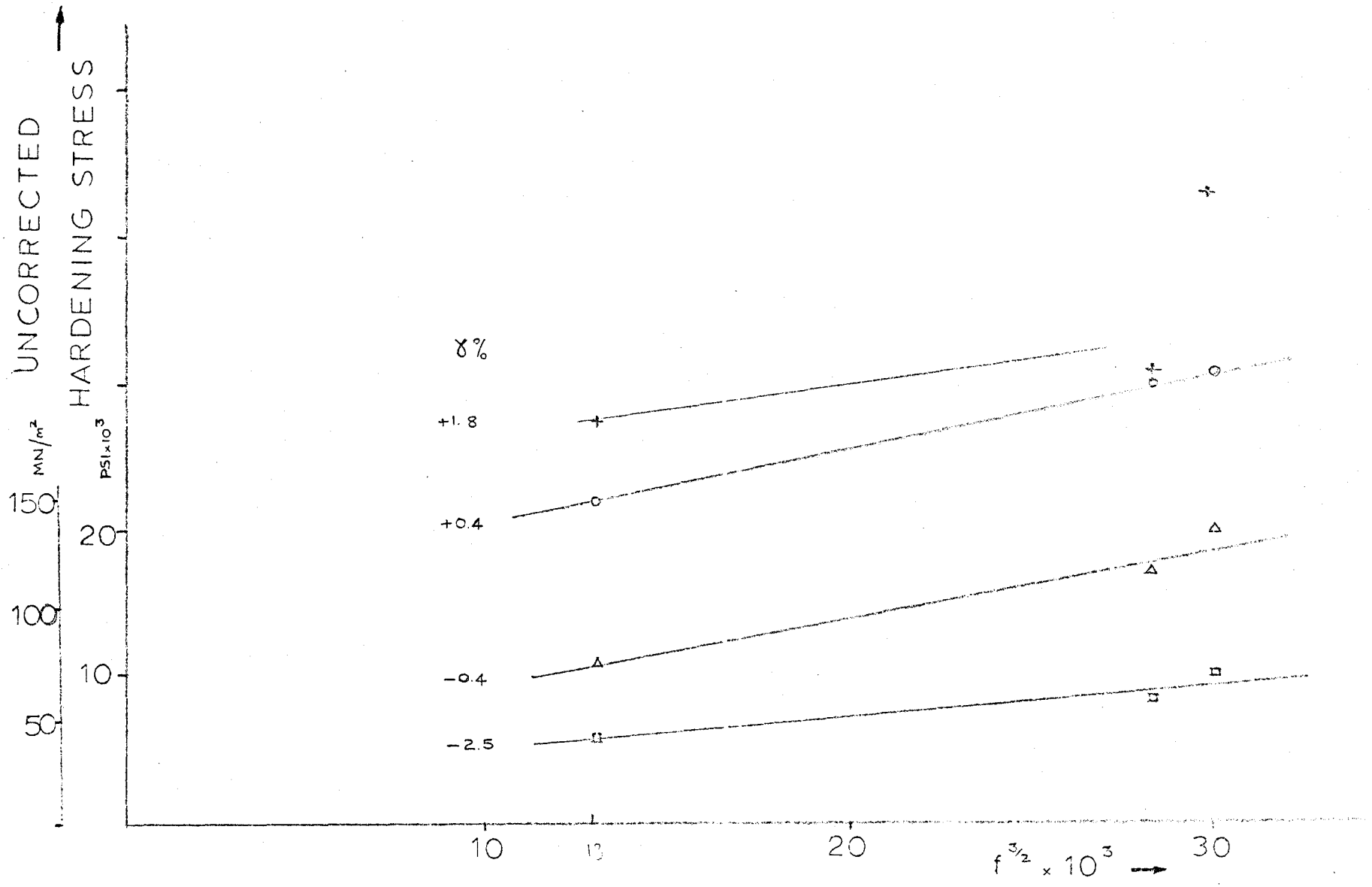

FIG. A5: DATA FROM HOFF & FISCHER